# The Marine Carbonate System: Ionic Interactions and Biogeochemical Processes

**Adam Ulfsbo**

THESIS FOR THE DEGREE OF DOCTOR OF PHILOSOPHY IN SCIENCE
IN THE FIELD OF CHEMISTRY

Akademisk avhandling för filosofie doktorsexamen i Naturvetenskap, inriktning kemi som med tillstånd från Naturvetenskapliga fakulteten kommer att offentligt försvaras fredagen den 28 maj kl. 10:00 i KB, Institutionen för kemi och molekylärbiologi, Kemigården 4, Göteborgs universitet, Göteborg

Fakultetsopponent: Prof. Dr. Dieter A. Wolf-Gladrow, Alfred Wegener Institute Helmholtz Centre for Polar and Marine Research, Bremerhaven, Tyskland.

UNIVERSITY OF GOTHENBURG
DEPARTMENT OF CHEMISTRY
AND MOLECULAR BIOLOGY

2014

The Marine Carbonate System: Ionic Interactions and Biogeochemical Processes

ADAM ULFSBO

Department of Chemistry and Molecular Biology
University of Gothenburg
SE-412 96 Göteborg
Sweden

Cover picture: A sketch of a free ion in seawater. (Republished in accordance with Chemistry Central's Open Access Charter, from Millero, F. (2001), Speciation of metals in natural waters, *Geochem. Trans.*, 8); The picture also reflects, generally, the time as a PhD student and is the thesis Author's tribute to the incredible life work of Prof. Dr. Frank J. Millero.


ISBN 978-91-628-8998-2 (print)
ISBN 978-91-628-8999-9 (pdf)
Available online at: http://hdl.handle.net/2077/35246

Typeset with LaTeX.
Printed by Ale Tryckteam AB,
Bohus, Sweden 2014

*To my family for eternal oceans of support, dedication and love*
*This thesis is dedicated to the loving memory of Gunnar Ulfsbo*

## Abstract

The absorption of atmospheric carbon dioxide ($CO_2$) by seawater and subsequent equilibrium reactions within this ionic medium give rise to a complex chemical system often referred to as the marine carbonate system. This system is influenced by physical and biogeochemical processes in the ocean. The marine carbonate system is a major component of the global carbon cycle and is, by virtue of its interaction with atmospheric $CO_2$, of fundamental importance to the Earth's climate. Accurate knowledge of the properties of the marine carbonate system is a prerequisite for understanding the chemical forcing and consequences of key biogeochemical processes such as biological production, organic matter respiration, or uptake of anthropogenic carbon. The assessment of the marine carbonate system builds on precise measurements by state-of-the-art analytical methods as well as an understanding of the underlying fundamental chemistry in terms of ionic interactions and equilibrium thermodynamics. This thesis focuses on different aspects of the marine carbonate system with emphasis on biogeochemical processes and thermodynamic modelling of the seawater ionic medium. A quantitative understanding of the equilibrium solution chemistry of seawater ultimately relies on accurate estimations of activity coefficients of all the various components that make up the solution. Activity coefficients of the carbonate system in sodium chloride solution of varying ionic strength were estimated by Monte Carlo simulations at different temperatures, as well as activity coefficients of chloride and sulfate salts of a simplified seawater electrolyte, suggesting that a complete Monte Carlo description of seawater activity coefficients may be achievable using the hard sphere approach with a very limited number of fitted parameters. Chemical speciation modelling showed that the measured excess alkalinity of Baltic seawater is consistent with an organic alkalinity derived from humic substances of terrestrial origin. In deep waters of the Baltic Sea, oxygen and sulfate was found to be the major electron acceptors to the remineralization of organic matter under different redox conditions. It was further suggested that this organic matter predominantly had a terrestrial origin. The subsurface waters of the central Arctic Ocean were found to be a sink of anthropogenic $CO_2$, attributed to uptake by source waters of Atlantic origin. The sea-ice covered central Arctic Ocean was also shown to harbor low, but significant biological productivity. Late summer net community production was estimated using multiple approaches based on both discrete and underway measurements and results showed large spatial variability between the deep basins with extremes at the marginal ice zone.

## Populärvetenskaplig sammanfattning

Haven utgör en central del i den globala kolcykeln. Processer i havet som påverkar kolcykeln är därför betydelsefulla för det globala klimatet då de påverkar utbytet av koldioxid ($CO_2$) med atmosfären. För att förstå klimatutvecklingen är det därför viktigt att ha god kunskap om de relevanta processerna i havet. Idag är detta än mer viktigt då, i huvudsak, förbränning av fossila bränslen medför stora utsläpp av $CO_2$ till atmosfären. En effekt av dessa utsläpp är det välkända faktum att havens pH har minskat, vilket idag är ett aktuellt och omfattande internationellt forskningsområde, ocean acidification (havsförsurning).

När $CO_2$ löser sig i havsvatten bildas den svaga syran kolsyra. Kolsyran omvandlas i sin tur till bikarbonat- och karbonatjoner, medan vätejoner frisläpps, d.v.s. vattnet blir surare (lägre pH). Dessa jämviktsreaktioner ger upphov till ett komplext kemiskt system som brukar kallas för det marina karbonatsystemet. Detta system påverkas av flera fysiska, biologiska, geologiska och kemiska processer, eller ofta uttryckt som fysiska och biogeokemiska processer, i havet. Kunskap om kolcykeln och de biogeokemiska processerna, t ex biologisk produktion, nedbrytning av organiskt material eller upptag av antropogen $CO_2$ (från mänsklig aktivitet), kräver god förståelse av karbonatsystemets olika ingående delar. Karbonatsystemet kan bestämmas genom att mäta två av de fyra mätbara parametrarna: totalt löst oorganiskt kol, total alkalinitet, partialtrycket av $CO_2$ samt pH. Utvärderingen bygger på termodynamiska jämviktsförhållanden och joninteraktioner i havsvatten. Denna avhandling behandlar olika delar av det marina karbonatsystemet med fokus på biogeokemiska processer och termodynamisk modellering av havsvatten.

En kvantitativ förståelse av havsvattens lösningskemi vid jämvikt bygger på att aktivitetskoefficienter för alla olika ingående komponenter (joner och molekyler) kan uppskattas efter bästa möjliga förmåga. En aktivitetskoefficient är en faktor som tar hänsyn till elektrostatiska interaktioner mellan joner i lösning och relaterar koncentrationen av en löst komponent med dess aktivitet, där aktiviteten kan ses som den effektiva koncentrationen. Jonernas aktivitet minskar som följd av att jonerna skärmar varandra från interaktion med andra joner. I denna avhandling uppskattades aktivitetskoefficienter av karbonatsystemets ingående komponenter i natriumkloridslösning vid olika koncentrationer och temperaturer genom Monte Carlo-simuleringar, som grundar sig i statistisk mekanik. Vidare uppskattades aktivitetskoefficienter av klorid- och sulfatsalter i en förenklad havsvattenselektrolyt. Fördelen med denna metod är att den bygger på endast ett fåtal anpassade parametrar, såsom jonradier, jämfört med den uppsjö av termodynamisk data som krävs för andra gällande jonpars- och specifika joninteraktionsmodeller. En nackdel med Monte Carlo-metoden i detta sammanhang är att den kräver extremt mycket datorkraft.

Kemiska specieringsberäkningar visade att uppmätt överskott av alkalinitet i Östersjön var förenligt med organisk alkalinitet från humusämnen som tillförts

från land med floderna. Detta var första gången en specifik joninteraktionsmodell kopplades med en oförändrad humusmodell. Östersjön är ett bräckt inlandshav som karaktäriseras av kraftig flodvattentillförsel och begränsat vattenutbyte med haven utanför de grunda och trånga sunden mellan Sverige och Danmark. En effekt av detta är att ytvattnet har betydligt lägre salthalt än vattnen i de djupa delarna. Det begränsade vattenutbytet tillsammans med övergödning resulterar i att de djupa delarna till största delen är syrefria, där även svavelväte bildas då organiskt material bryts ner i vattenpelare och sediment. I detta arbete undersöktes kopplingen mellan pH och biogeokemiska processer i Gotlandsdjupet i Egentliga Östersjön under två år med olika syreförhållanden. Låga, men konstanta, pH-värden observerades under båda år och ackumulering av alkalinitet och löst oorganiskt kol påvisades under syrefria förhållanden i djupvattnet. Genom applicering av en organisk modellsubstans påvisades syre och sulfat vara de viktigaste oxidationsmedel vid nedbrytning av organiskt material under olika reduktions-oxidationsförhållanden. Det organiska materialet var förenligt med material av terrestert ursprung.

Arktiska Oceanen (eller Norra Ishavet) är ett hav i snabb förändring med, bl.a. en snabbare klimatförändring än i någon annan del av världen. Sommaren 2012 var havsisens utbredning i Arktis den minsta i modern tid samtidigt som medeltemperaturen i Arktis har ökat dubbelt så mycket som den globala medeltemperaturen under de senaste 100 åren. Förändringarna kommer sannolikt att ha både miljömässiga och socioekonomiska konsekvenser, även utanför polarområdena. Det har rapporterats att Arktiska Oceanens upptag av $CO_2$ från atmosfären utgör upp till tio procent av det globala upptaget från atmosfären, men denna uppskattning är osäker. Det råder även stora oklarheter kring huruvida Arktiska Oceanen kommer att bli en sänka eller källa för $CO_2$ vid isfria förhållanden under sommarhalvåret. Utfallet kommer till stor del att bero på framtida förändringar i primärproduktion, då växtplankton tar upp och omvandlar $CO_2$ till organiskt kol genom fotosyntes. Efterföljande export av detta kol till djupvattnet, den biologiska pumpen, är direkt kopplad till nettoproduktionen. De flesta vetenskapliga studier av primärproduktion och biologisk nettoproduktion i Arktiska Oceanen har fokuserat på de produktiva randhaven, eftersom centrala Arktis ofta är svårtillgängligt i början av den produktiva säsongen. Rådande uppskattningar av den årliga och säsongsbaserade primär- och nettoproduktionen är låga i de centrala delarna jämfört med de produktiva randhaven. I denna avhandling har påvisats betydande biologisk produktivitet i centrala Arktis. Den biologiska nettoproduktionen var generellt låg, men signifikant i de istäckta djupbassängerna med en stor rumslig variation. Extremt hög produktivitet och nettoproduktion observerades vid iskanterna. Studien baserades på fyra olika metoder där både diskreta och kontinuerliga mätningar användes. En annan studie visade att de intermediära vattenmassorna i centrala Arktis är en sänka för antropogen koldioxid, baserat på analys av mätdata från forskningsexpeditioner med isbrytare mellan 1991 och 2011. Ökningen i antropogen $CO_2$ i de intermediära vattenmassorna tillskrevs ett tidigare upptag av $CO_2$ i de vatten av Atlantiskt ursprung som flödar in i Arktiska Oceanen.

# Part A: Table of contents


**1 Introduction** **1**

**2 The Marine Carbonate System** **5**

2.1 Total Dissolved Inorganic Carbon . . . . . 8

2.2 Total Alkalinity . . . . . 10

2.3 pH . . . . . 15

2.4 The Partial Pressure or Fugacity of $CO_2$ . . . . . 18

2.5 Internal Consistency of the Carbonate System . . . . . 19

**3 Biogeochemical Processes** **22**

3.1 The Arctic Ocean . . . . . 25

3.2 The Baltic Sea . . . . . 34

**4 Ionic Interactions** **39**

4.1 Ion-pairing Models . . . . . 43

4.2 Pitzer Equations . . . . . 45

4.3 Monte Carlo Simulations . . . . . 47

**5 Summary** **50**

**6 Future Outlook** **53**

# Part B: List of Publications

This thesis is based on investigations presented in the following papers, hereafter referred to by their roman numerals. The papers are appended at the end of the thesis.

**I** **Ulfsbo, A.**, Hulth, S., Anderson, L. G. (2011), pH and biogeochemical processes in the Gotland Basin of the Baltic Sea, *Marine Chemistry*, 127, 20-30, doi: 10.1016/j.marchem.2011.07.004.

**II** Abbas, Z., **Ulfsbo, A.**, Turner, D. R. (2013). Monte Carlo simulation of the dissociation constants of $CO_2$ in 0 to 1 molal sodium chloride between 0 and 25 °C, *Marine Chemistry*, 150, 1-10, doi: 10.1016/j.marchem.2013.01.002.

**III** **Ulfsbo, A.**, Cassar, N., Korhonen, M., van Heuven, S., Hoppema, M., Kattner, G., Anderson, L. G. (2014). Late summer net community production in the central Arctic Ocean using multiple approaches, *Global Biogeochemical Cycles*, submitted February 2014.

**IV** Ericson, Y., **Ulfsbo, A.**, van Heuven, S., Kattner, G., Anderson, L. G. (2014). Increasing carbon inventory of the intermediate layers of the Arctic Ocean, *Journal of Geophysical Research: Oceans*, doi: 10.1002/2013JC009514.

**V** **Ulfsbo, A.**, Kulinski, K., Anderson, L. G., Turner, D.R. (2014). Modelling organic alkalinity in the Baltic Sea using a Humic-Pitzer approach, manuscript in preparation for *Marine Chemistry.*

**VI** **Ulfsbo, A.**, Abbas, Z., Turner, D. R. (2014). Activity coefficients of a simplified seawater electrolyte at varying salinity (5-40) and temperature (0-25°C) using Monte Carlo simulations, manuscript in preparation for *Marine Chemistry.*

# Contribution Report

There are multiple authors on the papers presented here and my contribution to each of them is listed below.

**I** Responsible, together with L.A., for the planning, data evaluation and interpretation, and writing of the manuscript.

**II** Contributed to data interpretation and writing of the manuscript. Responsible for the Pitzer calculations. Z.A. did all MC simulations.

**III** Responsible for the planning, data evaluation and interpretation, and writing of the manuscript.

**IV** Contributed to sample analysis, data evaluation and interpretation, and writing of the manuscript.

**V** Responsible for the planning and writing of the manuscript together with D.T., whom developed the model. Responsible for data evaluation and interpretation.

**VI** Responsible for the planning, Pitzer calculations, interpretation and writing of the manuscript. Z.A. did all MC simulations.

# Chapter 1

# Introduction and Objectives

> "In the composition of sea-water the carbonic acid, on account of its intimate relations to life, forms an item of particular interest."
>
> John Murray, one of the naturalists of the expedition,
> *Report on the scientific results of the Voyage of H.M.S. Challenger during the years 1873-76*
> (1884)

The absorption of atmospheric carbon dioxide ($CO_2$) by seawater and subsequent equilibrium reactions within this *ionic medium* give rise to a complex chemical system, often referred to as *the marine carbonate system* (or alternatively referred to as the marine $CO_2$ system or the seawater $CO_2$-carbonate system). This system is influenced by physical, chemical, biological, and geological processes, i.e., physical and *biogeochemical processes*, in the ocean.

The marine carbonate system is a major component of the global carbon cycle and is, by virtue of its interaction with atmospheric $CO_2$, of fundamental importance to the Earth's climate. The oceanic reservoir of inorganic carbon is roughly 60 times that of the atmosphere (*Sabine et al.*, 2004). Therefore even small changes in the natural components of the marine carbon cycle have the potential to significantly feedback to the Earth's climate system (*Tanhua et al.*, 2013).

Approximately 30% of the total human emissions of $CO_2$ (anthropogenic $CO_2$) to the atmosphere is accumulating in the ocean (*Le Quéré et al.*, 2010). The uptake of $CO_2$ by the ocean changes the chemical balance of seawater through the thermodynamic equilibrium of $CO_2$ with seawater, with implications for surface ocean chemistry, physical properties, individual marine organisms, and ocean ecosystems. Dissolved $CO_2$ forms the weak carbonic acid ($H_2CO_3$) and, as $CO_2$ in seawater increases, the pH, carbonate ion ($CO_3^{2-}$), and calcium carbonate ($CaCO_3$) saturation state of seawater decreases,

while bicarbonate ($HCO_3^-$) increases. The mean pH of surface waters ranges between 7.8 and 8.4 in the open ocean, so the ocean remains mildly alkaline (pH >7) at present (*Feely et al.*, 2009). Ocean uptake of $CO_2$ results in gradual acidification of seawater in a process termed 'ocean acidification' (e.g., *Caldeira and Wickett*, 2003; *Doney et al.*, 2009). The observed decrease in ocean pH of 0.1 since the beginning of the industrial era corresponds to a ∼30% increase in the hydrogen ion concentration (*Feely et al.*, 2009). Direct measurements on ocean time-series stations in the North Atlantic and North Pacific (Figure 1.1) record decreasing pH with rates ranging from -0.0014 and -0.0024 pH units per year (*Rhein et al.*, 2013; *Bates et al.*, 2014). The largest ocean acidification influences for the environment are expected to occur in the polar regions (*Orr et al.*, 2005).

The Arctic Ocean has great potential for taking up atmospheric $CO_2$ owing to high biological production in the large ocean margin areas and the cooling of warm inflowing waters. The Arctic is widely viewed as the area on Earth most sensitive to climate changes (*Rhein et al.*, 2013), with acidification more pronounced than that of any other ocean (*Steinacher et al.*, 2009). Sea ice melt in the Arctic Ocean has increased steadily over recent decades, proceeding faster than any model prediction. It has been postulated that an ice-free condition in the Arctic Ocean basins would allow for uptake of a substantial amount of additional $CO_2$ from the atmosphere (*Bates and Mathis*, 2009), although contrasting views exist (*Cai et al.*, 2010b; *Steiner et al.*, 2013). In Paper IV, the anthropogenic $CO_2$ inventory of the subsurface waters of the central Arctic Ocean was investigated based on measurements of the marine carbonate system from research expedititions with icebreakers. In Paper III, large-scale patterns of late summer net community production in the ice covered central Arctic Ocean were estimated by different approaches, based on both discrete and underway measurements.

In marginal coastal systems, the situation is more complex. River runoff dilutes the seawater, which may or may not decrease the buffer capacity, depending on the composition of the runoff. In some areas rivers drain land rich in limestone, adding high alkalinity water to the coastal seas. Also, highly productive areas, impacted by eutrophication, could lower the oxygen content of the bottom waters in particular, thereby impacting the carbonate system through a series of redox reactions. In coastal, or estuarine waters such as the Baltic Sea, the temporal pH variability is substantial and often masks the decline from uptake of anthropogenic $CO_2$ (*Borges and Gypens*, 2010).The pH sensitivity is generally amplified by the reduced buffer capacity and the pronounced terrestrial input. As much as 30% of the ocean $CO_2$ uptake may originate from the continental shelves (*Chen and Borges*, 2009), making these areas important when considering the marine carbon cycle. In Paper I, the coupling of pH and biogeochemical processes was investigated in the deep waters of the Baltic Sea, under contrasting redox conditions. In Paper V, the contribution of weak organic protolytes (polydisperse humic substances) to the measured total alkalinity was investigated by a chemical speciation modelling approach.

Accurate knowledge of the properties of the marine carbonate system is a prerequisite for understanding the chemical forcing and consequences of key biogeochemical processes such as biological production, organic matter respiration, or uptake of anthropogenic carbon. The assessment of the marine carbonate system relies on state-of-the-art analytical methods as well as the underlying fundamental chemistry in terms of ionic interactions and equilibrium thermodynamics. A quantitative understanding of the equilibrium solution chemistry of seawater relies ultimately on a knowledge of the chemical potentials (or the activities) of all the various components that make up the solution. As the direct measurement of these quantities is an improbable task, much effort has gone into the development of empirical methods for estimating activity coefficients, i.e., the ratios between activities and concentrations. In Papers II and VI, a Monte Carlo method was used to estimate the stoichiometric dissociation constants of the carbonate system in sodium chloride solution and mean activity coefficients of a simplified seawater electrolyte of varying ionic strength (salinity) at different temperatures, respectively.

The first part of this thesis is divided into three main chapters, where the appended papers are put into context. Chaper 2 gives an introduction to the marine carbonate system, its parameters and their associated definitions and analytical procedures. Chapter 3 gives examples of biogeochemical processes affecting the marine carbonate system with emphasis on the central Arctic Ocean and the Baltic Sea. Chapter 4 introduces the concept of activities in the seawater ionic medium and different approaches for estimating the inter-related activity coefficients. A short summary of each paper is given in Chapter 5, followed by some thoughts on the future outlook in Chapter 6.

[1]BATS: http://www.bios.edu/research/projects/bats
[2]HOT: http://hahana.soest.hawaii.edu/hot/hot_jgofs.html
[3]ESTOC: http://www.eurosites.info/estoc.php
[4]MLOH: http://www.esrl.noaa.gov/gmd/ccgg/trends/

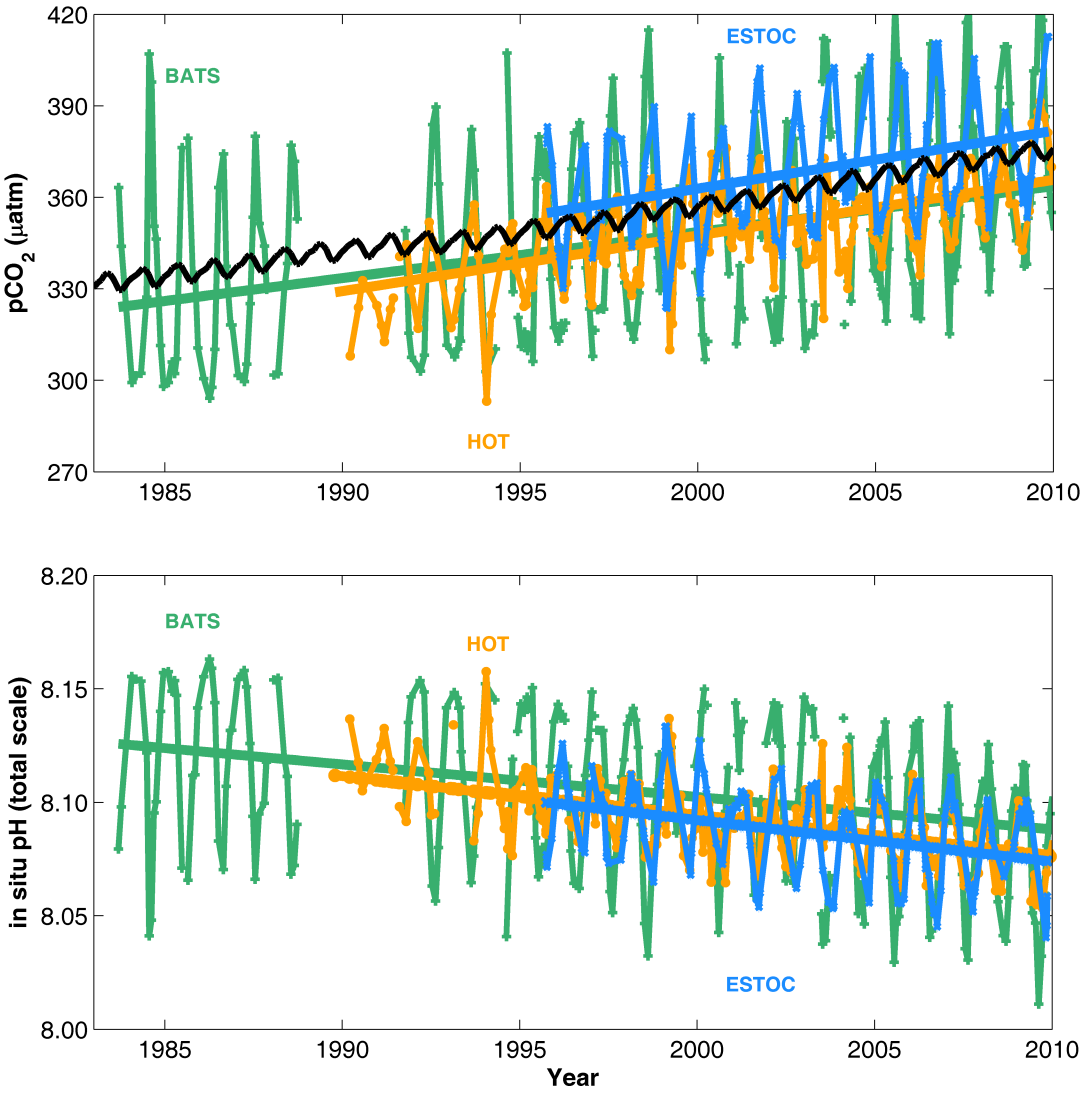


Figure 1.1: Long-term trends of surface seawater partial pressure of $CO_2$ ($pCO_2$) (top) and pH (bottom) at three subtropical ocean times series in the North Atlantic and North Pacific Ocean, including (a) Bermuda Atlantic Time-series Study[1] (BATS, 31°40'N, 64°10'W; green) from 1988 to 2010, including the nearby Hydrostation S from 1983 to 1988; (b) Hawaii Ocean Time-series[2] (HOT) at Station ALOHA (A Long-term Oligotrophic Habitat Assessment; 22°45'N, 158°00'W; orange) from 1988 to 2010 and (c) European Station for Time series in the OCean[3] (ESTOC, 29°10'N, 15°30'W; blue) from 1994 to 2010. Atmospheric $pCO_2$ (25°C, 1 atm, 100% humidity) from the Mauna Loa Observatory Hawaii[4] is shown in the top panel (black). Lines represent schematic linear fits to the data. After *Rhein et al.* (2013).

# Chapter 2

# The Marine Carbonate System

> "Die Wasserstoffzahl des Meerwassers (pH) wird, nach den Ergebnissen der neueren Untersuchungen über das Kohlensäuregleichgewicht im Meerwasser, fast ausschliesslich von der Kohlensäure und den Karbonaten des Wassers bestimmt."
>
> Kurt Buch und Stina Gripenberg, *J. Cons. int. Explor. Mer* (1932)

The assessment of the global ocean carbon cycle is obviously a task of Herculean proportions, where joint international collaborative efforts are necessary. The first comprehensive survey and collection of inorganic carbon in the open ocean was included as part of the Geochemical Ocean Sections Study (GEOSECS) program, initiated in 1969 (*Sabine et al.*, 2010). This led to several large, subsequent scientific expeditions and programs such as the Transient Tracers in the Ocean (TTO) in the early 1980s, and the World Ocean Circulation Experiment (WOCE) and Joint Global Ocean Flux Study (JGOFS), with global ocean surveys completed by the end of the 1990s (*Tanhua et al.*, 2013). Since these programs, inorganic carbon measurements along repeat hydrography sections have continued mainly within CLIVAR-$CO_2$ (Climate Variabilty program) and GO-SHIP (the Global Ocean Ship-based Hydrographic Investigations Program) (*Tanhua et al.*, 2013). Measurements are, e.g., also included in the International Study of Marine Biogeochemical Cycles of Trace Elements and their Isotopes (GEOTRACES), with the goal of generating a three-dimensional map of the concentrations of key trace elements and isotopes in the world ocean by the year 2020.

In order to understand potential effects of the ocean uptake of anthropogenic $CO_2$, ocean acidification, natural variability and feedback potential of the marine carbon cycle, the latter needs to be well constrained through direct and accurate evaluation. This was already recognized at the time of the WOCE/JGOFS $CO_2$ surveys (*Dickson*, 2010) and led to the synthesis of standard operating procedures (SOPs) in the *Handbook of Methods*

*for the Analysis of the Various Parameters of the Carbon Dioxide System in Seawater* (*DOE*, 1994). This has since been replaced by the updated *Guide to best practices for ocean $CO_2$ measurements* (*Dickson et al.*, 2007). Additionally, the *Guide to best practices for ocean acidification research and data reporting* (*Riebesell et al.*, 2010) was a result from the European Project on Ocean Acidification (EPOCA) for the growing ocean acidification scientific community. The book *$CO_2$ in seawater: Equilibrium, kinetics, isotopes* (*Zeebe and Wolf-Gladrow*, 2001) is also an important contribution and is nowadays a standard reference in marine chemistry, covering many ascpects of the marine carbonate system.

In the ocean and other natural waters, pH is largely controlled by $CO_2$ through its equilibrium with the atmosphere. In the atmosphere, $CO_2$ exhibits a single chemical form, whereas in seawater four inorganic carbon species are present: $CO_2$(g), $CO_2^*$(aq), $HCO_3^-$(aq), and $CO_3^{2-}$(aq), where

$$CO_2^*(aq) = CO_2(aq) + H_2CO_3(aq). \tag{2.1}$$

The use of the $CO_2^*$ species is, due to analytical difficulties in distinguishing $CO_2$(aq) from $H_2CO_3$(aq), defined by convention (*Dickson et al.*, 2007). When gaseous $CO_2$ dissolves and equilibrates with the large pool of dissolved $CO_2$ in seawater, the following equilibrium equations of the carbonate system hold:

$$\begin{aligned}
CO_2(g) &\longleftrightarrow CO_2(aq), && (2.2)\\
CO_2(aq) + H_2O &\longleftrightarrow H_2CO_3(aq), && (2.3)\\
H_2CO_3(aq) &\longleftrightarrow H^+(aq) + HCO_3^-(aq), && (2.4)\\
HCO_3^-(aq) &\longleftrightarrow H^+(aq) + CO_3^{2-}(aq). && (2.5)
\end{aligned}$$

The hydration reaction in (2.3) is slow and most of the $CO_2$ in seawater remains in the physically dissolved state rather than in the combined form of true carbonic acid ($H_2CO_3$(aq)). The phase state, i.e., the gas state (g) and aqueous state (aq), will principally be omitted henceforth in the thesis for simplicity and the aqueous phase (aq) should be assumed for all species if not specified explicitly. The equilibrium reactions (2.2-2.5) simplify to:

$$\begin{aligned}
CO_2^* + H_2O &\longleftrightarrow H^+ + HCO_3^- \qquad K_1 && (2.6)\\
HCO_3^- &\longleftrightarrow H^+ + CO_3^{2-} \qquad K_2 && (2.7)
\end{aligned}$$

where $K_1$ and $K_2$ are equilibrium constants (see 2.13 and 2.14). They are referred to as the first and second dissociation constants of carbonic acid, respectively. In the thermodynamic equilibrium (2.2), the $CO_2$ concentration is proportional to the partial pressure of $CO_2$ ($pCO_2$; Section 2.4), and is given by Henry's law:

$$CO_2^* = K_0 * pCO_2 \tag{2.8}$$

where $K_0$ is Henry's constant and, in this context, the solubility coefficient of $CO_2$. To account for the non-ideal behavior of $CO_2$ in the seawater ionic medium, the fugacity of $CO_2$ ($fCO_2$) is normally used (see Section 2.4). However in this work henceforth, $pCO_2$ will be used in calculations and discussions. For the description of the carbonate system in seawater, stoichiometric equilibrium constants, or stoichiometric dissociation constants, or conditional stability constants, or concentration products are used, which are related to concentrations rather than activities (Section 2.5).

The marine carbonate system can be determined from any two of the four[1] analytically quantifiable parameters, total dissolved inorganic carbon (DIC), total alkalinity (TA), $pCO_2$, and pH, together with known values of stoichiometric acid-base dissociation constants and total concentrations. Simplified, the marine carbonate system can be decribed by three mass balance equations (2.9-2.11) and five conditional stability constants (2.12-2.16):

$$\mathrm{TA} = [\mathrm{HCO_3^-}] + 2[\mathrm{CO_3^{2-}}] + [\mathrm{B(OH)_4^-}] + [\mathrm{OH^-}] - [\mathrm{H^+}] \quad (2.9)$$

$$\mathrm{DIC} = [\mathrm{CO_2^*}] + [\mathrm{HCO_3^-}] + [\mathrm{CO_3^{2-}}] \quad (2.10)$$

$$\mathrm{TB} = [\mathrm{B(OH)_3}] + [\mathrm{B(OH)_4^-}] \quad (2.11)$$

$$\mathrm{K_0} = [\mathrm{CO_2^*}]/pCO_2 \quad (2.12)$$

$$\mathrm{K_1^*} = \{\mathrm{H^+}\}[\mathrm{HCO_3^-}]/[\mathrm{CO_2^*}] \quad (2.13)$$

$$\mathrm{K_2^*} = \{\mathrm{H^+}\}[\mathrm{CO_3^{2-}}]/[\mathrm{HCO_3^-}] \quad (2.14)$$

$$\mathrm{K_B^*} = \{\mathrm{H^+}\}[\mathrm{B(OH)_4^-}]/[\mathrm{B(OH)_3}] \quad (2.15)$$

$$\mathrm{K_W^*} = \{\mathrm{H^+}\}[\mathrm{OH^-}] \quad (2.16)$$

where $\{H^+\}$ indicates the dependency of pH scale in use and not the activity of the hydrogen ion. See Section 2.2 for the full definition of TA and Section 2.3 for the concept of pH scales. These eight equations have ten unkowns, provided all stability constants and the total borate concentrations are known, and the carbonate system is thus solvable if two of the four analytical parameters TA, DIC, $pCO_2$, or pH are known.

Performing and interpreting $CO_2$-related measurements in seawater were fundamental parts of this thesis (Papers III, IV, and V) and in the following sections, the different parameters of the carbonate system are described by their definitions and associated analytical methods. For a more thorough description of the carbonate system chemistry and analytical methods, the reader is referred to *Zeebe and Wolf-Gladrow* (2001), *Dickson et al.* (2007), and *Grasshoff et al.* (1999).

[1] Analytical methods for direct determination of $CO_3^{2-}$(aq) were recently developed (*Byrne and Yao*, 2008; *Martz et al.*, 2009; *Easley et al.*, 2012). Although not yet implemented in the SOPs, the methods constitute important complements for studying the fundamental chemistry of the marine carbonate system and its internal consistency, as well as the saturation state of metal carbonates.

## 2.1 Total Dissolved Inorganic Carbon

DIC constitutes the basis of the carbonate system in seawater and is defined as the sum of the concentrations of aqueous $CO_2^*$, bicarbonate ion and carbonate ion

$$\mathrm{DIC} = [CO_2^*] + [HCO_3^-] + [CO_3^{2-}] \tag{2.17}$$

where the brackets represent concentrations, preferably in $\mu$mol kg$^{-1}$ (*Dyrssen and Sillén*, 1967). It should be noted that other abbreviations of DIC often appear in the literature (e.g., $TCO_2$, $\Sigma CO_2$, $C_T$) and that their definition or meaning may differ slightly from the analytical expression (Equation 2.17). The chemical speciation of the species of DIC is governed by temperature, salinity, pressure, pH, and TA. At typical seawater conditions (S = 35, T = 25°C, pH = 8.1, DIC = 2000 $\mu$mol kg$^{-1}$), the inorganic species are distributed as $[CO_2^*] : [HCO_3^-] : [CO_3^{2-}] \simeq 0.6\% : 90\% : 9.4\%$, which means that bicarbonate dominates, followed by carbonate. Due to uptake of anthropogenic $CO_2$ ($CO_2^{\mathrm{ant}}$) from the atmosphere, the measured DIC of a seawater sample is the sum of the natural occuring amount ($C_{\mathrm{nat}}$) that would be present irrespective of human emissions, and the anthropogenic amount ($C_{\mathrm{ant}}$) taken up by the ocean from the atmosphere. Within DIC, the fraction $C_{\mathrm{ant}}$ cannot be analytically distinguished from $C_{\mathrm{nat}}$ (Section 3.1).

### Analytical methods: DIC

DIC is typically determined by the acidification of a known mass of sample to a pH where all the inorganic carbon species are converted to $CO_2$. The $CO_2$ is then extracted by a carrier gas (typically $N_2$ or He), dried, and quantified either by coulometry (*Johnson et al.*, 1985, 1987, 1993), manometry (*Dickson*, 2010), or by non-dispersive infrared (NDIR) analysis (*O'Sullivan and Millero*, 1998; *Kaltin et al.*, 2005). Systems appropriate for field measurements of DIC, using liquid core waveguides and low power spectrophotometers (*Byrne et al.*, 2002; *Wang et al.*, 2007; *Liu et al.*, 2013), as well as continuous surface measurements by isotope dilution ($^{13}$C-labeled $NaHCO_3$) and cavity ring-down spectrometry (*Huang et al.*, 2013), have also been developed.

In this work (Papers III-IV), DIC was quantified by coulometric titration according to *Johnson et al.* (1985) using a modified SOMMA (Single-Operator Multiparameter Metabolic Analyzer) system; MIDSOMMA (Much sImpler Designed than SOMMA; *Mintrop* (2005)), a predecessor to the VINDTA 3C system (Versatile INstrument for the Determination of Total Alkalinity, designed and built by Dr. Ludger Mintrop, MARIANDA, Kiel, Germany), which is a commonly used shipboard instrumentation for determining DIC and TA. The MIDSOMMA used in this work comprise of a seawater sample extraction unit, a $CO_2$ coulometer (Model 5012, UIC Inc., Joliet, IL, USA) and an automated burette (Metrohm 415, Herisau, Switzerland). The instrument is controlled by a PC running LabView software (National Instruments Inc., Austin, TX, USA).

An accurately known volume of sample (~15 ml) is dispensed from a thermostated glass pipette into a glass 'stripper', which already contains ~0.5 ml of ~10% phosphoric acid ($H_3PO_4$). The acidified sample is rapidly and quantitatively purged of $CO_2$ by $N_2$ gas (flow rate ~150 ml $min^{-1}$). The $CO_2$ gas is carried through a condenser (~4°C) to remove water vapor. The $N_2$-$CO_2$ gas stream is subsequently introduced into ~100 ml cathode solution (platinum electrode) of the titration cell, which is separated from the anode solution (silver electrode) by a ceramic frit. The cathode solution contains dimethylsulfoxide (DMSO), ethanolamine and thymolphthalein indicator. The $CO_2$ reacts quantitatively with the ethanolamine to form hydroxyethylcarbamic acid:

$$CO_2 + HO(CH_2)_2NH_2 \longrightarrow HO(CH_2)_2NHCOOH \tag{2.18}$$

The weak acid formed in (2.18) partly dissociates, effectively decreasing the pH of the solution:

$$HO(CH_2)_2NHCOOH \longleftrightarrow HO(CH_2)_2NHCOO^- + H^+ \tag{2.19}$$

This results in a fading of the deep blue color of the thymolphtalein indicator, which is photometrically detected by the coulometric setup, monitoring the transmittance of the solution. Subsequently, the acid is coulometrically titrated by hydroxide ions ($OH^-$) generated at the cathode (2.20) that gradually restore the pH of the reagent solution (2.21):

$$H_2O + e^- \longleftrightarrow OH^- + ½H_2 \tag{2.20}$$

$$HO(CH_2)_2NHCOOH + OH^- \longleftrightarrow HO(CH_2)_2NHCOO^- + H_2O \tag{2.21}$$

In the anode solution (saturated potassium iodide (KI) DMSO solution), the silver electrode is oxidized, producing electrons and silver ions (2.22), which subsequently form a complex with the iodide ions (2.23):

$$Ag(s) \longrightarrow Ag^+ + e^- \tag{2.22}$$

$$Ag^+ + 2I^- \longrightarrow AgI_2^- \tag{2.23}$$

Reactions (2.18-2.23) can be summarized by the overall reaction (*Johnson et al.*, 1985):

$$Ag(s) + 2I^- + CO_2 + HO(CH_2)_2NH_2 \longrightarrow AgI_2^- + ½H_2 + HO(CH_2)_2NHCOO^- \tag{2.24}$$

The titration current is integrated over the time required to restore the initial transmission of the reagent solution. This integral of the current, i.e., the charge in coulombs, is linearly related to the amount of $CO_2$ absorbed by the cathode solution, after subtraction of the integrated background current of the coulometer (the blank).

The accuracy is set by routine analysis of Certified Reference Materials (CRMs, provided by A.G. Dickson, Scripps Institution of Oceanography, La Jolla, CA, USA) and

the precision is given by replicate analysis of samples. The precision or uncertainty of this state-of-the-art coulometric method is often reported in the range of $\pm$1-2 $\mu$mol kg$^{-1}$ (e.g., *Johnson et al.*, 1993). This is the best case scenario when performing analysis in the lab, although *Dickson* (2010) states uncertainties of 2-3 $\mu$mol kg$^{-1}$, provided the analysis has been 'performed by an experienced laboratory with well-trained analysts, and with a good quality assurance program in place'. It is not uncommon to find similar uncertainties reported in the literature for shipboard work. However, shipboard analysis is more sensitive to the environmental conditions (e.g., laboratory temperature) and poorer quality can occasionally be expected (cf. Paper IV).

## 2.2 Total Alkalinity

Total alkalinity or titration alkalinity, often denoted TA or $A_T$, is a non-trivial concept of many different definitions and applications (e.g., *Peng et al.*, 1987; *Stumm and Morgan*, 1996; *Morel and Hering*, 1993; *Wolf-Gladrow et al.*, 2007; *Dickson*, 1981), but may essentially be understood to represent the buffer capacity or charge balance of seawater. It is of direct importance to the solution chemistry of DIC and the determination of the marine carbonate system. The currently most precise definition of TA was given by *Dickson* (1981): *"The total alkalinity of a natural water is thus defined as the number of moles of hydrogen ion equivalent to the excess of proton acceptors (bases formed from weak acids with a dissociation constant $K \leq 10^{-4.5}$, at 25°C and zero ionic strength) over proton donors (acids with $K > 10^{-4.5}$) in one kilogram of sample"*, and the following expression is derived for the acid-base system in seawater:

$$\begin{aligned} \mathrm{TA} &= [\mathrm{HCO_3^-}] + 2[\mathrm{CO_3^{2-}}] + [\mathrm{B(OH)_4^-}] + [\mathrm{OH^-}] + [\mathrm{HPO_4^{2-}}] \\ &+ 2[\mathrm{PO_4^{3-}}] + [\mathrm{SiO(OH)_3^-}] + [\mathrm{NH_3}] + [\mathrm{HS^-}] + ... \\ &- [\mathrm{H^+}]_\mathrm{F} - [\mathrm{HSO_4^-}] - [\mathrm{HF}] - [\mathrm{H_3PO_4}] - ... \end{aligned} \tag{2.25}$$

where the ellipses represent unidentified or negligible dilute weak acid-base species. $[\mathrm{H^+}]_\mathrm{F}$ is the free concentration of hydrogen ion (see Section 2.3). The small contributions (usually $< 1$ $\mu$mol kg$^{-1}$) from hydroxide, phosphate, silicate and other bases can often be ignored in the open ocean (*Anderson et al.*, 1999), whereas in regions, such as the Baltic Sea (Paper I and V), of high nutrient concetrations (e.g., phosphate, ammonia, and phosphates) or reduced compounds (sulfides), the full definition should be considered (*Dickson*, 1981). From (2.25), TA is defined as a measure of the proton deficit in a solution with respect to a defined zero level of protons. For the carbonate species, $CO_2$ is chosen as the zero level of protons by convention (*Wolf-Gladrow et al.*, 2007). $HCO_3^-$ can accept one proton (level -1) with respect to $CO_2$, whereas $CO_3^{2-}$ can accept two protons (level -2). The choice of a particular chemical species defines the zero level of protons for a single set of related acid-base species. However, by specifying a single

pK value, $pK_{zlp}$, which applies for all acid-base systems as a dividing point, the chemical species that dominates at pH = $pK_{zlp}$, defines the zero level of protons. Acids with $pK \leq pK_{zlp}$ are proton donors and, consequently, bases formed from weak acids with $pK > pK_{zlp}$ are proton acceptors. Conventionally, the choice of $pK_{zlp}$ = 4.5 by *Dickson* (1981) is used and it was chosen to correspond roughly to the pH of the alkalinity titration end-point. The $pK_{zlp}$ = 4.5 is less than the $pK_1$ of the carbonate system and $CO_2$ is thus the zero level of protons for carbonic acid. Furthermore, by choosing $pK_{zlp}$ that is higher than those of hydrogen sulfate (pK = 2) and hydrogen fluoride (pK = 3.2), they do not contribute to TA (*Wolf-Gladrow et al.*, 2007). The balance between proton acceptors and proton donors are denoted by the proton condition (2.26). It defines the pH at which proton donors exactly balance the proton acceptors. The proton condition is also referred to as the second equivalence point, determined from titration data:

$$\begin{aligned}[H^+]_F + [HSO_4^-] + [HF] + [H_3PO_4] &= [HCO_3^-] + 2[CO_3^{2-}] + [B(OH)_4^-] + [OH^-] + [HPO_4^{2-}] \\ &+ 2[PO_4^{3-}] + [SiO(OH)_3^-] + [NH_3] + [HS^-] \end{aligned} \quad (2.26)$$

where the proton donors appear on the left-hand side and the proton acceptors on the right-hand side.

Becuase the oceans are electrically neutral, the sum of dissolved charged constituents needs to be charge balanced. Since the sum of the major cations (e.g., $Na^+$, $K^+$, $Mg^{2+}$, $Ca^{2+}$) is not exactly balanced by the major anions (e.g., $Cl^-$, $SO_4^{2-}$, $Br^-$), TA defined above must be identical to the charge imbalance between these major cations and anions. Therefore, one may encounter TA to be alternatively defined as:

$$\begin{aligned}TA &= [Na^+] + 2[Mg^{2+}] + 2[Ca^{2+}] + [K^+] + 2[Sr^{2+}] + ... \\ &- [Cl^-] - 2[SO_4^{2-}] - [Br^-] - ... \end{aligned} \quad (2.27)$$

*Wolf-Gladrow et al.* (2007) presented the *explicit conservative equation for total alkalinity* ($TA_{ec}$; Eq. (2.28), restating the two above definitions using only conservative terms, i.e., terms that are not affected by variability of temperature, pressure or mixing processes. As noted by *Wolf-Gladrow et al.* (2007), this is not a new definition of TA, but rather an expression that is different from but equivalent to expressions (2.25 and 2.27).

$$\begin{aligned}TA_{ec} &= [Na^+] + 2[Mg^{2+}] + 2[Ca^{2+}] + [K^+] + 2[Sr^{2+}] + ... \\ &- [Cl^-] - 2[SO_4^{2-}] - [Br^-] - ... \\ &- TPO_4 + TNH_3 - 2TSO_4 - THF - THNO_2 \end{aligned} \quad (2.28)$$

in which,

$$\begin{aligned} \mathrm{TPO_4} &= [\mathrm{H_3PO_4}] + [\mathrm{H_2PO_4^-}] + [\mathrm{HPO_4^{2-}}] + [\mathrm{PO_4^{3-}}] \\ \mathrm{TNH_3} &= [\mathrm{NH_3}] + [\mathrm{NH_4^+}] \\ \mathrm{TSO_4} &= [\mathrm{SO_4^{2-}}] + [\mathrm{HSO_4^-}] \\ \mathrm{THF} &= [\mathrm{F^-}] + [\mathrm{HF}] \\ \mathrm{THNO_2} &= [\mathrm{NO_2^-}] + [\mathrm{HNO_2}] \end{aligned}$$

This expression is useful for the interpretation of the effect of biogeochemical processes on alkalinity compared to the expression (2.25). For example, TA does not change as a result of air-sea exchange of $CO_2$. From (2.25), it is not obvious that the sum of the carbonate species stays constant during invasion of $CO_2$ (although not included in the definition), which decreases pH. However, invasion or release of $CO_2$ does not affect any concentration in $TA_{ec}$ and TA thus stays constant.

### Analytical methods: TA

There are various methods for measuring TA in seawater (see *Byrne*, 2014, and references therein). The most frequently used method for measuring TA in seawater is potentiometric titration, which involves stepwise additions of small aliquots of dilute strong acid to a sample, observing the consequent change in the electromotive force (emf; potential) of free protons, as measured by an electrochemical cell (a 'pH electrode'). Simplified, first, added $H^+$ are neutralized by the conversion of $CO_3^{2-}$ to $HCO_3^-$ and as a result the measured decrease in pH (i.e., increase of $[H^+]$) as inferred from the measured emf is much less than the actual added amount of $H^+$. A rapid drop in pH is observed at the point where all $CO_3^{2-}$ has been converted to $HCO_3^-$, the first inflection point on the titration curve, which is roughly equal to the first equivalence point. Next, upon further additions, the added protons are neutralized by the conversion of $HCO_3^-$ to $CO_2^*$ until all $HCO_3^-$ is converted, at which point the pH again drops rapidly, the second inflection point. The total amount of added $H^+$ is now equal to $[HCO_3^-]$ + $2[CO_3^{2-}]$ as initially present. As previously stated, this is somewhat simplified since other weak acid-base species are present in seawater (Eq. 2.25) and different methods are used to evaluate the final TA value from potentiometric titration data.

Various titration techniques are in use, with varying strengths and drawbacks with respect to precision, accuracy, throughput, automation, sample size requirement, or whether it is a closed-cell or open-cell titration (e.g., *Dickson et al.*, 2007; *Johansson and Wedborg*, 1982). In this work (Papers III-IV), TA was determined by open-cell potentiometric titration with dilute acid (0.05 + 0.65 mol $l^{-1}$ HCl and NaCl, respectively), according to the setup of *Haraldsson et al.* (1997) and their non-modified Gran evaulation approach

(see below). The sample is dispensed into a semi-open acrylic titration cell from a thermostated pipette of known volume (~40 ml), after which it is constantly stirred. During titration, the emf of free protons is measured by an electrochemical cell consisting of a combination Ag/AgCl-pH glass electrode(s) (Orion 9102AP, Thermo Fischer Scientific, Waltham, MA, US), which was quality tested by its Nernstian response. The instrument setup is semi-automatic and is controlled by a PC running an executable, with code written in PASCAL (by Dr. Conny Haraldsson; *Haraldsson et al.* (1997)).

The accuracy is, as for DIC, set by routine analysis of Certified Reference Materials (CRMs, provided by A.G. Dickson, Scripps Institution of Oceanography, La Jolla, CA, US) and the precision is given by replicate analysis of samples. The precision is typically better than $\pm$ 1-2 $\mu$mol kg$^{-1}$, which is in accordance to the expected performance, when implementing standard operating procedures (*Dickson et al.*, 2007). Because shipboard titrations require volumetric metering of a strong acid, shipboard TA precision is typically worse than the precision of onshore TA measurements.

### Evaluation of raw analytical titration data

*Dyrssen* (1965) first applied the *Gran function* method to calculate TA and DIC of seawater samples from potentiometric data. Gran functions (*Gran*, 1952, 1981) are used to estimate $v_1$ and $v_2$; the volumes of acid added to reach the carbonate/bicarbonate and bicarbonate/carbonic acid equivalence points. The TA can be determined directly from $v_2$, while DIC corresponds to the difference between $v_2$ and $v_1$. The simple Gran function method assumes that for $v>v_2$, all $H^+$ added forms free hydrogen ions. The mass balance condition for $H^+$ is then:

$$(v_0 + v) = t(v - v_2) \qquad \text{for} \qquad (v > v_2) \tag{2.29}$$

where $v_0$ is the initial sample volume and $t$ the concentration of the titrant. The measured emf (E) for $v>v_2$ is proportional to the excess of hydrogen ions and via the Nernst equation the Gran function is given by:

$$F2 = (v_0)10^{(E/59.16)} \qquad \propto (v - v_2) \tag{2.30}$$

where 59.16 (mV) is the Nernst slope at 25°C (cf. Paper V). When plotting F2 against v and if the above assumptions are true, F2 is linear and intersects the x-axis at the equivalence volume. This method ignores the contribution of non-carbonate species. Furthermore, only ranges of data points where the Gran function is linear can be used, while points near the inflection points are omitted as a result of non-linear response. *Haraldsson et al.* (1997) used a titration procedure with a five-point non-modified Gran function, positioning the data points in such a way to minimize the contribution of side reaction with sulfate and fluoride.

Remembering the proton condition in Equation (2.26) for the second equivalence point, one recognizes that the initial analytical total concentration of hydrogen ion ($H_{TOT}$) in the solution is the negative of the alkalinity (i.e., $H_{TOT} = -TA$). $H_{TOT}$ can, at any point in the titration, be described by the mass ($m$) and concentration of the acid ($C$), the initial total amount of hydrogen ion ($m_0$TA) and the total sample mass ($m_0 + m$):

$$\begin{aligned}\frac{mC - m_0\mathrm{TA}}{m_0 + m} &= [\mathrm{H}^+]_\mathrm{F} + [\mathrm{HSO}_4^-] + [\mathrm{HF}] + [\mathrm{H_3PO_4}] - [\mathrm{HCO}_3^-] - 2[\mathrm{CO}_3^{2-}] - [\mathrm{B(OH)}_4^-] - [\mathrm{OH}^-] \\ &- [\mathrm{HPO}_4^{2-}] - 2[\mathrm{PO}_4^{3-}] - [\mathrm{SiO(OH)}_3^-] - [\mathrm{NH_3}] - [\mathrm{HS}^-] \end{aligned} \quad (2.31)$$

This equation is the basis for the two most common methods used to estimate TA (and DIC) from potentiometric titration data. These are (i) the modified Gran function (F2') (*Hansson and Jagner*, 1973; *Grasshoff et al.*, 1999) where Eq. (2.31) is rearranged to a linear form and then fitted iteratively by least-squares and (ii) the use of a non-linear least-squares approach that fits a model curve to the titration curve based on the experimental parameters acid volume (*Johansson and Wedborg*, 1982) or the emf (*Dickson*, 1981; *Dickson et al.*, 2007). In the latter approach, Equation (2.32) is used to define a vector of residuals. The sum-of-squares of these residuales are minimized by adjusting the four parameters: $f$, TA, DIC, and $K_1$:

$$\begin{aligned}\mathrm{TA} &- \mathrm{DIC}\left(\frac{K_1 f[\mathrm{H}'] + 2K_1K_2}{(f[\mathrm{H}'])^2 + K_1 f[\mathrm{H}'] + K_1K_2}\right) - \mathrm{T_B}\left(\frac{1}{1 + (f[\mathrm{H}'])/K_\mathrm{B}}\right) \\ &- \mathrm{T_P}\left(\frac{K_{1\mathrm{P}}K_{2\mathrm{P}} f[\mathrm{H}'] + 2K_{1\mathrm{P}}K_{2\mathrm{P}}K_{3\mathrm{P}} - (f[\mathrm{H}'])^3}{(f[\mathrm{H}'])^3 + K_{1\mathrm{P}}(f[\mathrm{H}'])^2 + K_{1\mathrm{P}}K_{2\mathrm{P}}(f[\mathrm{H}']) + K_{1\mathrm{P}}K_{2\mathrm{P}}K_{3\mathrm{P}}}\right) \\ &- \mathrm{T_{Si}}\left(\frac{1}{1 + (f[\mathrm{H}'])/K_\mathrm{Si}}\right) - \mathrm{T_{NH_3}}\left(\frac{1}{1 + (f[\mathrm{H}'])/K_{\mathrm{NH_3}}}\right) \\ &- \mathrm{T_{H_2S}}\left(\frac{1}{1 + (f[\mathrm{H}'])/K_{\mathrm{H_2S}}}\right) - \mathrm{T_S}\left(\frac{1}{1 + K_\mathrm{S}Z/(f[\mathrm{H}'])}\right) \\ &- \mathrm{T_F}\left(\frac{1}{1 + K_\mathrm{F}/(f[\mathrm{H}'])}\right) + \left(\frac{m_0 + m}{m_0}\right)\left(\frac{f[\mathrm{H}']}{Z} - \frac{K_\mathrm{w}}{f[\mathrm{H}']}\right) - \frac{m}{m_0}C = 0 \end{aligned} \quad (2.32)$$

where $f = [\mathrm{H}^+]/[\mathrm{H}']$ is a multiplier related to the initial estimates of $\mathrm{E}^\circ$, and $[\mathrm{H}']$ is computed from an initial estimate of $\mathrm{E}^\circ$ via the Nernst equation. The fitting routine thus adjusts $f$, rather than adjusting the value of $\mathrm{E}^\circ$ directly. A variety of software routines are currently in use by the many research groups. Although most routines are based on the same thermodynamic considerations and comparable mathematical methods, subtle differences exist, mostly depending on the choice of dissociation constants for the non-abundant ions. The development of a well-documented, flexible, multiplatform routine for the calculation of TA from titrations results would be a significant benefit to the community (*van Heuven*, 2013).

Since these methods are based on the 'standard' chemical model of Equation (2.25), it is assumed that the full acid-base system of the seawater sample analyzed is known, as

well as the total concentrations, either measured or derived from salinity relationships, and dissociation constants needed for the determination of the acid-base system. This has shown to be an issue in, e.g., coastal waters rich in dissolved organic matter, which include weak organic acids (see Chapter 3.2 and Paper V for further discussion). For example, humic substances show a continuum of pK values in the pH range 2 to 10. Inclusion of humic substances would therefore invalidate the assumption behind equation (2.25), that no proton exchange reactions are occurring in the region of the titration endpoint at pH $\approx 4.5$ (see Paper V).

## 2.3 pH

pH is an important property of seawater because it affects chemical and biochemical properties such as chemical reactions, equilibrium conditions and biological toxicity and availability of nutrients (*Marion et al.*, 2011). More than forty elements in the periodic table, found in seawater, are strongly influenced by pH with respect to hydrolyzed species or carbonate complexes (*Byrne*, 2002). In fact, pH controls such a variety of processes that pH is referred to as the *master* variable for physical and biological processes in the ocean (e.g., *Clayton et al.*, 1995; *Millero*, 1986). Despite the intense historic and current research in pH of seawater, a universally accepted definition of pH for the seawater ionic medium does not exist.

In dilute solutions, pH is defined as a function of the hydrogen ion activity (*Bates*, 1948; *Covington et al.*, 1985; *Buck et al.*, 2002), where the activity of an ion is the effective ion concentration, i.e., the concentration corrected for non-ideal behavior of the ion in the presence of other charged particles (see Chapter 4).

$$\mathrm{pH} = -\log(a_{\mathrm{H}}) = -\log\left(\frac{m_{\mathrm{H}}\gamma_{\mathrm{H}}}{m^{\circ}}\right) \tag{2.33}$$

Here $a_{\mathrm{H}}$ is the activity, $\gamma_{\mathrm{H}}$ is the molal activity coefficient at the molal concentration of proton ($m_{\mathrm{H}}$) in solution, and $m^{\circ}$ is the standard molality (1 mol kg$^{-1}$-$H_2O$). The activity of a single ion is however immeasurable since a single ion cannot be varied independently in solution because electroneutrality is required. Instead, the International Union of Pure and Applied Chemistry (IUPAC) established an operational definition, the NBS[1] pH scale ($\mathrm{pH_{NBS}}$ or $\mathrm{pH_{IUPAC}}$). This scale is defined by a series of standard buffer solutions with assigned pH values close to the best estimates of $-\log(a_{\mathrm{H}})$, based on a conventional division of salt activity, where the activity coefficient $\gamma_{\mathrm{H}}$ approaches unity when $m_{\mathrm{H}}$ approaches zero in pure water. Pure water buffers are, however, only valid in low ionic media, and pH on the NBS scale is restricted to solutions where the ionic

[1]NBS: National Bureau of Standards), now NIST: National Institute of Standards and Technology

strength is $< 0.1$ mol kg$^{-1}$ (salinity ~5). At present, the NBS scale has mainly been replaced by other pH scales proposed for use in seawater, based on concentration scales (cf. Paper I). These are the free pH scale ($pH_F$), the total (or Hansson) pH scale ($pH_T$), and the seawater pH scale ($pH_{SWS}$), defined by (*Waters and Millero*, 2013):

$$pH_F = -\log\left(\frac{m_{H_F}}{m^\circ}\right) \tag{2.34}$$

$$pH_T \approx -\log\left(\frac{m_{H_F} + m_{HSO_4}}{m^\circ}\right) \tag{2.35}$$

$$pH_{SWS} \approx -\log\left(\frac{m_{H_F} + m_{HSO_4} + m_{HF}}{m^\circ}\right) \tag{2.36}$$

where the total (2.35) and seawater (2.36) scales are alternatively given by:

$$pH_T = pH_F - \log\left(\frac{1 + m_{SO_4}/K^*_{HSO_4}}{m^\circ}\right) \tag{2.37}$$

$$pH_{SWS} = pH_F - \log\left(\frac{1 + m_{SO_4}/K^*_{HSO_4} + m_F/K^*_{HF}}{m^\circ}\right) \tag{2.38}$$

Here $K^*_{HSO_4}$ and $K^*_{HF}$ are the stoichiometric dissociation constants for the species $HSO_4^-$ and HF, and $m_{SO_4}$ and $m_F$ are the total molal concentrations of $SO_4^{2-}$ and $F^-$ in solution. Conversion between the scales thus relies on $K^*_{HSO_4}$ (and $K^*_{HF}$), which have been determined (*Dickson*, 1990), although it is difficult to do it accurately in seawater (*Dickson*, 1984). Efforts are now being made at NIST for determining new accurate values of $K^*_{HSO_4}$ in seawater. The difference between the total and seawater scales is rather small (~0.01 pH units) because of the smaller concentration of HF than of $HSO_4^-$ in seawater. In contrast, there is a large difference between the free scale and the other two scales (~0.12 pH units) and it is thus of utmost importance to define and report which pH scale that is being used (*Zeebe and Wolf-Gladrow*, 2001). Still, after 30 years of intense research on pH in seawater by the marine chemistry community, I stand humble before the statement by *Dickson* (1984); "The field of pH scales ... in sea water is one of the more confused areas of marine chemistry."

### Analytical methods: pH

Many different analytical methods have been developed for pH measurements in seawater using, e.g., potentiometry (*Dickson et al.*, 2007; *Martz et al.*, 2010), spectrophotometry (*Clayton and Byrne*, 1993; *Dickson et al.*, 2007; *Carter et al.*, 2013), fluorometry (*Hakonen et al.*, 2013), and photometry (*Yang et al.*, 2014). Despite the lack of a standard definition, the pH of seawater is traceable to the emf of HCl in artificial seawater

solutions including the buffer 2-amino-2-hydroxymethyl-1,3-propanediol (Tris) (*Hansson*, 1973; *Pratt*, 2014), measured using reference hydrogen and silver-silver chloride electrodes (*Khoo et al.*, 1977; *Dickson*, 1990; *Campbell et al.*, 1993). As the pH of real seawater solutions cannot be directly measured with a hydrogen electrode, due to interference caused by interactions between $F^-$ and $Br^-$ with $Ag^+$ of the reference electrode, the artificial seawater Tris buffer solutions (not including $F^-$ or $Br^-$) are used as standards for the standard operating procedures of potentiometric and spectroscopic determination of pH in seawater (*Waters*, 2012).

In this work (Papers III-IV), pH was determined spectrophotometrically (Agilent 8453) using the sulfonephthalein dye, *m*-cresol purple (mCP), as colorimetric indicator (*Clayton and Byrne*, 1993). The indicator exists as three acid-base species, $H_2I$, $HI^-$, $I^{2-}$, each having a unique color and molar absorptivity. In solutions with pH typical of seawater, the reaction of interest is the second dissociation:

$$HI^- \longleftrightarrow I^{2-} + H^+ \tag{2.39}$$

The ratio of the deprotonated and protonated species are related to the wavelength absorbance ratio ($R$) and the molar absorptivity ($\varepsilon_i$) ratios ($e_i$):

$$\frac{I^{2-}}{HI^-} = \frac{R - e_1}{e_2 - Re_3} \tag{2.40}$$

where $R$ is the ratio of absorbance at the wavelength 578 nm and 434 nm, and $e_1$, $e_2$, $e_3$ are mCP molar absorptivity ratios equal to $e_1 =_{578} \varepsilon_{HI}/_{434}\varepsilon_{HI}$, $e_2 =_{578} \varepsilon_I/_{434}\varepsilon_{HI}$, $e_3 =_{434} \varepsilon_I/_{434}\varepsilon_{HI}$ at the specified wavelengths. The pH on the total scale is calculated as:

$$pH_T = pK_2 + \log\left(\frac{R - e_1}{e_2 - Re_3}\right) \tag{2.41}$$

where $pK_2$ is on the total scale and is a function of temperature and salinity (*Clayton and Byrne*, 1993). Physical-chemical characterizations have been made of other colorimetric indicators where, in addition to mCP, thymol blue is suitable for typical pH of seawater (*Zhang and Byrne*, 1996), cresol red is suitable for more acidic seawater (*Patsavas et al.*, 2013a), and bromocresol purple and phenol red are applicable in determining freshwater pH (*Yao and Byrne*, 2001).

The current setup is based on the absorption ratio of the indicator at wavelengths 434, 578, and 730 nm (background correction) using a 1-cm flow cuvette. Each run consists of three steps; *i)* rinsing of tubing and cuvette with sample (5 ml) *ii)* sample blank (25 mL) and *iii)* sample run (20 ml) including indicator (0.5 ml). The sample is pumped and mixed using a Kloehn pump. Sample temperature is measured after the cuvette. The magnitude of the perturbation of seawater pH caused by the addition of indicator

solution is calculated and corrected for using the method described in *Chierici et al.* (1999). The instrument is controlled by a PC running a LabView program (*Fransson et al.*, 2013).

The overall precision from duplicate sample analysis was ±0.0004 pH units within this work, similar to previous demonstrations (*Liu et al.*, 2011; *Clayton and Byrne*, 1993). The accuracy is mainly set by the accuracy in the temperature measurements and the determination of the equilibrium constants of the indicator, and has been reported to be of the order of ±0.002 units (*Dickson*, 1993). Recently, it has been shown that the bulk mCP indicators contain impurities, which can significantly affect the accuracy depending on brand and batch (*Liu et al.*, 2011; *Patsavas et al.*, 2013b). Unfortunately, non-purified mCP was used in this work. Purified indicators will, however, be implemented in future work.

## 2.4 The Partial Pressure or Fugacity of $CO_2$

According to Dalton's law, the total pressure of an ideal gas mixture is equal to the sum of the partial pressures of all component gases (*Körtzinger*, 1999; *Zeebe and Wolf-Gladrow*, 2001). The partial pressure of component $i$ is defined as the product of its mole fraction $x_i$ and the total pressure $p$ of a gas mixture containing $k$ components:

$$p_i = px_i = p\frac{n_i}{\sum_{j=1}^{k} n_j} \tag{2.42}$$

where $n_i$ is the number of moles of component $i$. The atmospheric $CO_2$ content is commonly reported as the mole fraction in dry air, $x\mathrm{CO_2}$, since the partial pressure of $CO_2$ ($p\mathrm{CO_2}$) depends on the total pressure and the water vapor pressure. The $p\mathrm{CO_2}$ assigned a seawater sample more accurately denotes the partial pressure in a gas phase that is in equilibrium with the sample. The air equilibrated with the seawater is assumed to be at 100% humidity and the $p\mathrm{CO_2}$ is related to the mole fraction by:

$$p\mathrm{CO_2} = x\mathrm{CO_2}(p - p\mathrm{H_2O}) \tag{2.43}$$

where $p\mathrm{H_2O}$ (atm) is the saturation vapor pressure of water (*Weiss and Price*, 1980). In dry air and at 1 atm total pressure, the $p\mathrm{CO_2}$ thus eqauls the $x\mathrm{CO_2}$. Partial pressure is, however, a concept for ideal gases. Since $CO_2$ is a non-ideal, or real gas, it is more appropriate to use the fugacity, which corrects for non-ideal behavior (see Chapter 4). The fugacity ($\mu$atm) can be calculated from its partial pressure (*Körtzinger*, 1999; *Zeebe and Wolf-Gladrow*, 2001):

$$f\mathrm{CO_2} = p\mathrm{CO_2}\exp\left(p\frac{B+2\delta}{RT}\right) \tag{2.44}$$

where $R$ is the gas constant, $T$ is the absolute temperature, and $B$ and $\delta$ are the virial coefficients of $CO_2$ (*Weiss*, 1974). In seawater, however, the correction for the non-ideal behavior of the gas in solution ($fCO_2$) is generally less than 3 $\mu$atm (*Pierrot et al.*, 2009), or 3-4‰ smaller than the $pCO_2$ (*Zeebe and Wolf-Gladrow*, 2001), and the partial pressure will henceforth be used in this thesis.

#### Analytical methods: $pCO_2$

Discrete measurements of $pCO_2$ (*Wanninkhof and Thoning*, 1993) have nowadays mostly been replaced by continuous surface seawater analysis. Generally, equilibrator instruments are used, in which a constant stream of seawater is allowed to exchange $CO_2$ with a relatively small amount of recirculated air in a gas headspace. An infrared gas analyzer is used to determine the mixing ratio of $CO_2$ in the air stream, which is proportional to the $pCO_2$ of the seawater when the proper corrections for air pressure, moisture content and temperature are taken into account (*van Heuven*, 2013). In this work (Paper III), surface seawater $pCO_2$ data was used which was measured underway by a General Oceanics system (GO8050) with a non-dispersive infrared (NDIR) $CO_2$ sensor (LI-COR® 7000). Calibration was performed several times per day against a series of 4 standard gases. The $pCO_2$ data were processed according to *Pierrot et al.* (2009) and SOCAT[1] approved methods (*Pfeil et al.*, 2013) and the overall uncertainty was estimated to $\pm$2 ppm.

## 2.5 Internal Consistency of the Carbonate System

If more than two of the four analytical parameters of the carbonate system are determined, the system is over-determined since it is possible to calculate any of the measured parameters from the other parameters. This allows one to examine the internal consistency, or apparent accuracy, of the measurements and is a common approach to examine the reliability of field measurements (*Lamb et al.*, 2001; *Millero*, 2007, Papers III-IV). Depending on the combination of input parameters, different uncertainties are expected for different combinations with respect to the target parameter. For example, the input of pH-$pCO_2$ gives the largest errors in the calculated values of TA and DIC. For all combinations of input parameters, the probable uncertainties due to experimental errors in the calculated parameters are approximately in the the range of $\pm$2-20 $\mu$mol kg$^{-1}$, $\pm$3-20 $\mu$mol kg$^{-1}$, $\pm$2-6 $\mu$atm, and $\pm$0.0025-0.0060 units for TA, DIC, $pCO_2$, and pH, respectively (*Millero*, 2007). Added to these are uncertainties in the stoichiometric dissociation constants, since they are derived from experimental data, fitted as a function

[1] Surface Ocean $CO_2$ Atlas; http://www.socat.info

of salinity and temperature. Input of TA-DIC also has a relatively high associated error and can lead to calculated values of $pCO_2$ up to 30% undersaturation (*Hoppe et al.*, 2012). Parts of this large error can be attributed to the high uncertainty in $K_2^*$ (*Millero*, 2007). The uncertainty has been suggested to be related to the interactions of boric acid with the carbonate ion. Investigations have shown that small additions of boric acid lead to a decrease in $K_2^*$ in seawater, whereas addition of larger concentrations of boric acid lead to an increase in $K_2^*$ (*Bustos-Serrano*, 2010; *Mojica Prieto and Millero*, 2002). Dissolved organic carbon (DOC) has also been suggested to have an effect on the $K_2^*$ value, but has, as of yet, not shown any obvious correlations (*Bustos-Serrano*, 2010). However, the propagation of the error associated with $K_2^*$ may not be enough to fully explain undersaturations of the magnitude as given above (*Hoppe et al.*, 2012). In order to achieve high accuracy in the calculated $CO_2$ parameters, calculations should preferably be made with pH-DIC (*Byrne*, 2014).

Despite the larger relative error introduced in the calculated pH and $pCO_2$, DIC and TA are recommended for ship-based surveys when only two of the carbon parameters are measured (*Orr et al.*, 2009). This recommendation is largely because of the CRM program for ocean $CO_2$ measurements (*Dickson et al.*, 2003), where the periodic analysis of a CRM allows for the assessment of the accuracy for DIC and TA measurements (*Waters*, 2012). Furthermore, TA and DIC are state variables in biogeochemical modelling due to their conservative behavior. It is recommended to always overdetermine the marine carbonate system by measuring more than two parameters.

Several sets of the dissociation constants of carbonic acid ($K_1^*$ and $K_2^*$) are available. These are based on measurements in both artificial and real seawater, on different pH scales, as well as over different range of salinity and temperature. Care should therefore be taken when choosing constants depending on the user's intended application. For example, in estuarine or low salinity coastal waters the constants by *Millero et al.* (2006) (Paper I) and *Millero* (2010) should represent the most appropriate choices due to their salinity range. The latter is a compilation and refit of earlier measurements of $K_1^*$ and $K_2^*$ from *Mehrbach et al.* (1973); *Mojica Prieto and Millero* (2002); *Millero et al.* (2006) given on different pH scales, with the fit forced though measurements of the pure water (thermodynamic) constants (*Harned and Scholes*, 1941; *Harned and Bonner*, 1945). In cold polar waters (Papers III-IV), the constants of *Roy et al.* (1993) and *Mehrbach et al.* (1973) refitted by *Dickson and Millero* (1987) typically provide the best estimations. Calculations of the carbonate system also rely on the standard mean composition of sea salt to be conservative with respect to changes in salinity. The total boron/borate concentration, for example, is derived from salinity (*Uppström*, 1974) and has recently been updated for oceanic waters (*Lee et al.*, 2010). However, while these relationships apply in most oceanic waters, deviations from these universal relationships are to be expected in estuarine systems, such as the Baltic Sea (*Dyrssen and Uppström*, 1974; *Kremling*, 1970; *Gripenberg*, 1960).

There are many freely available software packages for determining the carbonate system (Table 2.1). The most common package is CO2SYS and the MATLAB version (*Van Heuven et al.*, 2011) was used in this work (Papers III-IV), as well as AquaEnv (*Hofmann et al.*, 2010, Paper I). Although all packages are based on the same thermodynamic relationships, small differences (sub-micromolar) exist in the calculated parameters between the different packages (*Orr et al.*, 2014). These minor differences are, although important to resolve, of minor importance for the practical user considering the analytical uncertaines (*Zeebe*, 2014). The different packages may also differ in the availability of dissociation constants and input-output parameters.

Table 2.1: Carbonate system software packages. Modified and updated from *Orr et al.* (2014).

| Package | Language | Reference |
|---|---|---|
| CO2SYS[a] | DOS | *Lewis and Wallace* (1998) |
| CO2SYS[b] | Excel/VBA | *Pelletier et al.* (2007) |
| CO2SYS[a] | Excel/VBA | *Pierrot et al.* (2006) |
| CO2SYS[a] | MATLAB | *Van Heuven et al.* (2011) |
| CO2calc[c] | VBA/iOS | *Robbins et al.* (2010) |
| csys[d] | MATLAB | *Zeebe and Wolf-Gladrow* (2001) |
| ODV[e] | C++/GUI* | *Schlitzer* (2002) |
| mocsy[f] | Fortran 95/Python* | *Orr and Epitalon* (2014) |
| seacarb[g] | R | *Lavigne and Gattuso* (2011) |
| swco2[h] | Excel/VBA | *Hunter* (2007); *Mosley et al.* (2010) |
| AquaEnv[i] | R | *Hofmann et al.* (2010) |

[a] http://cdiac.ornl.gov/oceans/co2rprt.html
[b] http://envsci.rutgers.edu/˜reinfelder/aquaticnotes/co2sys.xls
[c] http://pubs.usgs.gov/of/2010/1280/
[d] http://www.soest.hawaii.edu/oceanography/faculty/zeebe_files/CO2_System_in_Seawater/csys.html
[e] http://odv.awi.de; *Embedded function in Ocean Data View
[f] http://ocmip5.ipsl.jussieu.fr/mocsy; *Python callable
[g] http://cran.r-project.org/web/packages/seacarb
[h] http://http://neon.otago.ac.nz/research/mfc/people/keith_hunter/software/swco2/
[i] http://http://cran.r-project.org/web/packages/AquaEnv/

# Chapter 3

# Biogeochemical Processes

> "In küstennahem Wasser, wo man durch die Süsswasserzufuhr mit Einmengung von Humus- oder anderen organischen vielleicht auch unorganischen pH beeinflussenden Stoffen rechnen kann, ist es vorgekommen, dass das System versagt hat. In diesem Falle muss die experimentelle Bestimmung der Titrationsalkalinität durch eine Bestimmung des Totalkohlensäuregehaltes ersetzt werden."
>
> Kurt Buch, *Das Kohlensäure Gleichgewichtsystem im Meerwasser* (1951)

The erosion, or weathering, of terrestrial sedimentary and igneous rock provides the ocean with dissolved constituents via the vast river systems and catchment areas. Among these dissolved components are all the constituents of sea salt (in fact all elements in the periodic table except the short-lived synthetic radioisotopes), including dissolved inorganic carbon and the non-carbonate acid-base species of total alkalinity. The observed concentrations of these constituents in the ocean is determined by the relative rates of the riverine input and the removal to the sediment and burial in sediments deposits of the ocean floor (*Broecker*, 1971). The balance between these source and sink terms, and the continuous circulation of the ocean, result in a fairly homogeneous average composition of the dissolved constituents in seawater. However, several processes contribute to significant alterations to this uniform distribution. Within the ocean, carbon is transported by three different mechanisms (e.g., *Rhein et al.*, 2013): (1) the 'solubility pump', (2) the 'biological pump', and (3) the 'marine carbonate pump'.

The solubility pump (alternatively referred to as the physical pump or the gas-exchange pump) denotes the physico-chemical process driven by the salinity and temperature dependent solubility of $CO_2$. When surface waters cool, more $CO_2$ can dissolve causing undersaturation with respect to the atmosphere, upon which a net flux of $CO_2$ from the

atmosphere may take place. At high latitudes, this mechanism is notable in the formation of deep water when warm surface waters are cooled to near-freezing temperatures, resulting in enrichment of DIC in these cool deep waters. The rate of exchange of $CO_2$ across air-sea interface is governed by the concentrations difference of $CO_2$ between the ocean and the atmospehre. The air-sea flux of $CO_2$ ($F$, in mol $m^{-2}$ $s^{-1}$) is commonly expressed as the product of the gas transfer velocity ($k$, in m $s^{-1}$), the solubility constant of $CO_2$ ($K_0^*$, in mol $m^{-3}$ $atm^{-1}$), and the difference of the partial pressure of $CO_2$ between ocean and atmosphere ($pCO_2$, in $\mu$atm):

$$F = kK_o^*(pCO_2^{\text{sea}} - pCO_2^{\text{atm}}) \tag{3.1}$$

The gas transfer velocity $k$ is approximated as a function of wind speed, with stronger winds facilitating higher gas exchange due to, e.g., enhanced turbulence and bubble formation. Various empirical wind-speed parameterizations of $k$ are available, which generally differ at high wind speed (*Wanninkhof et al.*, 2009, and references therein). This as yet unresolved variation in definitions leads to substantial uncertainty in the estimation of $CO_2$-fluxes (e.g., *Sweeney et al.*, 2007). In polar regions, the gas transfer velocity may be strongly reduced by the variable presence of sea ice (*Ito et al.*, 2004, Paper III). Since the atmospheric $CO_2$ content is fairly constant on short time scales, one may say that it is the seawater $pCO_2$ that mainly drives the flux, or processes that affect the surface $pCO_2$.

The increase of atmospheric anthropogenic $CO_2$ leads to an increased net flux of $CO_2$ from the atmosphere into the ocean. As direct consequence of the consumption of carbonate ions (protonated to bicarbonate) by addition of $CO_2$ is that the uptake capacity of additional $CO_2$ decreases (estimated by the Revelle factor). This process may be expected to become the primary cause of the gradual decrease of the oceanic sink strength, together with ocean warming and biologically driven feedbacks (*van Heuven*, 2013).

The biological pump (alternatively referred to as the soft-tissue pump) is the ocean's biologically driven uptake and physical transport of $CO_2$ from the atmosphere to the deep ocean (e.g., *Sarmiento and Gruber*, 2006). Based on measurements of the composition of phytoplankton in the ocean, the traditional stoichiometric formula for the composition of marine phytoplankton organic matter is (*Redfield et al.*, 1963):

$$106\,CO_2 + 16\,HNO_3 + H_3PO_4 + 122\,H_2O \underset{\text{Respiration}}{\overset{\text{Photosynthesis}}{\rightleftharpoons}} (CH_2O)_{106}(NH_3)_{16}H_3PO_4 + 138\,O_2 \tag{3.2}$$

and denotes the production (or, reversely, remineralization) of photosynthesising organisms that utilise light, nutrients, and trace elements for their growth and the conversion of inorganic carbon into organic carbon. The stoichiometric ratios of C:N:P:$O_2$ of 106:16:1:-138 are termed Redfield(-Ketchum-Richards; RKR) ratios. The ratios have regularly seen minor revisions over the last decades (e.g., *Anderson and Sarmiento*, 1994; *Körtzinger et al.*, 2001; *Takahashi et al.*, 1985; *Sterner et al.*, 2008), but the

concept of proportionality has proved remarkably valid in different water masses and regions over longer time scales. As is seen from reaction (3.2), $CO_2$ is consumed during photosynthesis, which causes $pCO_2$ to decrease and also lowers DIC, but increases pH. Loss of $CO_2$ does not change TA, as previously mentioned. However, the uptake of nutrients by the organisms has a slight effect on TA due to the requirement of electroneutrality. Simplified, uptake of a negatively charged species must be compensated by release of a positively charged species (e.g., $H^+$), or the reverse (see *Wolf-Gladrow et al.*, 2007). Since photosynthesis lowers the $pCO_2$ of the surface waters, it has the potential to increase the uptake of $CO_2$ from the atmosphere.

Some of the organic matter will be remineralized in the photic zone during photosynthesis and carbon and nutrients will again be available for the primary producers. The recycling is promoted by zooplankton grazing of the phytoplankton. The fecal pellets of the zooplankton and the dead phytoplankton join the pool of sinking detritus. While sinking, the detritus will be mineralized and carbon and nutrients will recycle to the dissolved inorganic state in the deeper layers. This carbon pool is, generally, unavailable for new primary production due to insufficient light conditions. Furthermore, zooplankton migrate to large depths, especially during winter, where they respire. All these processes involved in sedimentation result in carbon being transported from the surface further down the water column.

The marine carbonate pump is generated by the formation of calcareous shells of certain oceanic microorganisms in the surface ocean, which after sinking to depth, are remineralized back into DIC and calcium ions. The carbonate pump operates counter to the marine biological soft-tissue pump with respect to its effect on $CO_2$. Simplified, in the formation of calcareous shells, two bicarbonate ions are split into one carbonate and one dissolved $CO_2$ molecule, which increases the $pCO_2$ in surface waters. Only a small fraction of the carbon exported by the latter two pumps from the surface reaches the sea floor where it can be stored in sediments for millennia and longer (*Denman et al.*, 2007).

Biogeochemical processes of qualitative and quantitative importance during carbon cycling are tightly coupled to the redox state of the environment and are therefore often classified as oxidation-reduction (redox) reactions. The organic matter (reductant) is oxidized by an electron acceptor (oxidant). In waters with oxic conditions, the preferred electron acceptor is molecular oxygen ($O_2$). In shallow coastal ecosystems, a substantial fraction of organic material produced in the photic zone reaches the sediment surface (Berelson et al., 1996), while in the deep parts of the ocean up to 99% of the organic material exported from the surface is remineralized in the water column (Suess, 1980). The large amount of organic matter reaching the sediment in coastal environments is often associated with high rates of oxygen consumption. As oxygen is depleted, microorganisms switch to a succession of alternative electron acceptors (diagenetic sequence; Table 3.1) in order of decreasing themodynamic advantage which depends on the free energy ($\Delta G^\circ$) of the reaction.

Table 3.1: The diagenetic sequence of reactions that oxidize organic matter ($CH_2O$) in marine environments. Reactions are listed in order of decreasing yield of free energy ($\Delta G^\circ$) during standard state. $\Delta G^\circ$ values are in kJ $mol^{-1}$ $CH_2O$. After Berner (1980).

| Pathway | Reaction | $\Delta G^\circ$ |
|---|---|---|
| Oxygen respiration | $CH_2O + O_2 \longrightarrow CO_2 + H_2O$ | -475 |
| Denitrification | $CH_2O + \frac{4}{5}NO_3^- \longrightarrow \frac{4}{5}HCO_3^- + \frac{1}{5}CO_2 + \frac{2}{5}N_2 + \frac{3}{5}H_2O$ | -448 |
| Manganese(IV) reduction | $CH_2O + 3CO_2 + H_2O + 2MnO_2 \longrightarrow 2Mn^{2+} + 4HCO_3^-$ | -349 |
| Iron(III) reduction | $CH_2O + 7CO_2 + 4Fe(OH)_3 \longrightarrow 4\,Fe^{2+} + 8HCO_3^- + 3H_2O$ | -114 |
| Sulphate reduction | $CH_2O + \frac{1}{4}SO_4^{2-} \longrightarrow \frac{1}{2}H_2S + HCO_3^-$ | -77 |

Which of the processes that control carbon transformations under the wide suite of environmental conditions, as well as what kind of microorganisms that mediate these reactions, mainly rely on the availability and balance between oxidants and reductants. Concentrations of reactants provide the fundamental base for the thermodynamic state of the environment and thus the energy balance of reactions.

Various aspects of the above processes were investigated in more detail in this thesis. In the central Arctic Ocean, the anthropogenic carbon inventory was investigated from six expeditions between 1991-2011 (Paper IV), as well as the spatial variability of net community production from the latter expedition, using different approaches (Paper III). In the Baltic Sea, the coupling of biogeochemical processes and pH was investigated from historic measurements under contrasting redox conditions (Paper I). Additionally, the contribution of excess 'organic alkalinity' to total alkalinity in the Baltic Sea was studied using a humic ion-binding chemical speciation modelling approach (Paper VI).

## 3.1 The Arctic Ocean

### Arctic Ocean Characteristics

The central Arctic Ocean (Figure 3.1) is divided into the Eurasian and Canadian (or Amerasian) Basins by the Lomonosov Ridge that stretches between the surrounding continents. The Eurasian Basin includes the Amundsen Basin and the Nansen Basin, with the Gakkel Ridge rising in between, while the Alpha and Mendeleev Ridge subdivides the Canadian Basin into the Makarov and Canada Basins (*Rudels et al.*, 2012). The ridges direct currents and restrict deep water exchange between the basins (*Björk et al.*, 2010). The central basins are surrounded by shallow shelf seas which constitutes ~50% of the total area (*Jakobsson et al.*, 2003). They are mainly located on the Siberian side, with the deepest being the Barents Sea with an average depth of ~200 m and the larger

part being shallower than 50 m. There are two main inflows of seawater, of Pacific and

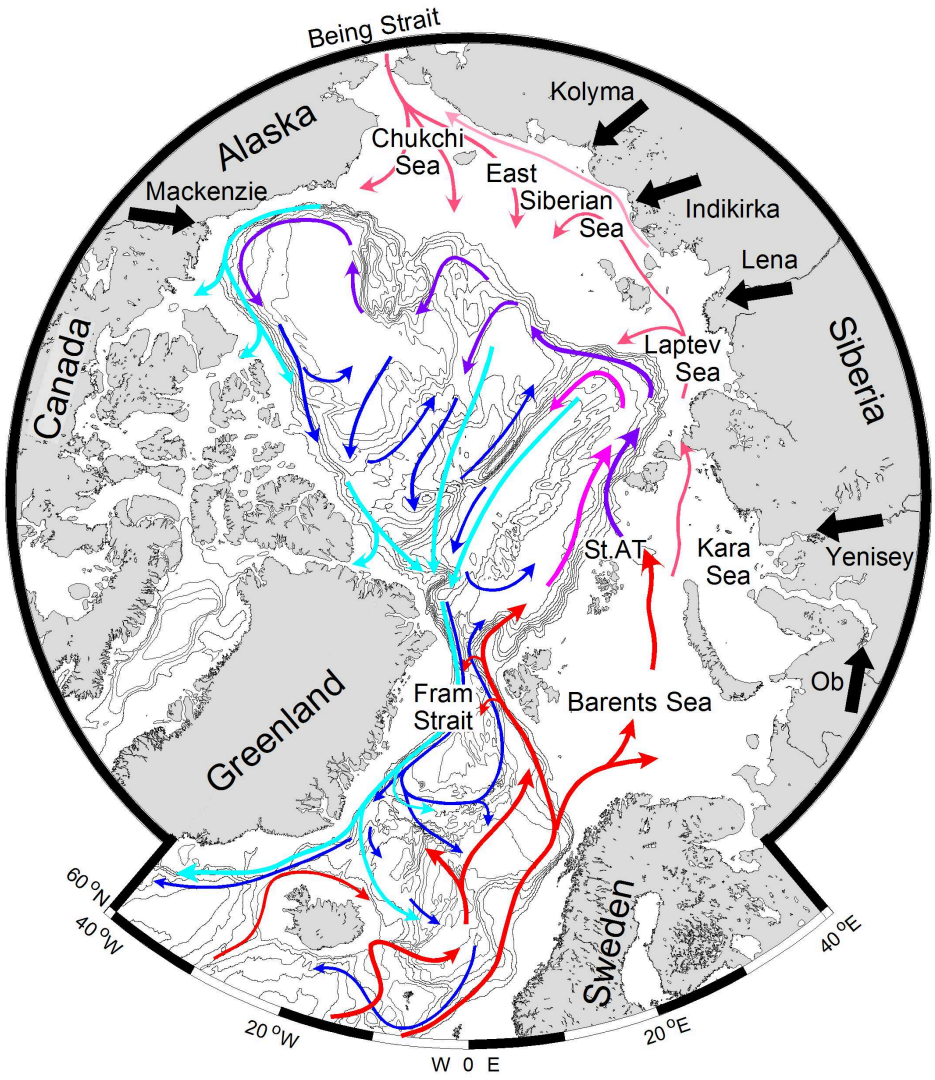


Figure 3.1: General mean circulation in the Arctic Ocean together with the dominating rivers entering this domain. Surface currents are illustrated by red, pink, and light blue colors, while deep currents are illustrated by dark blue and purple colors. Modified after *Rudels et al.* (1994).

Atlantic origin, to the Arctic Ocean. The Pacific water enters through the Bering Strait into the Chukchi Sea. Through the Chukchi Sea, the Pacific water is diverted into an eastward flow north of Alaska and one north into the central Arctic Ocean. These waters flow east along the continental margin and exit through the Canadian Archipelago and the Western Fram Strait (*Jones et al.*, 1998). There is also a westerly flow into the

East Siberian Sea, where it mixes with other waters before it eventually enters the deep central basins.

Warm Atlantic water enters the Arctic Ocean through the Fram Strait and the Barents Sea. The Fram Strait branch is supplied by the West Spitsbergen Current (WSC), where a fraction, the Fram Strait branch water (FSBW), flows eastward along the Eurasian continental slope forming a boundary current (*Rudels et al.*, 2012). The Barents Sea branch water (BSBW) is modified by cooling from heat loss to the atmosphere and freshened by sea-ice melt water during summer and brine addition from sea ice production in winter, as well as mixing with the Norwegian Coastal Current (*Gascard et al.*, 2004). Part of Barents Sea branch enters the Arctic Ocean through St. Anna Trough, at a depth that corresponds to its density and then follows the circulation pattern of the Fram Strait branch. Part of the Barents Sea branch also crosses the Kara Sea, while mixing with freshwater from Ob and Yenisey Rivers, and continues into the Laptev Sea (*Anderson et al.*, 1994). Confluence of the BSBW and FSBW takes place east of the St. Anna Trough and is characterized by considerable mixing (*Walsh et al.*, 2007). The contributions of the two Atlantic branches to the boundary current are of similar magnitude, but a substantial fraction of the FSBW is diverted into the interior of the Nansen Basin (*Aksenov et al.*, 2010).

The submarine ridges influence the boundary flow producing complex systems of basin-wide gyres (*Schauer et al.*, 1999), with mainly BSBW in the Amundsen Basin and over the Lomonosov Ridge and largely FSBW over the Gakkel Ridge and the northern Nansen Basin (*Rudels et al.*, 2012). An important bifurcation of the boundary current takes place north of the Laptev Sea, where one part flows along the Lomonosov Ridge towards Greenland while the other continues into the Canadian Basin (*Schauer et al.*, 1999). The boundary current within the Canadian Basin splits at each topographic feature that it encounters before it eventually recrosses the Lomonosov Ridge north of Greenland. The interior of the Canada and Makarov Basins are filled with water of more or less Atlantic origin from the halocline and deeper (*Rudels et al.*, 2012), as well as Pacific influenced shelf water, e.g., of Chukchi and East Siberian Sea origin in the surface and upper halocline (Smethie et al., 2000).

The water circulation of the Arctic Ocean below the halocline is largely topographically driven, with cyclonic circulation within the four deep basins; the Nansen, Amundsen, Canada and Makarov Basins (*Rudels et al.*, 1994). The surface water circulation pattern is divided into two major regimes; one large anti-cyclonic circulation in the Canada and Makarov Basins, i.e., the Beaufort Gyre, and one more direct flow of water from the Siberian Shelf region towards Fram Strait via the Nansen and Amundsen Basins, i.e., the Transpolar Drift (*Jones et al.*, 1998). The boundary between these two circulation patterns varies with time and is determined by the large-scale atmospheric pressure field (e.g., *Bourgain et al.*, 2013).

The central Arctic Ocean is largely ice covered all year long and the shelves are seasonally ice covered. In spring, the melting of sea ice on the shelves, together with a peak of freshwater from the rivers, creates a well-mixed surface layer, forming a strong halocline. The strong halocline largely caps the warm and more saline Atlantic water (*Karcher and Oberhuber*, 2002), preventing the large reservoir of heat to melt sea ice, with exception for the southern Nansen Basin (*Korhonen et al.*, 2013). In autumn, brine release by sea ice formation triggers convection which leads to a homogeneous winter mixed layer. This layer has a depth that varies from more than 100 m north of the Barents Sea where the Atlantic water enters the deep Arctic Ocean, to less than 50 m in the central regions (*Rudels et al.*, 1996, Paper III). Dense water production is essentially related to either modification of Atlantic waters on the shelves (*Årthun et al.*, 2011), or intense brine release during ice formation, above all, in coastal polynyas (*Dethleff*, 2010). Subsequent shelf-slope convection and entrainment renew the intermediate and deep layers of the Arctic Ocean (*Anderson et al.*, 1999).

## The central Arctic Ocean: a biological desert?

There are two possible main drivers for uptake of atmospheric $CO_2$ in the central Arctic Ocean, one being that the surface waters that enters from surrounding seas have low $pCO_2$ as a result of cooling and primary production before entering, and the other being local primary production. For the latter, it is important for the sequestration of $CO_2$ that the produced organic matter sediments out of the winter surface mixed layer so it is not mixed back into the summer surface mixed layer the next season.

The Arctic shelf seas include areas of high primary production, high air-sea fluxes of $CO_2$ and deep water formation, e.g., in the Barents and Chukchi Seas (*McGuire et al.*, 2009). While some of the shelf seas act as $CO_2$ sinks, e.g., the Barents Sea supplies the Arctic Ocean with approximately one third of the atmospheric uptake (*Fransson et al.*, 2001), other regions experience high loads of organic matter from river runoff, which when remineralized, become sources of $CO_2$ to the atmosphere (*Anderson et al.*, 2009). In contrast, the role of the central Arctic Ocean in carbon sequestration is still somewhat controversial. An early view was that the central Arctic Ocean is one of the most unproductive regions in the world, due primarily to the ice cover and lack of light during the long polar winter (*Cai et al.*, 2010a). In the last decade, however, primary production levels assigned to the Arctic Ocean has increased considerably as spatial and temporal sampling have improved (*Matrai et al.*, 2013). Generally, it is difficult to obtain reasonably constrained estimates of the primary production due to the regional heterogeniety, the strong seasonal changes, the poor quality of much of the data, and the limited access to the central Arctic Ocean. Nevertheless, considering the full Arctic Ocean system, including the vast shelf areas, the Arctic primary production rivals the

range that can be found in the rest of the world ocean (*Sakshaug*, 2004; *Codispoti et al.*, 2005; *Hill and Cota*, 2005, Table 3.2).

Table 3.2: Annual primary production estimates (g C $m^{-2}$ $yr^{-1}$) selected from *Sakshaug* (2004). Modified after *Codispoti et al.* (2013).

| Region | Total PP | New PP |
|---|---|---|
| Central Deep Arctic Ocean[a] | >11 | <1 |
| Arctic Shelf Seas (average)[b] | 32 | 1 |
| Beaufort Sea | 30-70 | 7-17 |
| Barents Sea | <20-200 | <8-100 |
| Bering Sea | >230 | - |
| Canadian Arctic | 20-40 | 5-10 |
| Chukchi Sea | 20 to >400 | 5 to >160 |

[a] Amerasian and Eurasian Basins.

[b] Average for the Barents and its north slope, and the White, Kara, Laptev, East Siberian, Chukchi, Beaufort, and Lincoln Seas, the North East Water Polynya, and the North Water Polynya.

Spring and summer have long been recognized as periods of high biological productivity on most Arctic Ocean shelves, driving both pelagic (e.g., Barents Shelf) and benthic (e.g., Chukchi Shelf) food webs (*Reigstad et al.*, 2002; *Grebmeier et al.*, 2006). In comparison, the central Arctic Ocean basins supports much less production, but is far from the biological desert suggested decades ago (*Hill et al.*, 2013; *Gosselin et al.*, 1997; *Boetius et al.*, 2013, Paper III).

Export of organic carbon from the surface layer depends on, among other things, the net community production (NCP). NCP is the difference between gross primary production and the community's combined auto- and heterotrophic respiration. Since storage of organic carbon in the mixed layer is likely to be modest with respect to NCP over large spatial and temporal scales, NCP approximates carbon export production (*Falkowski et al.*, 2003). Remembering the statement by *Dickson* (1984) in Section 2.3 regarding the different pH scales, the concept of different biological production terms may need some further clarification.

Primary production is distinguished as either *gross* or *net* primary production (GPP and NPP, respectively). GPP is the overall production, or chemical energy produced, by primary producers. Some of this energy is used by the primary producers for their cellular respiration. The difference between GPP and the primary producers' own respiration is referred to as NPP and this remaining organic carbon is available for heterotrophs (e.g., *Lindeman*, 1942; *Falkowski et al.*, 2003). Furthermore, from NPP, *new* production is based on nutrients (mainly nitrogen-based) that are supplied from outside the euphotic zone, by upwelling, mixing of nutrient-rich water, or input from rivers. Additionally, *regenerative* production is based on almost immediate uptake of nutrients released by organisms within the euphotic zone (*Sakshaug*, 2004; *Dugdale and Goering*, 1967).

The fraction of total production accounted for by new production is refered to as the $f$-ratio, which can be calculated either in terms of new and regenerated nitrogen uptake or in terms of carbon uptake (*Falkowski et al.*, 2003; *Codispoti et al.*, 2013). Stated differently, NCP is the difference between NPP and heterotrophic respiration (cf. above definition).

All of the presented production terms above are operationally defined and there are various methods for estimating primary production in the ocean. Techniques for daily productivity estimates typically rely on *in vitro* incubations using isotope tracers (e.g., $^{14}C$, $^{15}NO_3$, $^{15}NH_4$, $^{18}O_2$), where the productivity is estimated from rates of assimilation or evolution of these over a certain time period (e.g., *Williams*, 1993). Depending on the type of production estimated (e.g., GPP, NPP, NCP), different or the same methods have been used. This may result in some difficulties in obtaining unambiguous estimates (*Codispoti et al.*, 2013, and references therein). Generally, for any given system the inequality GPP $\geq$ NPP $\geq$ NCP should apply (*Codispoti et al.*, 2013). Seasonal NCP is commonly estimated from draw-down of dissolved inorganic matter (nitrate, phosphate, DIC), as the difference between summer concentrations in the surface mixed layer and winter surface water concentrations, either by using seasonal data or by inferring winter concentrations from summer profiles (e.g., *Mathis et al.*, 2010; *Jennings et al.*, 1984; *Bates*, 2006, Paper III).

In Paper III, NCP was estimated during the late summer cruise ARK-XXVI/3 TransArc (Trans-Arctic Survey of the Arctic Ocean in Transition) with the *R/V Polarstern* to the central Arctic Ocean between 5 August - 7 October, 2011. In this study, several approaches were exploited using (i) continuous measurements of surface water oxygen to argon ratios ($O_2$/Ar), (ii) underway measurements of surface $pCO_2$, (iii) discrete samples of DIC, and (iv) of nutrients (nitrate and phosphate). The results show very high productivity in the marginal ice zone (MIZ) north of Franz Josef Land and Severnaya Zemlya. During periods of sea ice melt, the margins are generally areas of increased biological activity. Conditions are favourable as a result of a stabilized vertically mixed water column leading to sufficient light conditions (e.g., *Perrette et al.*, 2011).

Low values of late summer NCP was found in the sea-ice covered deep basins, with a strong spatial variability in NCP depending on region. Lowest values (even negative) were found in the Amundsen Basin. Moderate NCP were observed in the Nansen and Makarov Basins, with slightly higher estimates over the Mendeleev Ridge (see Figure 5 in Paper III). Overall, the results are comparable to the reported values in the recent synthesis by *Codispoti et al.* (2013) of nitrate and phosphate based estimates of seasonal NCP in the Artic Ocean system (Table 3.3).

However, important differences in methodology exist. The estimates by *Codispoti et al.* (2013) are based on compilations of discrete nutrient samples from different years, organizing the data in 100 x 100 km grid cells, and arbitrarily chosen integration depths

Table 3.3: Estimates of seasonal NCP and annual primary production in the Arctic Ocean system selected from *Codispoti et al.* (2013).

| Sub-region | NCP[a] (g C $m^{-2}$) | NCP[b] (Tg C $a^{-1}$) | PP[c] (Tg C $a^{-1}$) | PP[d] (Tg C $a^{-1}$) | PP (deep)[e] (Tg C $a^{-1}$) |
|---|---|---|---|---|---|
| Bering Sea | 100 (50-200) | 54 | 135 | 69 | 134 |
| Chukchi Southern | 70 (40-120) | 37 | 124 | 26 | 80 |
| Chukchi Northern | 10 (5-20) | 6 | 32 | 1 | 1 |
| Barents Sea | 40 (30-50) | 76 | 190 | 106 | 212 |
| Canadian Archipelago | 35 (20-50) | 47 | 116 | 24 | 93 |
| Nordic Seas | 30 (25-30) | 52 | 131 | 162 | 308 |
| Beaufort Southern | 15 (10-30) | 4 | 15 | 2 | 2 |
| Beaufort Northern | 1 (0.5-5) | 1 | 5 | 1 | 1 |
| ESS + Laptev Sea | 15 (5-30) | 12 | 47 | 20 | 20 |
| Kara Sea | 15 (5-30) | 13 | 47 | 17 | 16 |
| Arctic Basin[f] | | | 119 | 1 | 1 |
| Eurasian Basin | 15 (5-25) | 22 | 54 | | |
| Amerasian Basin | 3 (0.5-5) | 7 | 65 | | |

[a] *Codispoti et al.* (2013), best estimate with ranges given in parantheses
[b] *Codispoti et al.* (2013), up-scaled using sub-region area
[c] *Codispoti et al.* (2013), PP using $f$-ratio and up-scaled NCP
[d] *Hill et al.* (2013), integrated PP within surface mixed layer
[e] *Hill et al.* (2013), integrated PP including depths below surface mixed layer
[f] sum of Eurasian and Amerasian Basins due to different sub-region division between studies

depending on the basins. In Paper III, draw-down of phosphate and nitrate was also used, although a slightly different approach was applied, using assumed winter concentrations found at the depth of the winter mixed layer as inferred from summer CTD profiles. The resulting integration depth is, however, generally of similar scale to the choice of *Codispoti et al.* (2013) for the different basins. Although each of the various methods is associated with uncertainties of similar and different types, the NCP estimates are constrained by the overall agreement between the methods.

High-resolution measurements, although only applicable in the uppermost surface layer, add important details of the spatial variability in productivity as seen within the different basins. For example, an intriguing 'hotspot', with respect to biological activity, was seen during the crossing of a shallow seamount at the Gakkel Ridge (Figure 3.2). This feature was not evident from discrete sampling.

While certain shelf seas respond to the shrinking ice cover with increased primary production (*Wang et al.*, 2005) and export production (*Lalande et al.*, 2009), others do not (*Reigstad et al.*, 2011). The processes on the shelves cannot easily be extrapolated to the deep Arctic Ocean. Nonetheless, potential sequestration of carbon follows in the wake of shrinking sea ice cover due to changes in primary production, although this is highly uncertain and will depend on future light availability, stratification, nutrient supply and

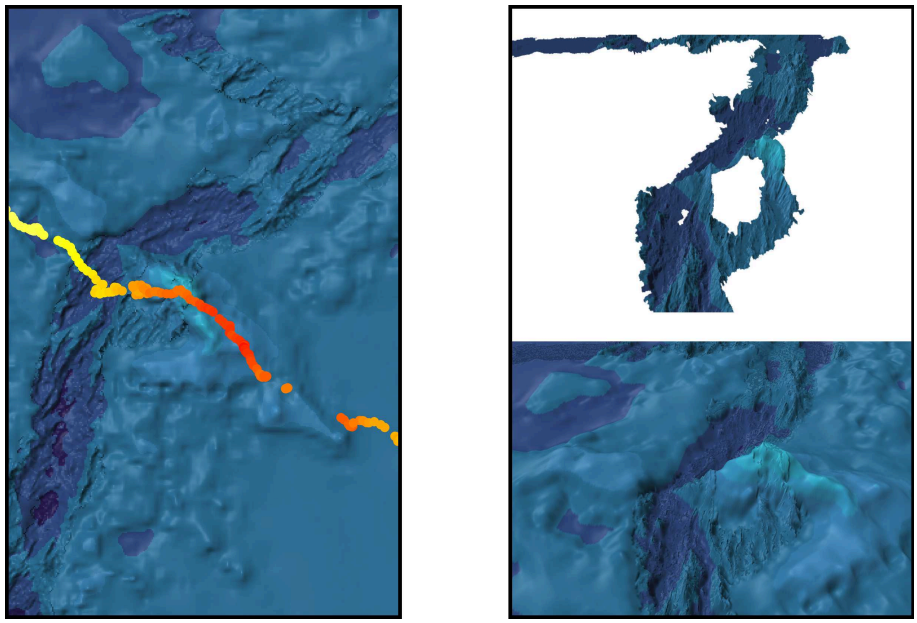

Figure 3.2: Biological oxygen supersaturation along the crossing of a shallow seamount (~600 m) at the Gakkel Ridge (left). The colors represent an approximate range of 0-15%, where red is towards higher values. View of the seamount of gridded bathymetry from the IBCAO v3 compilation and the actual multibeam track (right, *Jakobsson et al.*, 2012), which can also be seen in the left figure.

planktonic communities. An increased export production will be reflected in the deep water properties by a build up of the concentrations of nutrients and DIC, as well as a decrease in oxygen concentration through microbial remineralization.

## The central Arctic Ocean: a sink of anthropogenic $CO_2$?

In order to predict the future oceanic carbon sink and ultimately the climate evolution, it is necessary to comprehend the absorption rate of anthropogenic $CO_2$ ($C_{ant}$ uptake) as well as how and where $C_{ant}$ is distributed within the ocean ($C_{ant}$ inventory) (*Sabine and Tanhua*, 2010). These processes are governed by the physical and chemical responses to rising atmospheric $CO_2$. Biological processes within the ocean mediate the natural distribution of carbon, but there is no clear evidence that they affect $C_{ant}$ uptake and storage so far (*Sabine and Tanhua*, 2010).

There is relatively little information about the inventory and uptake rate of anthropogenic $CO_2$ in the Arctic Ocean (*Tanhua et al.*, 2013). This is mainly due to the fact that the Arctic Ocean is heavily under-sampled with respect to the carbon cycle and the

scarcity of carbonate system data from which to determine anthropogenic inventory and uptake rates. As a result, the Arctic Ocean has not typically been considered in the global estimates of anthropogenic $CO_2$ (e.g., *Sabine et al.*, 2004; *Khatiwala et al.*, 2013). However, in Paper IV, it is clearly demonstrated that the $C_{ant}$ that has been taken up from the atmosphere in the Atlantic Ocean is added to the intermediate waters of the central Arctic Ocean. The earliest estimate of $C_{ant}$ inventory in the Arctic Ocean was 1.35 $\pm$ 0.12 Pg C (*Anderson et al.*, 1998), this in relation to the estimated global ocean inventory of 155 $\pm$ 31 Pg C ($\pm$20% uncertainty) (*Khatiwala et al.*, 2013).

$C_{ant}$ uptake from the atmosphere and oceanic $C_{ant}$ storage are two measures of the oceanic carbon cycle that are closely related to each other, and ultimately equal if the net uptake is integrated over sufficient time and space. Nevertheless, it is of importance to separate between the two as oceanic circulation may transport anthropogenic carbon that has been absorbed from the atmosphere in one place to store it in another region (*Anderson and Olsen*, 2002, Paper IV).

There are different techniques for estimating $C_{ant}$ uptake and $C_{ant}$ inventory, of which the latter uses ocean interior measurements (Table 3.4). Changes in $C_{ant}$ inventory are commonly determined utilizing either regression-based methods or transient tracers (e.g., *Sabine and Tanhua*, 2010; *Thacker*, 2012; *van Heuven*, 2013, cf. Paper IV).

Table 3.4: A selection of techniques available for the calculation of $C_{ant}$, or the increase therein ($\Delta C_{ant}$), in the ocean. Modified after *van Heuven* (2013).

| Technique | Reference | Required measurements |
|---|---|---|
| *Determining $C_{ant}$* | | |
| $C_T^0$ | *Brewer* (1978); *Chen and Millero* (1979) | $O_2$, DIC, TA |
| $\Delta C^*$ | *Gruber et al.* (1996) | $O_2$, DIC, TA, transient tracer |
| TTD | *Hall et al.* (2002) | transient tracer |
| TrOCA | *Touratier and Goyet* (2004a,b) | $O_2$, DIC, TA |
| TSS | *Tanhua et al.* (2007) | $\Delta C_{ant}$ (see below) |
| *Determining $\Delta C_{ant}$* | | |
| change in DIC | *van Heuven* (2013) | DIC |
| change in $C_T^0$ | *Peng et al.* (1998) | $O_2$, DIC, TA |
| MLR | *Wallace* (1995) | $O_2$, DIC, TA, nutrients |
| eMLR | *Friis et al.* (2005) | $O_2$, DIC, TA, nutrients |
| TSR | *van Heuven* (2013) | $O_2$, DIC, TA, nutrients |

The idea behind the two first techniques in Table 3.4 ($C_T^0$ and $\Delta C^*$), is to subtract the pre-industrial value of DIC from the measured DIC, which contains both the natural and anthropogenic part. Corrections have to be made for the decay of biological soft parts and dissolution of metal carbonates, which both increase DIC. This requires knowledge of the carbonate system parameters, oxygen saturation, nutrients, and the use of the Redfield ratio. Since pre-industrial values of the the carbonate system parameters cannot

be measured, they have to be estimated. Other techniques, such as the Transit Time Distribution (TTD; Table 3.4), uses transient tracers, e.g., chlorofluorocarbons (CFCs), to estimate the age of the water mass. All techniques have their inherent assumptions and drawbacks. Larger studies often include several techniques, where applicable, to get a range of the estimates (e.g., *Khatiwala et al.*, 2013). *Vázquez-Rodríguez et al.* (2009) compared five techniques in the Antlantic Ocean between 60°N-40°S and found similar spatial distributions and magnitude of $C_{ant}$, with discrepancies particularly in the Southern Ocean and Nordic Seas.

## 3.2 The Baltic Sea

### Baltic Sea Characteristics

The Baltic Sea is a semi-enclosed sea, connected only to the oceanic waters of the North Sea through the shallow and narrow Danish straits (including Øresund). The Baltic Sea is characterized by a limited water exchange (see below), large input of river runoff and low salinity water. Bathymetric constraints, such as sills or horizontal contractions, divide the Baltic Sea into several sub-basins, where the larger ones, from north to south, are the Bothnian Bay, Bothnian Sea, Gulf of Finland, Gulf of Riga, Baltic Proper, Bornholm Basin, and the Arkona Basin, prior to the Danish straits and followed by the Kattegat and Skagerak (Figure 3.3). The average depth of the Baltic Sea is 55 m and the maximum depth of 460 m is found at the Landsort Deep, followed by the Gotland Deep (250 m). The Baltic 'seawater' is brackish due to large river discharges, which drive the large-scale estuarine circulation, with strong vertical salinity dependent stratification in the southern parts of the system. The largest river runoff is delivered to the Gulf of Bothnia, the Gulf of Finland, and the Gulf of Riga. Combined, these discharges are estimated to make up 70% of the total volume of freshwater delivered to the system. The Baltic drainage area is more than four times greater than the sea area (*Kuliński and Pempkowiak*, 2012). In the central Baltic Sea (Baltic Proper), the surface salinity is around 7, whereas bottom waters typically have salinity around 13. The surface and bottom layers are divided by a permanent halocline at ~60 m depth. In the shallower northern basins, the water mass is more easily mixed due to a weaker vertical salinity gradient. The Baltic Sea has a horizontal salinity gradient from the more saline surface waters of the Skagerak (20-25), to the extreme of Gulf of Bothnia in the north (2-4). In spring and summer, a seasonal thermocline develops, while during winter the surface layer is well mixed above the halocline. As a result of high primary productivity and large river discharge, concentrations of dissolved organic carbon in the Baltic Sea are three to five times higher than those in the open ocean (*Kuliński and Pempkowiak*, 2008; *Kuliński et al.*, 2011).

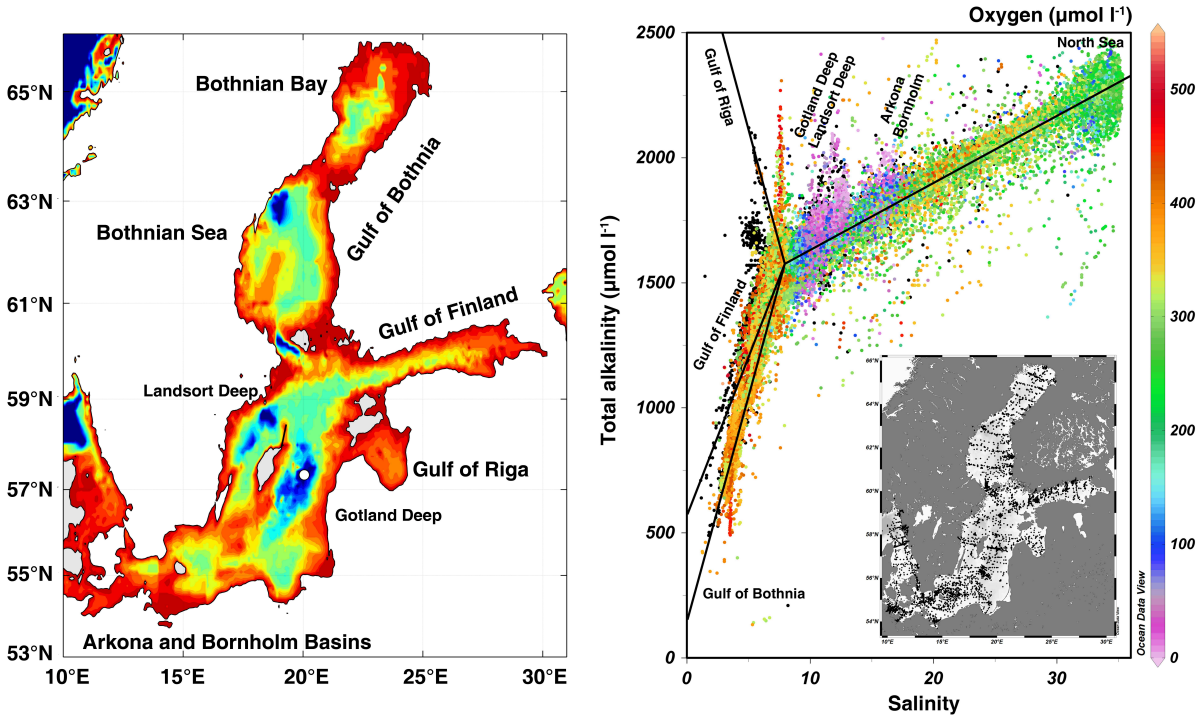


Figure 3.3: Left figure shows a bathymetric map of the Baltic Sea down to 200 m (modified after *Edman* (2013)). The monitoring station BY15 is indicated (open circle) in the Gotland Deep (250 m). Right figure shows total alkalinity versus salinity with overlain oxygen concentrations (data between 1911-2003, *Hjalmarsson et al.* (2008)). Lines indicate the schematic mixing regimes. Inset shows the distribution of sampling locations of the data (adapted after *Hjalmarsson et al.* (2008)).

There are both baroclinic and barotropic inflows to the Baltic Sea, where the former is driven by density gradients and the latter is driven by differences in sea level between Kattegat and the southern Baltic Sea. The barotropic inflows are responsible for the main water exhange of the deep water. Sea level differences are highly variable, which is reflected in the frequency and magnitude of the barotropic inflows. These inflows come as pulses of water of various salinity, temperature, and volume, which determine how far and how deep into the Baltic Sea the inflowing water reaches. Minor inflows are relatively frequent and contribute to the ventilation of the upper water masses. Renewal of deep water are infrequent and the two most recent large inflows were in 1993 and 2003 (Paper I). Between major inflows, the deep water becomes stagnant and depleted in oxygen, resulting in anoxic and euxinic (sulfidic) conditions below 100-150 m. Hypoxia, here defined as oxygen concentrations less than 2 mg $l^{-1}$ (125 $\mu$mol $l^{-1}$, or sometimes defined as 2 ml $l^{-1}$; 90 $\mu$mol $l^{-1}$), has expanded from less than 10 000 $km^2$ before 1950

to >60 000 $km^2$ since 2000. This is attributed to enhanced nutrient inputs from land and atmosphere (*HELCOM*, 2013) as well as by the stronger stratification and an upward movement of the halocline in the water column (*Carstensen et al.*, 2014).

## The Baltic carbonate system

Extensive investigations of the Baltic Sea have been performed for more than 100 years, resulting in long time series of hydrographic data, e.g., at the Gotland Deep (*Fonselius and Valderrama*, 2003). At the beginning only salinity (as chlorinity), temperature and dissolved oxygen were measured and one or two expeditions were carried out annually, mostly in summer. In the 1920s, alkalinity and pH were occasionally measured and are the two parameters of the carbonate system that are being measured today. National and joint environmental monitoring programs of the surrounding countries of the Baltic Sea have been employed, based on the HELCOM Monitoring and Assessment Strategy[1]. The Swedish Meteorological and Hydrological Institute (SMHI) is the national data host, appointed by the Swedish Agency for Marine and Water Management, where hydrographic data are freely available. As a result of analytical developments and implementations of new methods for TA and pH, the more recent data are deemed more reliable. For example, potentiometric measurements of $pH_{NBS}$ have been stated to be of sufficient high quality from 1993 and onwards. Efforts are now being made for implementing spectrophotometric methods for the determination of pH in the national monitoring program (see Section 2.3).

The relationship between TA and salinity is a fairly linear function in most oceanic waters. In the Baltic Sea, different or deviating relationships are observed (Figure 3.3). This is a result of long-term large river discharge from drainage basins of different geological composition. Rivers that enter the southern part of the Baltic Sea are rich in limestone, i.e., have higher TA than rivers that enter in the northern part, where granite dominates the bedrock of the drainage basins (e.g., *Hjalmarsson et al.*, 2008), adding less buffer capacity. Generally, TA decreases linearly with respect to salinity from the North Sea via the straits to the central Baltic Sea. The Gulf of Riga has extremely high TA with respect to salinity, whereas the Gulf of Finland and the Bothnian Bay and Sea experience seemingly lower TA than what is expected from the North Sea mixing line (Figure 3.3). The notion of 'excess alkalinity' is a well-known concept for the Baltic Sea, which also applies to the higher calcium concentrations with respect to salinity (*Dyrssen*, 1993; *Gripenberg*, 1937; *Kremling*, 1970). The horizontal distribution of surface TA also reflects the distribution of DIC. Recently (2008-2009), extensive measurements of DIC and TA were performed in all of the major basins (*Beldowski et al.*, 2010). From these,

[1]HELCOM; Baltic Marine Environment Protection Commission - Helsinki Commission, http://www.helcom.fi

it was concluded that surface water DIC is mainly controlled by TA where the biologically induced modulation of the TA-controlled DIC distribution was relatively small in the surface layer.

As in most oceans, the surface water $pCO_2$ shows a distinct seasonality with extremely low values (100-150 $\mu$atm), whereas the oversaturation observed during autumn/winter is more moderate (*Schneider et al.*, 2014). The $pCO_2$ drops below the atmospheric value with the development of a shallow thermocline and the concurrent onset of the production period in March/April and remains undersaturated with respect to the atmosphere until September/October when cooling and increasing winds cause a deepening of the mixed layer (*Schneider et al.*, 2014). Two distinct $pCO_2$ minima in May and July indicate the spring phytoplankton bloom and the large bloom of nitrogen fixing cyanobacteria, respectively (*Schneider et al.*, 2009).

Similarly to the oceans, the largest carbon resources in the Baltic Sea are present as DIC, followed by DOC. The amount of carbon that is exported from, and imported to, the Baltic depends mainly on the volume of flowing water, which is highly variable (e.g., *Omstedt et al.*, 2004). *Thomas et al.* (2005) estimated the net carbon export to 14 Tg C annually. This is in contrast to *Hjalmarsson et al.* (2010), who estimated the net export to 5.5 Tg C based on seasonal data and model volume transport. Scandinavian rivers have been suggested to supply the Baltic Sea with 0.12 Tg C annually, whereas continental rivers provide a substantially larger annual supply of 4.9 Tg C (*Thomas et al.*, 2003). Estimates of carbon deposition on the sediments vary by region, and 1.7 Tg C $yr^{-1}$ have been suggested for the Baltic Proper (*Kuliński and Pempkowiak*, 2012), whereas 1.1 Tg C $yr^{-1}$ have been suggested for the Gulf of Bothnia based on total organic carbon (TOC) accumulation rates in the uppermost sediment layers (*Algesten et al.*, 2006). For the deep basins, it has been suggested that the accumulation rate of TOC has increased two- to three-fold during the several last decades (*Emeis et al.*, 2000). It has been estimated that the Gulf of Bothnia annually releases 3.6-3.8 Tg C in the form of $CO_2$ to the atmosphere (*Algesten et al.*, 2004, 2006). In contrast, the other parts of the Baltic Sea are considered to absorb atmospheric $CO_2$ (*Ohlson*, 1991; *Thomas and Schneider*, 1999; *Kuss et al.*, 2006). *Ohlson* (1991) estimated the average annual atmospheric $CO_2$ uptake to 13.2 g C $m^{-2}$, which is similar to more recent estimates *Thomas and Schneider* (1999).

In the deep water layers the effect of remineralization of organic matter on DIC concentration is large and DIC is accumulating during long-lasting stagnation periods and large input of organic matter (*Beldowski et al.*, 2010, Paper I). The progressive remineralization of organic matter, together with the generally low buffer capacity in low salinity waters, results in a low but fairly constant pH environment (Paper I). Although oxygen and sulfate are the major electron acceptors in the central deep basins (Paper I), other electron acceptors, such as manganese and iron oxides, are likely to be important contributors in the remineralization of organic matter, especially at the oxic-anoxic interface (*Yakushev et al.*, 2007; *Schneider et al.*, 2010; *Jost et al.*, 2010). It has been estimated

that only 10% of the particulate organic matter collected at the sediment surface was derived from the overlying water column (*Schneider et al.*, 2002). The remaining 90% was suggested to enter the deeper part of the basin by near-bottom transport, which also has been suggested by others (*Schneider et al.*, 2010; *Almroth-Rosell et al.*, 2011, Paper I). This organic matter is partly allochthonous with a terrestrial origin. Recent budget calculations for organic carbon indicate that of the total allochthonous organic carbon supplied to the system, on average 56% is remineralized, 36% is exported out of the system, and the remainder is buried (*Gustafsson et al.*, 2014).

During stagnant periods, TA increases due to the formation of hydrogen sulfide. The suboxic and anoxic deepwaters are also suggested to be a significant source for humic substances (but not total organic carbon) (*Skoog et al.*, 2011). It is a challenge to make accurate measurements of TA in anoxic waters due to the presence of hydrogen sulfide (Paper I) and humic substances (Paper V). Fluorescence measurements indicate substantial concentrations of humic substances in most major basins, with a significant part being derived from terrestrial sources (*Skoog et al.*, 2011). *Kuliński et al.* (2014) recently reported measurements of 'excess organic alkalinity' on the order of ~30 $\mu$mol $kg^{-1}$ in the surface waters of the Baltic Sea. In Paper V, these titration alkalinity data were re-evaluated and modelled using a humic model approach and it was found that the reported organic alkalinity could be explained by humic substances in the form of fulvic acid. Due to the general difficulties in measuring TA in coastal waters that are rich in organic matter, it is recommended to measure DIC (and pH) instead. This was already pointed out by *Buch* (1951).

# Chapter 4

# Ionic Interactions

> "Lärljungen får intet grepp om vad som orsakar avvikelserna från massverkans lag i icke-ideala system, t. ex. starka lösningar. Kanske får han veta, att man i sådana fall ersätter koncentrationerna med något som kallas för aktiviteter, men de definieras ej; förklaringen att man inför dem »för att det ska stämma» är inte särskilt tillfredställande och väcker lätt misstanken att något slags fusk föreligger."
>
> Lars Gunnar Sillén, *Särtryck ur Elementa* (1942)

Equilibrium solution chemistry is the study of the distribution between species at equilibrium, while thermodynamics is the study of the content and flows of energy. According to the concepts of equilibrium thermodynamics, a component present in a closed system in a thermodynamically unstable state will progress to the equilibrium state of minimum free energy. The equilibrium condition is described by an equilibrium constant $K$, e.g.,

$$\mathrm{HCO_3^-} \longleftrightarrow \mathrm{H^+} + \mathrm{CO_3^{2-}} \tag{4.1}$$

$$K = [\mathrm{H^+}][\mathrm{CO_3^{2-}}]/[\mathrm{HCO_3^-}] \tag{4.2}$$

At constant temperature and pressure, the energy content of a closed system is given by the Gibbs free energy $G$:

$$G = H - TS \tag{4.3}$$

where $H$ is the enthalpy, $T$ is the absolute temperature and $S$ is the entropy. In practice we are concerned with changes in free energy:

$$\Delta G = \Delta H - T\Delta S \tag{4.4}$$

Chemical equilibrium in a given system is attained when its free energy $G$ is at minimum. The free energy change associated with a reversible chemical reaction is related to the equilibrium constant $K$:

$$\Delta G = -RT \ln K \tag{4.5}$$

where $R$ is the gas constant. In natural waters, however, a number of effects might prevent the attainment of equilibrium. The real system is open to a flux of matter, and the throughput might be faster than the rate of conversion to more stable forms. Additionally, reactions can be extremely slow, such that equilibrium will not be reached over a foreseeable period of time. Many natural chemical processes are dominated by the slow precipitation or dissolution of solid phases. However, there are numerous homogeneous reactions in natural waters proceeding at rates that are very rapid compared to the residence times of the reacting components. Under these circumstances, equilibrium thermodynamics, which strictly only applies to closed systems, can be used to good approximation (*Clegg and Whitfield*, 1991). The importance of kinetic and biological factors to the chemistry of natural waters can to certain extent be assessed by equilibrium models, which provide clearly defined 'base lines'.

A quantitative understanding of the equilibrium solution chemistry of natural waters such as seawater ultimately relies on accurate estimations of activity coefficients of all the various components that make up the solution. The seawater ionic medium is a mixed electrolyte consisting of 11 major dissolved components ($Na^+$, $Mg^{2+}$, $Ca^{2+}$, $K^+$, $Sr^{2+}$, $Cl^-$, $SO_4^{2-}$, $Br^-$, $F^-$, $HCO_3^-$, $B(OH)_3$) that make up >99.95% of the total dissolved constituents (*Clegg and Whitfield*, 1991). This medium corresponds to a non-ideal solution characterized by strong and weak electrostatic interactions between the different constituent ions in solution. Modelling the thermodynamics of the seawater ionic medium requires calculation of solute activity coefficients ($\gamma$) and the osmotic coefficient ($\phi$), the latter being a function of the activity of water, $a_w$.

The theory of ionic solutions is based on the thermodynamics of gases. An ideal gas obeys Boyle's law and there are no specific interactions between the gas atoms or molecules. The concept of chemical potential arises from the need to consider changes in the free energies of individual chemical species, not just the system as a whole. Just as for free energy, we focus on differences in chemical potential, which is achieved by defining chemical potential with reference to a standard state. For a gas, the standard state is a pressure of 1 atmosphere, so that the chemical potential $\mu$ for an ideal gas is

$$\mu = \mu^0 + RT \ln P \tag{4.6}$$

where $\mu^0$ is the chemical potential at the standard state. From Section 2.4, the composition of a gas mixture can be expressed as partial pressures $p_i$ or mole fractions $x_i$. If the mixture consists of ideal gases, then for each component $i$ we can write

$$\mu_i = \mu_i^0 + RT \ln p_i \tag{4.7}$$

This direct dependence between chemical potential (free energy) and partial pressure is true only for ideal gases. Non-ideal gases (such as $CO_2$) do not follow Boyle's law and therefore the relationship between partial pressure and chemical potential does not hold.

Instead, the property fugacity, $f$, is defined, which follows the same form of equation for chemical potential

$$\mu_i = \mu_i^0 + RT \ln f_i \tag{4.8}$$

Similarly for aqueous solutions, the chemical potential cannot be directly related to chemical composition. Instead the activity ($a$) is defined, analogous to fugacity in the gas phase. Generally, the activity of a constituent $i$ is given by

$$a_i = \frac{f_i}{f_i^0} \approx \frac{p_i}{p_0} \tag{4.9}$$

where $f_i$ is the fugacity, $f_i^0$ is the fugacity in the standard state, and the $p_i$ values are the partial pressures. For all constituents, the activity ($a_i$) is equal to unity in the standard state and for a gas, the standard state is where the fugacity ($f_i$) is equal to unity. Furthermore, for a solvent such as water or a solid phase such as a mineral, the standard state is the pure substance. The activity of a dissolved constituent, $a_i$, is related to the solute activity coefficient $\gamma_i$ by (*Pitzer*, 1995):

$$a_i = \gamma_i m_i \tag{4.10}$$

where $m_i$ is the molality (mol $kg^{-1}$-$H_2O$). For solutes, the standard state occurs at infinite dilution, where $a_i/m_i = 1$ as $m_i \to 0$, i.e., when $y_i \to 1$. The activity of the $i$th constituent is related to the chemical potential $\mu_i$ by

$$\mu_i = \mu_i^\circ + RT \ln(a_i) = \mu_i^\circ + RT \ln(\gamma_i m_i), \tag{4.11}$$

In practical terms, the chemical potential can be considered as a chemical species' free energy per mole. At constant temperature and pressure, the chemical potential is identical to the partial molal (or molar) Gibbs free energy $\bar{G}_i$:

$$\mu_i = \bar{G}_i = \left(\frac{\delta G}{\delta n_i}\right)_{T,P,n_{j\neq i}}, \tag{4.12}$$

where the subscripts denote which state variables are held constant and $j \neq i$ means that the amounts of all constituents other than $i$ are held constant. The excess Gibbs energy ($G^{\text{ex}}$) is defined as the difference between the actual Gibbs energy ($G$) and that of an ideal solution ($G^{\text{id}}$):

$$G^{\text{ex}}(T,P,n_i) = G(T,P,n_i) - G^{\text{id}}(T,P,n_i) \tag{4.13}$$

The three terms, from left to right, are related to $\gamma_i$, $a_i$, and $m_i$ of Equation (4.10), respectively. The activity coefficient and the osmotic coefficient measure the degree to which solute concentrations and the activity of water depart from ideal solutions, respectively.

Since solutions are rarely ideal, much effort has been put into the development of models for estimating $\gamma_i$ and $\phi$. An early model based on statistical mechanics, which became a milestone in the exploration of electrolyte solutions, was developed by *Debye and Hückel* (1923). Their equations are:

$$\ln(\gamma_i) = -3A_\phi z_i^2 I^{i/2} \tag{4.14}$$

and

$$1-\phi = \frac{2A_\phi I^{3/2}}{\sum m_i} \tag{4.15}$$

where $z_i$ is the ionic charge, $A_\phi$ is the product of several fundamental constants and is given by:

$$A_\phi = \frac{1}{3}\left(\frac{2\pi N_A d_w}{1000}\right)^{1/2}\left(\frac{e^2}{\varepsilon kT}\right)^{3/2} \tag{4.16}$$

where $N_A$ is the Avogadro constant, $d_w$ is the solvent density, $e$ is the electronic charge, $\varepsilon$ is the dielectric constant, $k$ is the Boltzmann constant, and $T$ is the absolute temperature. At 25°C, $A_\phi = 0.3915$ (*Pitzer*, 1995). The ionic strength ($I$) is defined by (*Lewis and Randall*, 1921):

$$I = \frac{1}{2}\sum m_i z_i^2 \tag{4.17}$$

or in relation to salinity (e.g., *Dickson et al.*, 2007):

$$I = \frac{19.924S}{1000-1.005S} \tag{4.18}$$

Oceanic waters of salinity 35 have an ionic strength of ~0.72 mol kg$^{-1}$, which is considerably higher compared to surface waters of the Baltic Sea (~0.14). The osmotic coefficient ($\phi$) is related to the activity of water ($a_w$) through:

$$a_w = \exp\left(\frac{-\phi\sum m_i}{55.50844}\right) \tag{4.19}$$

where the constant in the denominator is equal to $1000/M_w$, where $M_w$ is the molecular weight of water.

The theory of Debye-Hückel is normally presented as the limiting and extended limiting law, or the extended Davies equation:

$$\log_{10}\gamma_\pm = \begin{cases} -A|z_+z_-|\sqrt{I} & I < 0.005 \\ -A|z_+z_-|\dfrac{\sqrt{I}}{1+aB\sqrt{I}} & I < 0.1 \\ -A|z_+z_-|\left(\dfrac{\sqrt{I}}{1+\sqrt{I}} - 0.2I\right) & I < 0.5 \end{cases} \tag{4.20}$$

where $z$ is the integer charge of the ions, $a$ is the empirical size of effective diameter of the ion in Ångström, and $A$ and $B$ are constants[2]. For the Davies equation, the second term ($0.2I$) is an empirical derivation and there are different values given in the literature (~0.15 - 0.33). The range of ionic strengths for which the Davies equation is suggested to be valid differs significantly in the literature (e.g., *Stumm and Morgan*, 1996; *Davies*, 1962; *Millero and Schreiber*, 1982).

Calculations of chemical potentials and modelling of chemical speciation in seawater currently use either Pitzer equations (e.g., *Clegg and Whitfield*, 1991; *Marion et al.*, 2011) or an ion-pairing approach (e.g., *Turner et al.*, 1981; *Dickson and Whitfield*, 1981).

## 4.1 Ion-pairing Models

The ion-pairing model, or the ion-association model, is one of the most popular methods to account for the ionic interactions in natural waters and was originally developed by *Bjerrum* (1926). The concept of the ion pairing model is based on the assumption that a fraction of anion-cation couples lose their electrolytic properties when their coulombic attraction is strong (*Dickson and Whitfield*, 1981). This model is based on the arbitrary assumption made by *Bjerrum* (1926) that two ions of opposite charge could be considered as forming a new species (an ion pair) if the distance between them is less than the value $q$ given by

$$q = \frac{z_+ z_- e}{2DkT} \tag{4.21}$$

where $z_i$ is the charge of the ion $i$, $e$ is is the electrostatic charge, $D$ is the dielectric constant of pure water, $k$ is the Boltzmann constant and $T$ is the absolute temperature. *Garrels and Thompson* (1962) were the first to use the Bjerrum hypothesis to calculate single-ion activity coefficients in seawater. In this model, the activity coefficient of each solute species is assumed to depend only on ionic strength. The activity of a free ion ($a_i$) is given by

$$a_i = [\mathrm{i}]_\mathrm{F} \gamma_\mathrm{F}(\mathrm{i}) \tag{4.22}$$

where $[\mathrm{i}]_\mathrm{F}$ is the concentration and $\gamma_\mathrm{F}(\mathrm{i})$ is the activity coefficient of the free or uncomplexed species $i$. The activity is also related to the total concentration $[\mathrm{i}]_\mathrm{T}$ and activity coefficient $\gamma_\mathrm{T}(\mathrm{i})$ by

$$a_i = [\mathrm{i}]_\mathrm{T} \gamma_\mathrm{T}(\mathrm{i}) \tag{4.23}$$

Therefore, the total activity coefficient is given by the following relationship:

$$\gamma_\mathrm{T}(\mathrm{i}) = \left( \frac{[\mathrm{i}]_\mathrm{F}}{[\mathrm{i}]_\mathrm{T}} \right) \gamma_\mathrm{F}(\mathrm{i}) = \alpha_i \gamma_\mathrm{F}(\mathrm{i}) \tag{4.24}$$

[2] $A = 1.82 \cdot 10^6 (\varepsilon T)^{3/2}$ and $B = 50.3 (\varepsilon T)^{-1/2}$ (*Stumm and Morgan*, 1996)

Free ions and ion pairs are considered to be in chemical equilibrium:

$$M^+ + X^- \longleftrightarrow MX \tag{4.25}$$

which is characterized by an association constant $K^*_{MX}$ given by:

$$K^*_{MX} = [MX]/[M^+][X^-] \tag{4.26}$$
$$K^*_{MX} = K_{MX}[\gamma_F(M)\gamma_F(X)/\gamma_F(MX)] \tag{4.27}$$

where $K_{MX}$ is the thermodynamic constant in pure water, $K^*_{MX}$ is the stoichiometric constant and $\gamma_F(i)$ is the free activity coefficients of species $i$. The free ion activity coefficients are usually estimated from $Cl^-$ and $K^+$ salts using the MacInnes convention (*MacInnes*, 1919), where $\gamma_K = \gamma_{Cl}$ at every ionic strength. The total concentrations of M and X are given by

$$[M]_T = [M]_F + \sum[MX] \tag{4.28}$$

$$[X]_T = [X]_F + \sum[MX] \tag{4.29}$$

where $\sum[MX]$ is the sum of all the various ion pairs in the solution. By combining these equations with Equation (4.24), the following expressions are derived

$$\alpha_M = [M]_F/[M]_T = (1 + \sum K^*_{MX}[X]_F)^{-1} \tag{4.30}$$
$$\alpha_X = [X]_F/[X]_T = (1 + \sum K^*_{MX}[M]_F)^{-1} \tag{4.31}$$

These equations, from which the total activity coefficients can be estimated, are solvable by iterative methods if $K^*_{MX}$ is known. The results depend on the quality of the values of $K^*_{MX}$, which are functions of ionic strength and the composition of the solution (*Millero*, 2001). Several computer programs have been developed for this kind of iterative problems, e.g., HALTAFALL (*Ingri et al.*, 1967). Since the pioneering work of *Garrels and Thompson* (1962), the ion-pairing model has been extensively used for seawater type solutions (see *Millero and Hawke*, 1992), as well as updated and extended (e.g., *Dickson and Whitfield*, 1981; *Turner et al.*, 1981). The updated model allows reliable estimates of activity coefficients for a number of major and minor ions of natural waters up to 1 m ionic strength at 25°C. However, the use of this model becomes troublesome at higher ionic strength and at other temperatures, due to the lack of reliable data. For seawater, about fifty association constants are needed. There are also difficulties associated with the determination of the activity coefficients of ion pairs (*Millero and Schreiber*, 1982). The dependence of the ionic strength on the association constant values, besides the fact that it makes this concept ambiguous, introduces complexity in the calculations. The ionic strength and association constants are inter-dependent,

which requires solving of several simultaneous complicated equations by an iterative method. These problems contributed to the fact that the ion-pairing model in its pure form has now, for most part, been abandoned (*Pierrot*, 2002). However, the CO2SYS (and other similar programs) is an example of an ion-pairing model adapted to a specific purpose, i.e., calulations of the carbonate system in seawater, which uses experimentally determined stoichiometric constants based on total concentrations, e.g., for carbonate $[CO_3]_T = [CO_3^{2-}] + [MgCO_3^0] + [CaCO_3^0] + [SrCO_3^0]$.

## 4.2 Pitzer Equations

The specific interaction model of *Pitzer* (1991) is one of the most widely used interaction models in order to account for non-ideal behavior of electrolytes, such as the seawater ionic medium. It treats strong electrolytes as completely dissociated, and the properties of the solutions are described, as far as possible, in terms of interactions between free ions, in contrast to the ion-pairing model (*Dickson and Whitfield*, 1981). The Pitzer model is based on an extension of the Debye-Hückel theory using a virial expansion of terms in increasing powers of molality for the expression of the excess Gibbs free energy ($G^{ex}$) (*Pitzer*, 1995):

$$\frac{G^{ex}}{RT} = w_w f(I) + \frac{1}{w_w}\sum\sum\lambda_{ij}(I)n_i n_j + \frac{1}{w_w^2}\sum\sum\sum\mu_{ijk}n_i n_j n_k \qquad (4.32)$$

where $w_w$ is the amount of water (kg) and $n_i$ is the moles of species $i$, i.e., $n_i/w_w = m_i$ which is the molality. Here $f(I)$ is a function of ionic strength and accounts for long-range electrostatic forces and corresponds to the right-hand terms in the Debye-Hückel expressions (Eqs. 4.14 and 4.15). Its final form is empirically chosen to best fit the experimental data. The binary interaction parameter, $\lambda_{ij}$ represents the short-range interactions in the presence of the solvent between solute species $i$ and $j$. It is dependent on ionic strength for ions, but not for neutral species. The ternary interaction parameter, $\mu_{ijk}$, is a similar quantity for triple solute interactions, which may be significant at higher concentrations, but has not been found experimentally to depend on ionic strength (*Pierrot*, 2002; *Pitzer*, 1991). These interaction terms thus account for ion-ion, ion-neutral, and neutral-neutral species interactions and similar triple particle interactions. These specific species interaction terms are critical at higher concentrations and distinguish the Pitzer approach from the Debye-Hückel approach. Fourth or higher order interactions can be added, but are only necessary for very concentrated solutions. The $\lambda_{ij}$ and $\mu_{ijk}$ terms are summed over all possible solute combinations. The full details of the Pitzer equations have been described elsewhere (*Pitzer*, 1995, 1991; *Millero and Pierrot*, 1998; *Pierrot*, 2002) and will not be repeated here.

A simple example is the carbonate system in sodium chloride solution (Paper II), the single-ion (and single-molecule) activity coefficients are given by

$$\begin{aligned}
\ln\gamma(\mathrm{H}^+) &= f^\gamma + 2m_{\mathrm{Cl}}(B_{\mathrm{HCl}} + m_{\mathrm{Cl}}C_{\mathrm{HCl}}) + m_{\mathrm{Na}}m_{\mathrm{Cl}}(B'_{\mathrm{NaCl}} + C_{\mathrm{NaCl}}) \\
&+ m_{\mathrm{Na}}(2\Theta_{\text{Na-H}} + m_{\mathrm{Cl}}\Psi_{\mathrm{HNaCl}}) \qquad (4.33) \\
\ln\gamma(\mathrm{HCO}_3^-) &= f^\gamma + 2m_{\mathrm{Na}}(B_{\mathrm{NaHCO_3}} + m_{\mathrm{Cl}}C_{\mathrm{NaHCO_3}}) + m_{\mathrm{Na}}m_{\mathrm{Cl}}(B'_{\mathrm{NaCl}} + C_{\mathrm{NaCl}}) \\
&+ m_{\mathrm{Cl}}(2\Theta_{\text{Cl-HCO}_3} + m_{\mathrm{Na}}\Psi_{\text{Cl-HCO}_3\text{-Na}}) \qquad (4.34) \\
\ln\gamma(\mathrm{CO}_3^{2-}) &= 4f^\gamma + 2m_{\mathrm{Na}}(B_{\mathrm{NaCO_3}} + m_{Cl}C_{\mathrm{NaCO_3}}) + 4m_{\mathrm{Na}}m_{\mathrm{Cl}}B'_{\mathrm{NaCl}} \\
&+ 2m_{\mathrm{Na}}m_{\mathrm{Cl}}C_{\mathrm{NaCl}} + m_{\mathrm{Cl}}(2\Theta_{\text{Cl-CO}_3} + 2^E\theta_{\text{Cl-CO}_3}) \\
&+ m_{\mathrm{Na}}\Psi_{\text{Na-Cl-CO}_3} \qquad (4.35) \\
\ln\gamma(\mathrm{CO_2}) &= 2m_{\mathrm{Na}}(\lambda_{\text{Na-CO}_2} + \lambda_{\text{Cl-CO}_2}) + m_{\mathrm{Na}}m_{\mathrm{Cl}}\xi_{\text{NaCl-CO}_2} \qquad (4.36)
\end{aligned}$$

The term $\Theta_{ij}$ is related to the interactions of similarly charged ions $i$ and $j$. The term $\Psi_{ijk}$ is related to the triple ionic interactions of two similarly charged ions with an ion of opposite charge. These mixing parameters are determined from mixtures of two electrolytes with a common ion. The $\lambda_{in}$ and $\xi_{ijn}$ paramaters account for interactions with neutral species ($n$). Note that this $\lambda$ term is different from that in Equation (4.32). The term ${}^E\theta$ accounts for unsymmetrical mixing effects (see *Pitzer*, 1991). The limiting law is given by

$$f^\gamma = -A_\phi\left[I^{1/2}/\left(1+1.2I^{1/2}\right) + 2/1.2\ln\left(1+1.2I^{1/2}\right)\right] \qquad (4.37)$$

The values of $B_{\mathrm{MX}}$, $B'_{\mathrm{MX}}$ and $C_{\mathrm{MX}}$ in Equations (4.33)-(4.35) are given by

$$\begin{aligned}
B_{\mathrm{MX}} &= \beta^{(0)}_{\mathrm{MX}} + \left(\beta^{(1)}_{\mathrm{MX}}/2I\right)\left[1-\exp\left(-2I^{1/2}\right)\left(1+2I^{1/2}\right)\right] \qquad (4.38) \\
B'_{\mathrm{MX}} &= \left(\beta^{(1)}_{\mathrm{MX}}/2I^2\right)\left[-1+\exp\left(-2I^{1/2}\right)\left(1+2I^{1/2}+2I\right)\right] \qquad (4.39) \\
C_{\mathrm{MX}} &= C^\phi_{\mathrm{MX}}/\left(2|z_{\mathrm{M}}z_{\mathrm{X}}|^{1/2}\right) \qquad (4.40)
\end{aligned}$$

where $\beta^{(0)}$, $\beta^{(1)}$ and $C^\phi$ are empirical interaction parameters, or Pitzer parameters. The osmotic coefficient for the simple system here is given by

$$\phi - 1 = f^\phi + m_{\mathrm{Na}}B^\phi_{\mathrm{NaCl}} + m_{\mathrm{Na}}m_{\mathrm{Cl}}C^\phi_{\mathrm{NaCl}} \qquad (4.41)$$

where

$$\begin{aligned}
\ln a_w &= -(2m_{\mathrm{NaCl}}/55.51)\phi \qquad (4.42) \\
f^\phi &= -A_\phi\left[I^{1/2}/\left(1+1.2I^{1/2}\right)\right] \qquad (4.43) \\
B^\phi_{\mathrm{NaCl}} &= \beta^{(0)}_{\mathrm{NaCl}} + \beta^{(1)}_{\mathrm{NaCl}}\exp\left(-2I^{1/2}\right) \qquad (4.44)
\end{aligned}$$

Equations (4.38)-(4.40) were developed using data for 1-1 and 1-2 electrolytes. In cases of other valence types, it was found that these equations also represented the properties of 3-1 and 4-1 electrolytes (*Pierrot*, 2002). However, for 2-2 electrolytes (e.g., $MgSO_4$) a fourth interaction parameter, $\beta^{(2)}$, was needed to obtain good agreement with the experimental data (e.g., *Pitzer and Mayorga*, 1974). The need for this $\beta^{(2)}$ term arises from the tendency for 2-2 salts to form ion pairs at low and moderate molalities (*Pierrot*, 2002, Papers V-VI) and *Pitzer and Mayorga* (1974) have shown that $\beta^{(2)}$ is related to the association equilibrium constant, $K$, by $\beta^{(2)} = -K/2$.

The Pitzer model is mathematically simple, involving only the summation of linear terms. However, extending a simple electrolyte towards the composition of the seawater ionic medium, requires extensive parameterization and the need for consistent datasets. The simple carbonate system in sodium chloride above requires 20 interaction parameters derived from 58 coefficients for temperature dependence. In general, parameterizations of interaction and mixing parameters of electrolytes have been determined at 25 °C (*Harvie et al.*, 1984; *Pitzer*, 1991). Several extensions of the 25 °C parameterizations have been made over the years for use in natural systems. At the time of writing, the modified MIAMI Ion Interaction Model (*Waters and Millero*, 2013; *Millero and Pierrot*, 1998; *Campbell et al.*, 1993; *Clegg and Whitfield*, 1995; *Millero and Roy*, 1997), which uses the equations of *Pitzer* (1991), is applicable primarily to major ions in seawater (from 0 to 50 °C, and 0 to >40 salinity) containing the species $H^+$, $Na^+$, $K^+$, $Mg^{2+}$, $Ca^{2+}$, $Sr^{2+}$, $Cl^-$, $Br^-$, $OH^-$, $HCO_3^-$, $B(OH)_4^-$, $HSO_4^-$, $SO_4^{2-}$, $CO_3^{2-}$, $CO_2$, $B(OH)_3$, and $H_2O$. The matrix of Pitzer model parameters for a major ion seawater of such composition is considerable: 40 sets of cation-anion interactions, and potentially 250 ternary or "mixture" parameters, each which may vary with temperature and pressure. The measurements that are used to build models of mixtures such as seawater include: solvent and solute activities, apparent molar enthalpies and heat capacities (yielding the variation of the model parameters with temperature), apparent molar volumes (the variation of the parameters with pressure), and other data.

Although the Pitzer model treats strong electrolytes as completely dissociated, it is compatible with the ion-pairing approach at lower molalities (*Whitfield*, 1975; *Millero and Pierrot*, 1998, Papers II and VI). For some electrolyte systems that tend to show stronger ion pairing, it becomes necessary to take ion-association constants into account in order to fit the data to within the experimental precision. The carbonic, sulfuric and phosphoric acid systems are such examples.

## 4.3 Monte Carlo Simulations

The common feature of the ion-pairing and specific interaction approaches to chemical speciation modelling is that they require a great deal of thermodynamic data, since they

include a large number of parameters whose values must be determined experimentally. In this work (Papers II and VI), an alternative approach, Monte Carlo (MC) modelling, was explored. This approach demands very little experimental data. All that is needed is the dependence of water's dielectric constant on temperature, and the hard sphere radii of the ions and molecules to be modelled. Monte Carlo modelling does, however, require extensive computing resources.

The Debye-Hückel theory, as well as the Monte Carlo method used in this work, is based on a dielectric continuum model where particles (ions and non-electrolytes) are treated as hard spheres with radii $r_i$ and charges $z_i$. The solvent (water) is described solely by its temperature dependent dielectric constant $\varepsilon_i$. This representation of an electrolyte is usually referred to as the unrestricted primitive model (UPM) (*Carley*, 1967), compared to the simpler restricted primitive model (RPM) (*Friedman*, 1960) that considers ions as charged hard spheres of equal size dissolved in a solvent represented by its bulk dielectric constant. The potential energy of a particle $i$ interacting with another particle $j$ is described using Coulomb's law according to the following conditions;

$$u(r_{ij}) = \begin{cases} \dfrac{z_i z_j e^2}{4\pi\varepsilon_0\varepsilon_r r_{ij}} & r_{ij} \geq r_i + r_j \quad \text{(long range)} \\ +\infty & r_{ij} < r_i + r_j \quad \text{(short range)} \end{cases} \tag{4.45}$$

Here $r_{ij}$ is the distance between the two particles, $\varepsilon_0$ is the permittivity of vacuum and $e$ is the elementary charge (charge of electron). The sum of the hard sphere radii, $r_i + r_j$ can be regarded as the distance of closest approach. At large separation, for example between two cations, this sum becomes neglible. The distances between particles decrease at higher concentrations, which leads to higher contribution from short-range interactions and hence the importance of the hard sphere radii is increased. The treatment of the solvent as a structure-less medium containing hard spheres is obviously an approximation but, for our applications, a fairly good one (Papers II and VI).

In contrast to the Debye-Hückel theory, where the distribution of charge is approximated by an ionic atmosphere, the primary goal of the Monte Carlo (MC) method is to find this distribution by simulating the positions of the ions in solution.

The MC method used in this work was developed by *Svensson and Woodward* (1988) and was performed by the standard Metropolis algorithm (*Metropolis et al.*, 1953). A Canonical ensemble was constructed by using a cubic box with periodic boundary conditions using large systems, i.e., up to >5000 particles (ions) as hard charged spheres. Next, particles are moved, one at the time, to new random positions. After each move, the total Coulomb energy $U$ is calculated by adding all particle interactions

$$U = \sum_{i=1}^{N-1} \sum_{j=i+1}^{N} u(r_{ij}) \tag{4.46}$$

If the energy is lowered after one such move, the configuration is accepted. If on the other hand, the move leads to an increase in energy, the configuration is accepted with the probability $\exp(-\beta\Delta U)$:

$$\begin{aligned} \Delta U &< 0 \qquad \text{Accept move} \\ \Delta U &> 0 \qquad \text{Accept if} \qquad \xi < \exp(-\beta\Delta U) \end{aligned} \tag{4.47}$$

where $\xi$ is a random number between 0 and 1. In this way the particle distribution is simulated and $U$ reaches a stable value and the system is assumed to represent equilibrium.

After the system is equilibrated, the displacement of particles continues where a particle $\alpha$ is inserted at a random position. This allows calculation of the energy required to add the particle to the system which, by definition, is equal to the chemical potential

$$\mu_\alpha = \left(\frac{\delta G}{\delta n_\alpha}\right)_{T,P,n} \tag{4.48}$$

The activity coefficient, i.e., the excess chemical potential, is calculated according to Widom's method (*Widom*, 1963):

$$\ln\gamma = -\ln\langle\exp[-\beta\Delta U_\alpha(r)]\rangle \tag{4.49}$$

Here $\beta$ is $1/k_B T$, where $k_B$ is the Boltzmann constant and T is the absolute temperature. The exponential term enclosed in the angular brackets is the ensemble average of the energy change, $\Delta U_\alpha$, of adding the particle. The original Widom method becomes less accurate when dealing with ionic systems of finite sizes, since the addition of a charged particle will violate electroneutrality in the cell. This effect can be reduced considerably by using very large systems, but such simulations require enormous computation times. Instead a charge rescaling method was used to re-establish electroneutrality in the computation cell (*Svensson and Woodward*, 1988, Papers II and VI).

# Chapter 5

# Summary

> "Högskolestudenten av idag är icke intelligentare och har icke heller bättre omdöme än förr. Men han har större hjärna om han har lärt sig göra bruk av datamaskinerna."
>
> David Dyrssen, *Svensk Kemisk Tidskrift 79:4* (1967)

## Paper I

Data collected in 1995 and 2008 in the Gotland Deep, under contrasting redox conditions, were evaluated with the objective to assess how pH couples to biogeochemical processes. The largest decrease in pH was observed in the layer where oxygen decreased from $\sim$300 $\mu$mol kg$^{-1}$ to about zero. When oxygen was low or hydrogen sulfide was present pH was nearly constant both in 1995 and 2008 at a low level of $\sim$7.2. Oxygen and sulfate were the major electron acceptors in remineralization of organic matter, while nitrate played a minor role in the low oxygen or anoxic environment. The small variability in pH under conditions of low oxygen concentrations indicated that Fe(III)- and Mn(IV)-oxides were of minor importance as electron acceptors during organic matter mineralization at this site. In oxic environments, observed data were consistent with mineralization of the model substance $(CH_2O)_{45}(CH_2)_{44}(NHCH_2CO)_{16}(CHPO_4Me)$. Under anoxic conditions, however, the observed changes in pH and DIC could be explained by mineralization of organic matter with significantly lower lipid content, e.g., material of terrestrial origin.

## Paper II

Stoichiometric dissociation constants of the carbon dioxide system in NaCl solution between 0 and 1 mol kg$^{-1}$ and 0 to 25 °C were estimated by Monte Carlo (MC) simula-

tions, and compared with Pitzer calculations and experimental measurements. The MC results are in good agreement with the experimental data as well as with the Pitzer calculations. This study shows that Monte Carlo simulations in the temperature and ionic strength range relevant to seawater can provide pK values of the same quality as Pitzer calculations, and constitutes the first step in developing a temperature-dependent MC model for seawater.

## Paper III

Large-scale patterns of net community production (NCP) were estimated during the late summer cruise ARK-XXVI/3 (TransArc, Aug/Sep 2011) to the central Arctic Ocean. Several approaches were used based on: (i) continuous measurements of surface water oxygen to argon ratios ($O_2$/Ar), (ii) underway measurements of surface partial pressure of carbon dioxide ($pCO_2$), (iii) discrete samples of dissolved inorganic carbon (DIC), and (iv) dissolved inorganic nitrogen and phosphate. The NCP estimates agreed relatively well within the uncertainties associated with each approach. The highest late summer NCP (up to 6 mol C $m^{-2}$) were observed in the marginal sea ice zone region. Low values ($< 1$ mol C $m^{-2}$) was found in the sea-ice covered deep basins, with a strong spatial variability. Lowest values were found in the Amundsen Basin and moderate values were observed in the Nansen and Makarov Basins, with slightly higher estimates over the Mendeleev Ridge. Our findings support a coupling of NCP to sea ice coverage and nutrient supply and thus stress a potential change in spatial and temporal distribution of NCP in a future Arctic Ocean. To follow the evolution of NCP in space and time, it is suggested to apply one or several of these approaches in shipboard investigations with a time interval of three to five years.

## Paper IV

Subsurface waters of the central Arctic Ocean were investigated for temporal trends over the last two decades using concentrations of dissolved inorganic carbon (DIC), total alkalinity (TA), nutrients, and oxygen data from six cruises between 1991 to 2011, covering the Nansen, Amundsen and Makarov Basins. In each basin, for each property, differences were computed between the mean concentrations of the Arctic Atlantic Water (AAW) and the upper Polar Deep Water (uPDW), relative to the deep waters. In the intermediate water masses, significant positive time trends for DIC are observed, ranging from 0.6 to 0.9 $\mu$mol $kg^{-1}$ $y^{-1}$ (AAW) and 0.4 to 0.6 $\mu$mol $kg^{-1}$ $y^{-1}$ (uPDW). Absence of time trends in nutrients indicates no change in the rate of organic matter remineralization. Consequently, the buildup of DIC is attributed to increasing concentrations of anthropogenic carbon ($C_{ant}$) in the waters flowing into these depth layers of the Arctic

Ocean. The resulting rate of increase of the column inventory of $C_{ant}$ is estimated to be between 0.6 and 0.9 mol C $m^{-2}$ $yr^{-1}$, depending on the basin.

## Paper V

Significant excess alkalinity, of the order of 30 $\mu$mol $kg^{-1}$ and attributed to dissolved organic matter, has recently been measured in the Baltic Sea. Chemical speciation modelling shows that the measured excess alkalinity is consistent with an organic alkalinity derived from dissolved organic carbon, assuming that this dissolved organic carbon consists entirely of terrestrial humic substances. The contribution of polydisperse material such as humic substances to titration alkalinity invalidates the assumptions on which the current definition of titration alkalinity is based. It is therefore concluded that alkalinity should not be one of the parameters used to characterise the $CO_2$ system in organic-rich waters. The use of a simple relationship to estimate organic alkalinity from the dissolved organic carbon concentration is assessed for the limited Baltic Sea data set currently available.

## Paper VI

Mean salt activity coefficients of a simplified seawater electrolyte ($Na^+$, $Mg^{2+}$, $Ca^{2+}$, $Cl^-$, $SO_4^{2-}$) at varying salinity (5-40) and temperature (0-25 °C) were estimated by Monte Carlo (MC) simulations, and compared with Pitzer calculations. The MC simulations used experimentally determined dielectric constants of water at different temperatures, and optimal agreement with the experimental data and Pitzer calculations was achieved by adjusting the ionic radii. The results, together with a previous study of the carbon dioxide system in sodium chloride solution (Paper II), suggest that a complete Monte Carlo description of seawater activity coefficients may be achievable using the hard sphere approach with a very limited number of fitted parameters (effective ionic radii), in contrast to the large number of fitted parameters required for a Pitzer model.

# Chapter 6

# Future Outlook

"*Columnia regi sapienta*"

*Christina Regina Sueciae* (1632-1654)

Although the marine carbonate system is well-defined in theory, intriguing issues arise when implemented in practice. Inconsistencies between calculated and measured parameters can to some extent be traced back to the analytical procedures in use with respect to accuracy and precision. However, there are still inconsistencies reported within the marine communities that slip through unexplained. The evaluation of the internal consistency of the marine carbonate system relies on underlying thermodynamic principles. For example, the various acid-base systems in a seawater sample are assumed to be completely known and in equilibrium. It is assumed that these acid-base systems are well-characterized by equilibrium constants defined with ionic medium standard states, and that these can be closely approximated by concentration quotients that are a function of salinity, temperature, and pressure. This is seldom the case in a natural open system such as seawater, but reasonable consistency is most often achievable if care is taken during sampling, analysis, and evaluation. However, in coastal and estuarine systems, the available sets of stoichiometric constants risk to fail due to deviating ionic composition and abundant presence of organic protolytes compared to standard oceanic seawater. Determination of new dissociation constants of carbonic acid, e.g., for the Baltic Sea, would be a well-needed effort. There is also a need for the development of state-of-the-art analytical methods for measurements of the carbonate system parameters in anoxic and sulphidic waters, particularly in the wake of expanding hypoxia in the Baltic Sea and generally for coastal systems globally. The contribution of weak organic protolytes to total alkalinity needs to be further studied, both in coastal and oceanic systems. This is important for biogeochemical modelling as well as for the analytical procedures and subsequent evaluation. It is also desirable to complement the existing environmental

monitoring repertoire in the Baltic Sea with measurements of dissolved inorganic carbon. This would be an important contribution to the constrainment of the Baltic carbon cycle and an extra means of validation for the extensive modelling efforts that are being done in the Baltic Sea, underlying the management of the Baltic Sea Action Plan and policy making in the Baltic region.

Although there has been an increased sampling in recent years, the Arctic Ocean remains a highly under-sampled system despite its role in the global carbon cycle and Earth's climate. In order to understand the physical and biogeochemical processes in this system, it is important to accelerate the collection of data, both temporally and spatially. Most shipbased studies in this region are performed during the Arctic summer, when the sea ice conditions are more forgiving. Buoys, moorings, and ice-tethered profilers provide long time-series data, but mainly of physical parameters. Development of long-term stable sensors for the parameters of the carbonate system in Arctic conditions is desirable, but remains a challenge. As a complement to conventional discrete sampling, underway measurements provide the higher temporal or spatial resolution, although exclusive for the uppermost layer. Underway measurments of $pCO_2$ has been used extensively and important information on the dynamics of the surface carbonate system has been obtained. Preferably, these measurements should be complimented to a larger extent by, e.g., underway methods for measurements of DIC, pH, $O_2$/Ar, which are already available. The use of high-resolution continuous measurements is crucial in elucidating the spatial and temporal variability of the biogeochemical processes that governs the carbon cycling in the Arctic Ocean, processes that are likely to be missed by conventional discrete sampling. However, within the ice-covered deep basins of the Arctic, the gas exchange is still poorly constrained. Extensive studies are needed to elucidate the role of gas exchange, and what role it will have for the air-sea gas exchange in future scenarios with declining sea ice extent.

The changes in the sea ice cover of the Arctic Ocean, observed and predicted for the future, will likely have substantial impact on the fluxes of chemical constituents as well as the ventilation of deep waters. Moving from a state where the biological productivity mainly has been confined to the shelf areas to a situation with much more biological activity over the deep central basins, notably an increase in export production, changes the biogeochemistry of the deep and bottom waters. With more sedimentation of organic matter to the deep layers, remineralization increases which results in elevated bottom water nutrient and dissolved carbon concentrations, and decrease in oxygen concentration. The larger seasonal ice production, possibly in combination with a higher surface water salinity if mixing of the upper water layers increases, results in more brine formation that contribute to deep water formation. Standing on the threshold of these unprecedented changes, there is a strong need for high quality studies of relevant properties of the full water column and the biologically productive surface waters of the central Arctic Ocean on a regular basis within international collaborations.

The use of computer programs to carry out chemical speciation and other complex calculations for aqueous solutions and natural waters has traditionally involved obtaining the program from the authors, understanding the probably idiosyncratic input and output facilities (only intended for the authors' use), and learning to use the program without instructions or documentation. These obstacles have hampered the use of state-of-the-art models and the spread of best practice in modelling. Therefore, there is a strong need for the developement of a user-friendly, well-documented, multi-platform software package as well as a compilation of a consistent, quality-controlled database of Pitzer parameters, adapted for the range of salinity (0 - 35, concentrated brines), temperature (-2 - 40°C), and pressure (1 - 1000 atm) that are likely to be of interest in natural waters. This also applies to chemical speciation modelling of trace metals and their complexation with both inorganic and organic ligands, which need extensive parameterization and characterization.

In summary, the marine carbonate system is a well-known, and at the same time an intriguingly complex, chemical system of utter importance to the global biogeochemical cycling of carbon and to Earth's climate. Our understanding of the marine carbon cycle has increased immensely during the last few decades as a result of accurate and precise observations of the marine carbonate system, although still with large temporal and spatial gaps. In constrast to the chemistry, our knowledge of potential feedbacks from its natural components is much more uncertain. The biological responses to these are extremely hard to assess, particularly in the wake of the changing climate. Although much effort has been put into manipulative small- and medium-scale experiments to identify and quantify these, it remains a challenge to extrapolate these to a gobal scale, both in space and time.

Thus, in the composition of seawater the carbonic acid, on account of its intimate relations to life, still forms an item of particular interest.

# Acknowledgments

The work presented in this thesis and my time as a PhD student at the Department of Chemistry and Molecular Biology, University of Gothenburg, have been financially supported by: the Swedish Research Council Formas (contract no 214-2008-1383), the Swedish Research Council (contract no 621-2010-4084), the European Union project EPOCA (contract 211384), the European Union project CarboChange (project reference 264879), the Royal Swedish Academy of Sciences, the YMER-80 Foundation, ÅForsk (Ångpanneföreningen's Foundation for Research and Development), Selma and Fritz Kreisky's Foundation, the Adlerbert Foundation, and Paul and Marie Berghaus' Foundation.

---

Handledare docent Leif Anderson, professor i hydrosfärsvetenskap med inriktining mot marin kemi tillika Kungliga Vetenskapsakademins 1:e vice preses, det har varit en stor ära att få vara en del av din forskargrupp och allt som hör därtill, städse stöttande och uppmuntrande med kloka ord. Onekligen modigt att släppa iväg en novis till Nordpolen, och för detta är jag evigt tacksam. Det har varit en oerhört lärorik, frustrerande och episk resa, tack för allt! Även om kontoret ser ut som ett slagfält i skrivande stund, så är jag djupt tacksam för att ha haft marinkemins födsel, barndom, ungdom och bästa år att luta mig tillbaka mot. Med förhoppningar om ett smärtfritt första och sista ben!

Biträdande handledare doktor David Turner, professor i marin kemi, Sveriges främste marinkemist alla kategorier. Ett fantastiskt stort tack för visat tålamod och för utforskningen av den djupaste av djunglar. Blickar förväntansfullt mot framtiden!

Vice biträdande handledare docent Stefan Hulth, professor i mikrobiell marin kemi, alltid stöttande med sprudlande entusiasm och tjôt. Jag överlåter Kommandocentralen med varm hand.

Examinator docent Margareta Wedborg, professor i marin analytisk kemi, facit vad gäller examinatorskap. Stort tack för gott arbete under dessa år. Det har varit ett sant nöje att läsa dina alster. Ses i publiken!

An especially warm acknowledgement to all amazing co-authors: Zareen, Steven, Mario, Meri, Gerhard, Karol, and Nicolas. Your expertise and smooth collaboration has been a true pleasure to experience. Steven, you certainly gave 'nitpicking' a new meaning, highly appreciated. Thanks to Luke Gregor and Robin Matthews for contributing to the progress of this thesis.

I would like to thank the Captain, officers, crew, and chief scientist Ursula Schauer of the ARK-XXVI/3 expedition to the North Pole with FS Polarstern, for your helpfulness, dedication and professionalism. Many thanks to all in the scientific party for making this

a truly unforgettable cruise. Special thanks to the ever so helpful and friendly Sea-Ice Physics group.

Mario and Nicolas, it is the highest honor and a rare luxury to be part of the NPBBs.

Ola, sann vän och livsnjutare, väl kämpat! Tack för att du lockade in mig i candn. Många trevliga stunder har det blivit, i och utanför huset, på min ära. Vi ses i No'n bland gjusar och tak!

Stina, sista tiden hade varit fantastisk seg utan dig. Det har blivit många sena kvällar oavsett veckodag, men med pepp, hopp och inspiration. Tack och hoppas på riklig skörd!

Anna, starkt jobbat! Stort tack för alla dessa år, framför allt detta. För framtiden ryck in, marsch!

Ylva, helt klart den mest exemplariska expeditionskollega och medförfattare man kan tänka sig. Tack!

Tack till alla nuvarande och tidigare AMKare för att ni har gjort arbetsplatsen till ett sant nöje att gå till. Särskilt tack till Sara, Sofia, Johan E, Erik, Anders, Katarina, Martin A, Martin H, Per, Dasha, Misha, Melissa, My, Madeleine, Karin och Geert. Tack Julian för alla tips!

Thanks to all the people at the 4th floor for all the niceties. Tang Soo to all in GTSD!

Tack till alla mina vänner, gamla och trogna som nyfunna. Ni är på tok för många för att räkna upp, men ni vet vilka ni är och har alltid en plats i mitt hjärta.

Mårten, Johannes, Björn och Richard, tack för alla otaliga timmars trevligheter och mörrs. Hoppas på framtida motsvarigheter! Särskilt tack till Kuma för markunderstöd och lingvistisk magi. Suiton! Kura-ken no jutsu!

o o/ o(((7)))
Lämna av! vStrpC Drgtrp 517 FTP1 FoMZT Brennan, enastående sambandskontroll och understödsverksamhet under alla dessa år. Mycket bra! Jag ser ljust på framtiden (AZ2, kaimu, NBT, WDG, NH-tårta och 7G). Stäng flikar till höger 2!
o7 o

David, käre storebror, du är min förebild när det gäller det mesta. Tack för att du och din underbara familj, Lotta, Linnea, Love, Leon, Tesla och Kitty, finns och förgyller mitt liv! Tack Castro, Molly och Milo, immunologisk förmedlad överkänslighet till trots.

Mamma och Pappa, utan er hade ju det här aldrig gått. Min tacksamhet och kärlek går inte att beskriva nog med ord. Ni är och förblir mina förebilder och jag hoppas innerligen att jag får möjligheten att vara ert stöd och inspirationskälla i framtiden.

*Göteborg, 27 April 2014*

# References


Aksenov, Y., S. Bacon, A. C. Coward, and A. J. G. Nurser (2010), The North Atlantic inflow to the Arctic Ocean: High-resolution model study, *Journal of Marine Systems*, *79*(1-2), 1–22, doi:10.1016/j.jmarsys.2009.05.003.

Algesten, G., J. Wikner, S. Sobek, L. J. Tranvik, and M. Jansson (2004), Seasonal variation of $CO_2$ saturation in the Gulf of Bothnia: Indications of marine net heterotrophy, *Global Biogeochemical Cycles*, *18*(4), GB4021, doi:10.1029/2004GB002232.

Algesten, G., et al. (2006), Organic carbon budget for the Gulf of Bothnia, *Journal of Marine Systems*, *63*(3-4), 155–161, doi:10.1016/j.jmarsys.2006.06.004.

Almroth-Rosell, E., K. Eilola, R. Hordoir, H. E. M. Meier, and P. O. J. Hall (2011), Transport of fresh and resuspended particulate organic material in the Baltic Sea - a model study, *Journal of Marine Systems*, *87*(1), 1–12, doi:10.1016/j.jmarsys.2011.02.005.

Anderson, L. A., and J. L. Sarmiento (1994), Redfield ratios of remineralization determined by nutrient data analysis, *Global Biogeochemical Cycles*, *8*(1), 65–80, doi:10.1029/93GB03318.

Anderson, L. G., and A. Olsen (2002), Air-sea flux of anthropogenic carbon dioxide in the North Atlantic, *Geophysical Research Letters*, *29*(17), 1835, doi:10.1029/2002GL014820.

Anderson, L. G., et al. (1994), Water masses and circulation in the Eurasian Basin: Results from the Oden 91 expedition, *Journal of Geophysical Research: Oceans*, *99*(C2), 3273–3283, doi:10.1029/93JC02977.

Anderson, L. G., K. Olsson, E. P. Jones, M. Chierici, and A. Fransson (1998), Anthropogenic carbon dioxide in the Arctic Ocean: Inventory and sinks, *Journal of Geophysical Research: Oceans*, *103*(C12), 27,707–27,716, doi:10.1029/98JC02586.

Anderson, L. G., D. R. Turner, M. Wedborg, and D. Dyrssen (1999), Thermodynamic calculations of the $CO_2$ system in seawater, in *Methods of Seawater Analysis*, edited by K. Kremling and M. Ehrhards, pp. 141–148, third edition, Wiley-VCH, Weinheim, Germany.

Anderson, L. G., S. Jutterström, S. Hjalmarsson, I. Wrahlström, and I. P. Semiletov (2009), Out-gassing of $CO_2$ from Siberian Shelf seas by terrestrial organic matter decomposition, *Geophysical Research Letters*, *36*(20), L20,601, doi:10.1029/2009GL040046.

Bates, N. R. (2006), Air-sea $CO_2$ fluxes and the continental shelf pump of carbon in the Chukchi Sea adjacent to the Arctic Ocean, *Journal of Geophysical Research*, *111*(C10), doi: 10.1029/2005jc003083.

Bates, N. R., and J. T. Mathis (2009), The Arctic Ocean marine carbon cycle: evaluation of air-sea $CO_2$ exchanges, ocean acidification impacts and potential feedbacks, *Biogeosciences*, *6*(11), 2433–2459, doi:10.5194/bg-6-2433-2009, bG.

Bates, N. R., et al. (2014), A time-series view of changing ocean chemistry due to ocean uptake of anthropogenic $CO_2$ and ocean acidification, *Oceanography*, *27*(1), 126–141, doi: 10.5670/oceanog.2014.16.

Bates, R. G. (1948), Definitions of pH Scales, *Chemical Reviews*, *42*(1), 1–61, doi: 10.1021/cr60131a001.

Beldowski, J., A. Löffler, B. Schneider, and L. Joensuu (2010), Distribution and biogeochemical control of total $CO_2$ and total alkalinity in the Baltic Sea, *Journal of Marine Systems*, *81*(3), 252–259, doi:10.1016/j.jmarsys.2009.12.020.

Bjerrum, N. (1926), Ion association. I. Influence of ionic association on the activity of ion at moderate degree of association, *Kgl. Danske Videnskab Selskab. Mat-Fys. Medd.*, *7*(9), 1–48.

Björk, G., et al. (2010), Flow of Canadian basin deep water in the Western Eurasian Basin of the Arctic Ocean, *Deep Sea Research Part I*, *57*(4), 577–586, doi:10.1016/j.dsr.2010.01.006.

Boetius, A., et al. (2013), Export of Algal Biomass from the Melting Arctic Sea Ice, *Science*, *339*(6126), 1430–1432, doi:10.1126/science.1231346.

Borges, A. V., and N. Gypens (2010), Carbonate chemistry in the coastal zone responds more strongly to eutrophication than ocean acidification, *Limnology and Oceanography*, *55*(1), 346–353, doi:10.4319/lo.2010.55.1.0346.

Bourgain, P., J. C. Gascard, J. Shi, and J. Zhao (2013), Large-scale temperature and salinity changes in the upper Canadian Basin of the Arctic Ocean at a time of a drastic Arctic Oscillation inversion, *Ocean Sci.*, *9*(2), 447–460, doi:10.5194/os-9-447-2013, oS.

Brewer, P. G. (1978), Direct observation of the oceanic $CO_2$ increase, *Geophysical Research Letters*, *5*(12), 997–1000, doi:10.1029/GL005i012p00997.

Broecker, W. S. (1971), A kinetic model for the chemical composition of sea water, *Quaternary Research*, *1*(2), 188–207, doi:10.1016/0033-5894(71)90041-X.

Buch, K. (1951), Das Kohlensäure Gleichgewichtsystem im Meerwasser: Kritische Durchsicht und Neuberechnungen der Konstituenten, *Merentutkimuslaioksen Julkaisu, Havsforskningsinstitutets skrift*, *151*, 1–18.

Buck, R., et al. (2002), Measurement of pH. Definition, standards, and procedures (IUPAC Recommendations 2002), *Pure and Applied Chemistry*, *74*(11), 2169–2200, doi: 10.1351/pac200274112169.

Bustos-Serrano, H. (2010), The Carbonate System in Natural Waters, *Open Access Dissertations*, *Paper 493*, University of Miami.

Byrne, R. (2002), Inorganic speciation of dissolved elements in seawater: the influence of pH on concentration ratios, *Geochemical Transactions*, *3*(1), 11–16, doi:10.1186/1467-4866-3-11.

Byrne, R. H. (2014), Measuring Ocean Acidification: New Technology for a New Era of Ocean Chemistry, *Environmental Science & Technology*, doi:10.1021/es405819p.

Byrne, R. H., and W. Yao (2008), Procedures for measurement of carbonate ion concentrations in seawater by direct spectrophotometric observations of Pb(II) complexation, *Marine Chemistry*, *112*(1-2), 128–135, doi:10.1016/j.marchem.2008.07.009.

Byrne, R. H., X. Liu, E. A. Kaltenbacher, and K. Sell (2002), Spectrophotometric measurement of total inorganic carbon in aqueous solutions using a liquid core waveguide, *Analytica Chimica Acta*, *451*(2), 221–229, doi:10.1016/S0003-2670(01)01423-4.

Cai, P., M. Rutgers van der Loeff, I. Stimac, E. M. Nöthig, K. Lepore, and S. B. Moran (2010a), Low export flux of particulate organic carbon in the central Arctic Ocean as revealed by $^{234}$Th:$^{238}$U disequilibrium, *Journal of Geophysical Research: Oceans*, *115*(C10), C10,037, doi:10.1029/2009JC005595.

Cai, W. J., et al. (2010b), Decrease in the $CO_2$ Uptake Capacity in an Ice-Free Arctic Ocean Basin, *Science*, *329*(5991), 556–559, doi:10.1126/science.1189338.

Caldeira, K., and M. E. Wickett (2003), Oceanography: Anthropogenic carbon and ocean pH, *Nature*, *425*(6956), 365–365, 10.1038/425365a.

Campbell, D. M., F. J. Millero, R. Roy, L. Roy, M. Lawson, K. M. Vogel, and C. Porter Moore (1993), The standard potential for the hydrogen-silver, silver chloride electrode in synthetic seawater, *Marine Chemistry*, *44*(2-4), 221–233, doi:10.1016/0304-4203(93)90204-2.

Carley, D. D. (1967), Radial Distributions of Ions for a Primitive Model of an Electrolyte Solution, *The Journal of Chemical Physics*, *46*(10), 3783–3788, doi:10.1063/1.1840451.

Carstensen, J., et al. (2014), Hypoxia in the Baltic Sea: Biogeochemical Cycles, Benthic Fauna, and Management, *AMBIO*, *43*(1), 26–36, doi:10.1007/s13280-013-0474-7.

Carter, B., J. Radich, H. Doyle, and A. G. Dickson (2013), An automated system for spectrophotometric seawater pH measurements, *Limnology and Oceanography: Methods*, *11*, 16–27, doi:10.4319/lom.2013.11.16.

Chen, C.-T. A., and A. V. Borges (2009), Reconciling opposing views on carbon cycling in the coastal ocean: Continental shelves as sinks and near-shore ecosystems as sources of atmospheric $CO_2$, *Deep Sea Research Part II*, *56*(8-10), 578–590, doi:10.1016/j.dsr2.2009.01.001.

Chen, G.-T., and F. J. Millero (1979), Gradual increase of oceanic $CO_2$, *Nature*, *277*(5693), 205–206, 10.1038/277205a0.

Chierici, M., A. Fransson, and L. G. Anderson (1999), Influence of m-cresol purple indicator additions on the pH of seawater samples: correction factors evaluated from a chemical speciation model, *Marine Chemistry*, *65*(3-4), 281–290, doi:10.1016/S0304-4203(99)00020-1.

Clayton, T. D., and R. H. Byrne (1993), Spectrophotometric seawater pH measurements: total hydrogen ion concentration scale calibration of m-cresol purple and at-sea results, *Deep Sea Research Part I*, *40*(10), 2115–2129, doi:10.1016/0967-0637(93)90048-8.

Clayton, T. D., R. H. Byrne, J. A. Breland, R. A. Feely, F. J. Millero, D. M. Campbell, P. P. Murphy, and M. F. Lamb (1995), The role of pH measurements in modern oceanic $CO_2$-system characterizations: Precision and thermodynamic consistency, *Deep Sea Research Part II*, *42*(2-3), 411–429, doi:10.1016/0967-0645(95)00028-O.

Clegg, S., and M. Whitfield (1991), Activity coefficients in natural waters, in *Activity Coefficients in Electrolyte Solutions, 2nd edition*, edited by K. S. Pitzer, pp. 279–434, CRC Press, Boca Raton, Florida.

Clegg, S. L., and M. Whitfield (1995), A chemical model of seawater including dissolved ammonia and the stoichiometric dissociation constant of ammonia in estuarine water and seawater from -2 to 40°C, *Geochimica et Cosmochimica Acta*, *59*(12), 2403–2421, doi:10.1016/0016-7037(95)00135-2.

Codispoti, L. A., C. Flagg, V. Kelly, and J. H. Swift (2005), Hydrographic conditions during the 2002 SBI process experiments, *Deep Sea Research Part II*, *52*(24-26), 3199–3226, doi:10.1016/j.dsr2.2005.10.007.

Codispoti, L. A., V. Kelly, A. Thessen, P. Matrai, S. Suttles, V. Hill, M. Steele, and B. Light (2013), Synthesis of primary production in the Arctic Ocean: III. Nitrate and phosphate based estimates of net community production, *Progress in Oceanography*, *110*, 126–150, doi:10.1016/j.pocean.2012.11.006.

Covington, A., R. Bates, and R. Durst (1985), Definition of pH sclaes, standard reference values, measurement of pH and related terminology, *Pure and Applied Chemistry*, *57*(3), 531–542, doi:0.1351/pac198557030531.

Davies, C. W. (1962), *Ion association*, 190 pp., Butterworths, London, UK.

Debye, P., and E. Hückel (1923), Zur Theorie der Elektrolyte. I. Gefrierpunktserniedrigung und verwandte Erscheinungen, *Physikalische Zeitschrift*, *24*(9), 185–206.

Denman, K. L., et al. (2007), Couplings between changes in the climate system and biogeochemistry, in *Climate Change 2007: The Physical Science Basis. Contribution of Working Group I to the Fourth Assessment Report of the Intergovernmental Panel on Climate Change*, edited by S. Solomon, D. Qin, M. Manning, Z. Chen, K. B. Marquis, M. Averyt, M. Tignor, and H. L. Miller, Cambridge University Press, Cambridge, United Kingdom and New York, NY, USA.

Dethleff, D. (2010), Dense water formation in the Laptev Sea flaw lead, *Journal of Geophysical Research: Oceans*, *115*(C12), C12,022, doi:10.1029/2009JC006080.

Dickson, A. G. (1981), An exact definition of total alkalinity and a procedure for the estimation of alkalinity and total inorganic carbon from titration data, *Deep Sea Research Part A*, *28*(6), 609–623, doi:10.1016/0198-0149(81)90121-7.

Dickson, A. G. (1984), pH scales and proton-transfer reactions in saline media such as sea water, *Geochimica et Cosmochimica Acta*, *48*(11), 2299–2308, doi:10.1016/0016-7037(84)90225-4.

Dickson, A. G. (1990), Standard potential of the reaction: $AgCl(s) + 1/2H_2(g) = Ag(s) + HCl(aq)$, and the standard acidity constant of the ion $HSO_4^-$ in synthetic sea water from 273.15 to 318.15 K, *The Journal of Chemical Thermodynamics*, *22*(2), 113–127, doi:10.1016/0021-9614(90)90074-Z.

Dickson, A. G. (1993), The measurement of sea water pH, *Marine Chemistry*, *44*(2-4), 131–142, doi:10.1016/0304-4203(93)90198-W.

Dickson, A. G. (2010), Standards for ocean measurements, *Oceanography*, *23*(3), 34–47, doi:10.5670/oceanog.2010.22.

Dickson, A. G., and F. J. Millero (1987), A comparison of the equilibrium constants for the dissociation of carbonic acid in seawater media, *Deep Sea Research Part A*, *34*(10), 1733–1743, doi:10.1016/0198-0149(87)90021-5.

Dickson, A. G., and M. Whitfield (1981), An ion-association model for estimating acidity constants (at 25 °C and 1 atm. pressure) in electrolyte mixtures related to seawater (ionic strength $< 1$ mol $kg^{-1}H_2O$), *Marine Chemistry*, *10*, 315–333.

Dickson, A. G., J. D. Afghan, and G. C. Anderson (2003), Reference materials for oceanic $CO_2$ analysis: a method for the certification of total alkalinity, *Marine Chemistry*, *80*(2-3), 185–197, doi:10.1016/S0304-4203(02)00133-0.

Dickson, A. G., C. L. Sabine, and J. R. Christian (2007), *Guide to best practices for ocean $CO_2$ measurements*, PICES Special Publication, 173 pp., North Pacific Marine Science Organization (PICES), Sidney, British Columbia.

DOE (1994), in *Handbook of Methods for the Analysis of the Various Parameters of the Carbon Dioxide System in Seawater, version 2*, edited by A. G. Dickson and C. Goyet, ORNL/CDIAC-74.

Doney, S. C., V. J. Fabry, R. A. Feely, and J. A. Kleypas (2009), Ocean Acidification: The Other $CO_2$ Problem, *Annual Review of Marine Science*, *1*(1), 169–192, doi: 10.1146/annurev.marine.010908.163834.

Dugdale, R. C., and J. J. Goering (1967), Uptake of new and regenerated forms of nitrogen in primary productivity, *Limnology and Oceanography*, *12*(2), 196–206.

Dyrssen, D. (1965), A Gran Titration of Sea Water on Board Sagitta, *Acta Chemica Scandinavica*, *19*(5), 1265, doi:10.3891/acta.chem.scand.19-0653.

Dyrssen, D. (1993), The Baltic-Kattegat-Skagerrak estuarine system, *Estuaries*, *16*(3), 446–452, doi:10.2307/1352592.

Dyrssen, D., and L. G. Sillén (1967), Alkalinity and total carbonate in sea water. A plea for p-T-independent data, *Tellus*, *19*(1), 113–121, doi:10.1111/j.2153-3490.1967.tb01464.x.

Dyrssen, D., and L. R. Uppström (1974), The boron/chlorinity ratio in Baltic sea water, *Ambio*, *3*, 44–46.

Easley, R. A., M. C. Patsavas, R. H. Byrne, X. Liu, R. A. Feely, and J. T. Mathis (2012), Spectrophotometric Measurement of Calcium Carbonate Saturation States in Seawater, *Environmental Science & Technology*, *47*(3), 1468–1477, doi:10.1021/es303631g.

Edman, M. (2013), Modelling the Dissolved Inorganic Carbon System in the Baltic Sea, *Doctoral thesis*, *University of Gothenburg, Gothenburg, Sweden*.

Emeis, K. C., U. Struck, T. Leipe, F. Pollehne, H. Kunzendorf, and C. Christiansen (2000), Changes in the C, N, P burial rates in some Baltic Sea sediments over the last 150 years-relevance to P regeneration rates and the phosphorus cycle, *Marine Geology*, *167*(1-2), 43–59.

Falkowski, P. G., E. A. Laws, R. T. Barber, and J. W. Murray (2003), Phytoplankton and Their Role in Primary, New, and Export Production, in *Ocean Biogeochemistry*, edited by M. J. R. Fasham, Global Change - The IGBP Series (closed), chap. 5, pp. 99–121, Springer Berlin Heidelberg.

Feely, R. A., S. C. Doney, and S. R. Cooley (2009), Ocean acidification: Present conditions and future changes in a high-$CO_2$ world, *Oceanography*, *22*(4), 36–47, doi: 10.5670/oceanog.2009.95.

Fonselius, S., and J. Valderrama (2003), One hundred years of hydrographic measurements in the Baltic Sea, *Journal of Sea Research*, *49*(4), 229–241, doi:10.1016/S1385-1101(03)00035-2.

Fransson, A., M. Chierici, L. G. Anderson, I. Bussmann, G. Kattner, E. Peter Jones, and J. H. Swift (2001), The importance of shelf processes for the modification of chemical constituents in the waters of the Eurasian Arctic Ocean: implication for carbon fluxes, *Continental Shelf Research*, *21*(3), 225–242, doi:10.1016/S0278-4343(00)00088-1.

Fransson, A., J. Engelbrektsson, and M. Chierici (2013), Development and Optimization of a Labview program for spectrophotometric pH measurements of seawater, pHspec ver 2.5.

Friedman, H. L. (1960), Mayer's Ionic Solution Theory Applied to Electrolyte Mixtures, *The Journal of Chemical Physics*, *32*(4), 1134–1149, doi:10.1063/1.1730863.

Friis, K., A. Körtzinger, J. Pätsch, and D. W. R. Wallace (2005), On the temporal increase of anthropogenic $CO_2$ in the subpolar North Atlantic, *Deep Sea Research Part I*, *52*(5), 681–698, doi:10.1016/j.dsr.2004.11.017.

Garrels, R. M., and M. E. Thompson (1962), A chemical model for sea water at 25 degrees C and one atmosphere total pressure, *American Journal of Science*, *260*(1), 57–66, doi:10.2475/ajs.260.1.57.

Gascard, J.-C., G. Raisbeck, S. Sequeira, F. Yiou, and K. A. Mork (2004), The Norwegian Atlantic Current in the Lofoten basin inferred from hydrological and tracer data (129I) and its interaction with the Norwegian Coastal Current, *Geophysical Research Letters*, *31*(1), L01,308, doi:10.1029/2003GL018303.

Gosselin, M., M. Levasseur, P. A. Wheeler, R. A. Horner, and B. C. Booth (1997), New measurements of phytoplankton and ice algal production in the Arctic Ocean, *Deep Sea Research Part II*, *44*(8), 1623–1644, doi:10.1016/S0967-0645(97)00054-4.

Gran, G. (1952), Determination of the equivalence point in potentiometric titrations. Part II, *Analyst*, *77*(920), 661–671, doi:10.1039/AN9527700661.

Gran, G. (1981), Calculation of equivalence volumes in potentiometric titrations, *Doctoral thesis*, *The Royal Institute of Technology, Stockholm, Sweden*.

Grasshoff, K., K. Kremling, and M. Ehrhardt (1999), Methods of Seawater Analysis, pp. 600, Third edition, Wiley–VCH, Weinheim, Germany.

Grebmeier, J. M., et al. (2006), A Major Ecosystem Shift in the Northern Bering Sea, *Science*, *311*(5766), 1461–1464, doi:10.1126/science.1121365.

Gripenberg, S. (1937), The Calcium Content of Baltic Water, *J. Cons. int. Explor. Mer*, *12*(3), 293–304, doi:10.1093/icesjms/12.3.293.

Gripenberg, S. (1960), On the Alkalinity of Baltic Waters, *J. Cons. int. Explor. Mer*, *26*(1), 5–20, doi:10.1093/icesjms/26.1.5.

Gruber, N., J. L. Sarmiento, and T. F. Stocker (1996), An improved method for detecting anthropogenic $CO_2$ in the oceans, *Global Biogeochemical Cycles*, *10*(4), 809–837, doi:10.1029/96GB01608.

Gustafsson, E., B. Deutsch, B. G. Gustafsson, C. Humborg, and C. M. Mörth (2014), Carbon cycling in the Baltic Sea - The fate of allochthonous organic carbon and its impact on air-sea $CO_2$ exchange, *Journal of Marine Systems*, *129*(0), 289–302, doi:10.1016/j.jmarsys.2013.07.005.

Hakonen, A., L. G. Anderson, J. Engelbrektsson, S. Hulth, and B. Karlson (2013), A potential tool for high-resolution monitoring of ocean acidification, *Analytica Chimica Acta*, *786*, 1–7, doi:10.1016/j.aca.2013.04.040.

Hall, T. M., T. W. N. Haine, and D. W. Waugh (2002), Inferring the concentration of anthropogenic carbon in the ocean from tracers, *Global Biogeochemical Cycles*, *16*(4), 1131, doi: 10.1029/2001GB001835.

Hansson, I. (1973), A new set of pH-scales and standard buffers for sea water, *Deep Sea Research and Oceanographic Abstracts*, *20*(5), 479–491, doi:10.1016/0011-7471(73)90101-0.

Hansson, I., and D. Jagner (1973), Evaluation of the accuracy of gran plots by means of computer calculations: Application to the potentiometric titration of the total alkalinity and carbonate content in sea water, *Analytica Chimica Acta*, *65*(2), 363–373, doi:10.1016/S0003-2670(01)82503-4.

Haraldsson, C., L. G. Anderson, M. Hassellöv, S. Hulth, and K. Olsson (1997), Rapid, high-precision potentiometric titration of alkalinity in ocean and sediment pore waters, *Deep Sea Research Part I*, *44*(12), 2031–2044, doi:10.1016/S0967-0637(97)00088-5.

Harned, H. S., and F. T. Bonner (1945), The First Ionization of Carbonic Acid in Aqueous Solutions of Sodium Chloride, *Journal of the American Chemical Society*, *67*(6), 1026–1031, doi:10.1021/ja01222a037.

Harned, H. S., and S. R. Scholes (1941), The Ionization Constant of $HCO_3^-$ from 0 to 50°, *Journal of the American Chemical Society*, *63*(6), 1706–1709, doi:10.1021/ja01851a058.

Harvie, C. E., N. Mller, and J. H. Weare (1984), The prediction of mineral solubilities in natural waters: The Na-K-Mg-Ca-H-Cl-$SO_4$-OH-$HCO_3$-$CO_3$-$CO_2$-$H_2O$ system to high ionic strengths at 25°C, *Geochimica et Cosmochimica Acta*, *48*(4), 723–751, doi:10.1016/0016-7037(84)90098-X.

HELCOM (2013), Approaches and methods for eutrophication target setting in the Baltic Sea region, *Baltic Sea Environmental Proceedings in Marine Science*, *No. 133*, http://www.helcom.fi.

Hill, V., and G. Cota (2005), Spatial patterns of primary production on the shelf, slope and basin of the Western Arctic in 2002, *Deep Sea Research Part II*, *52*(24-26), 3344–3354, doi: 10.1016/j.dsr2.2005.10.001.

Hill, V. J., P. A. Matrai, E. Olson, S. Suttles, M. Steele, L. A. Codispoti, and R. C. Zimmerman (2013), Synthesis of integrated primary production in the Arctic Ocean: II. In situ and remotely sensed estimates, *Progress in Oceanography*, *110*, 107–125, doi: 10.1016/j.pocean.2012.11.005.

Hjalmarsson, S., K. Wesslander, L. G. Anderson, A. Omstedt, M. Perttilä, and L. Mintrop (2008), Distribution, long-term development and mass balance calculation of total alkalinity in the Baltic Sea, *Continental Shelf Research*, *28*(4-5), 593–601, doi:10.1016/j.csr.2007.11.010.

Hjalmarsson, S., L. G. Anderson, and J. She (2010), The exchange of dissolved inorganic carbon between the Baltic Sea and the North Sea in 2006 based on measured data and water transport estimates from a 3D model, *Marine Chemistry*, *121*(1-4), 200–205, doi: 10.1016/j.marchem.2010.04.008.

Hofmann, A. F., K. Soetaert, J. J. Middelburg, and F. J. R. Meysman (2010), AquaEnv: An Aquatic Acid-Base Modelling Environment in R, *Aquatic Geochemistry*, *16*(4), 507–546, doi: 10.1007/s10498-009-9084-1.

Hoppe, C. J. M., G. Langer, S. D. Rokitta, D. A. Wolf-Gladrow, and B. Rost (2012), Implications of observed inconsistencies in carbonate chemistry measurements for ocean acidification studies, *Biogeosciences*, *9*(7), 2401–2405, doi:10.5194/bg-9-2401-2012, bG.

Huang, K., N. Cassar, R. Wanninkhof, and M. L. Bender (2013), An isotope dilution method for high-frequency measurements of dissolved inorganic carbon concentration in the surface ocean, *Limnology and Oceanography: Methods*, *11*, 572–583, doi:10.4319/lom.2013.11.572.

Hunter, K. (2007), Seawater $CO_2$ Equilibrium Calculations Using Excel, *Version 2*, *University of Otago, New Zealand*.

Ingri, N., W. Kakolowicz, L. G. Sillén, and B. Warnqvist (1967), High-speed computers as a supplement to graphical methods-V: HALTAFALL, a general program for calculating the composition of equilibrium mixtures, *Talanta*, *14*(11), 1261–1286, doi:10.1016/0039-9140(67)80203-0.

Ito, T., M. J. Follows, and E. A. Boyle (2004), Is AOU a good measure of respiration in the oceans?, *Geophysical Research Letters*, *31*(17), L17,305, doi:10.1029/2004GL020900.

Jakobsson, M., A. Grantz, Y. Kristoffersen, and R. Macnab (2003), Physiographic provinces of the Arctic Ocean seafloor, *Geological Society of America Bulletin*, *115*(12), 1443–1455, doi:10.1130/b25216.1.

Jakobsson, M., et al. (2012), The International Bathymetric Chart of the Arctic Ocean (IBCAO) Version 3.0, *Geophysical Research Letters*, *39*(12), L12,609, doi:10.1029/2012GL052219.

Jennings, J. C., L. I. Gordon, and D. M. Nelson (1984), Nutrient depletion indicates high primary productivity in the Weddell Sea, *Nature*, *309*, 51–54.

Johansson, O., and M. Wedborg (1982), On the evaluation of potentiometric titrations of seawater with hydrochloric acid, *Oceanologica Acta*, *5*(2), 209–218.

Johnson, K. M., A. E. King, and J. M. Sieburth (1985), Coulometric $TCO_2$ analyses for marine studies; an introduction, *Marine Chemistry*, *16*(1), 61–82, doi:10.1016/0304-4203(85)90028-3.

Johnson, K. M., J. M. Sieburth, P. J. l. Williams, and L. Brändström (1987), Coulometric total carbon dioxide analysis for marine studies: Automation and calibration, *Marine Chemistry*, *21*(2), 117–133, doi:10.1016/0304-4203(87)90033-8.

Johnson, K. M., K. D. Wills, D. B. Butler, W. K. Johnson, and C. S. Wong (1993), Coulometric total carbon dioxide analysis for marine studies: maximizing the performance of an automated gas extraction system and coulometric detector, *Marine Chemistry*, *44*(2-4), 167–187, doi:10.1016/0304-4203(93)90201-X.

Jones, E. P., L. G. Anderson, and J. H. Swift (1998), Distribution of Atlantic and Pacific waters in the upper Arctic Ocean: Implications for circulation, *Geophysical Research Letters*, *25*(6), 765–768, doi:10.1029/98GL00464.

Jost, G., W. Martens-Habbena, F. Pollehne, B. Schnetger, and M. Labrenz (2010), Anaerobic sulfur oxidation in the absence of nitrate dominates microbial chemoautotrophy beneath the pelagic chemocline of the eastern Gotland Basin, Baltic Sea, *FEMS Microbiology Ecology*, *71*(2), 226–236, doi:10.1111/j.1574-6941.2009.00798.x.

Kaltin, S., C. Haraldsson, and L. G. Anderson (2005), A rapid method for determination of total dissolved inorganic carbon in seawater with high accuracy and precision, *Marine Chemistry*, *96*(1-2), 53–60, doi:10.1016/j.marchem.2004.10.005.

Karcher, M. J., and J. M. Oberhuber (2002), Pathways and modification of the upper and intermediate waters of the Arctic Ocean, *Journal of Geophysical Research: Oceans*, *107*(C6), 2–1–2–13, doi:10.1029/2000JC000530.

Khatiwala, S., et al. (2013), Global ocean storage of anthropogenic carbon, *Biogeosciences*, *10*(4), 2169–2191, doi:10.5194/bg-10-2169-2013, bG.

Khoo, K. H., R. W. Ramette, C. H. Culberson, and R. G. Bates (1977), Determination of hydrogen ion concentrations in seawater from 5 to 40°C: standard potentials at salinities from 20 to 45‰, *Analytical Chemistry*, *49*(1), 29–34, doi:10.1021/ac50009a016.

Korhonen, M., B. Rudels, M. Marnela, A. Wisotzki, and J. Zhao (2013), Time and space variability of freshwater content, heat content and seasonal ice melt in the Arctic Ocean from 1991 to 2011, *Ocean Sci.*, *9*(6), 1015–1055, doi:10.5194/os-9-1015-2013.

Körtzinger, A. (1999), Determination of carbon dioxide partial pressure ($p(CO_2)$), in *Methods of Seawater Analysis*, edited by K. Kremling and M. Ehrhards, pp. 149–158, third edition, Wiley-VCH, Weinheim, Germany.

Körtzinger, A., J. Hedges, and P. Quay (2001), Redfield ratios revisited: Removing the biasing effect of anthropogenic $CO_2$, *Limnology and Oceanography*, *46*(4), 964–970, doi:10.4319/lo.2001.46.4.0964.

Kremling, K. (1970), Untersuchungen über die chemische Zusammensetzung des Meerwassers aus der Ostsee II, *Kieler Meeresforschungen*, *26*(1-20).

Kuliński, K., and J. Pempkowiak (2008), Dissolved organic carbon in the southern Baltic Sea: Quantification of factors affecting its distribution, *Estuarine, Coastal and Shelf Science*, *78*(1), 38–44, doi:10.1016/j.ecss.2007.11.017.

Kuliński, K., and J. Pempkowiak (2012), Carbon Cycling in the Baltic Sea, *Geoplanet: Earth and Planetary Sciences*, *Springer-Verlag Berlin Heidelberg*, 5–47, doi:10.1007/978-3-642-19388-0_2.

Kuliński, K., J. She, and J. Pempkowiak (2011), Short and medium term dynamics of the carbon exchange between the Baltic Sea and the North Sea, *Continental Shelf Research*, *31*(15), 1611–1619, doi:10.1016/j.csr.2011.07.001.

Kuliński, K., B. Schneider, K. Hammer, U. Machulik, and D. Schulz-Bull (2014), The influence of dissolved organic matter on the acid-base system of the Baltic Sea, *Journal of Marine Systems*, *132*(0), 106–115, doi:10.1016/j.jmarsys.2014.01.011.

Kuss, J., W. Roeder, K. P. Wlost, and M. D. DeGrandpre (2006), Time-series of surface water $CO_2$ and oxygen measurements on a platform in the central Arkona Sea (Baltic Sea): Seasonality of uptake and release, *Marine Chemistry*, *101*(3-4), 220–232, doi:10.1016/j.marchem.2006.03.004.

Lalande, C., S. Bélanger, and L. Fortier (2009), Impact of a decreasing sea ice cover on the vertical export of particulate organic carbon in the northern Laptev Sea, Siberian Arctic Ocean, *Geophysical Research Letters*, *36*(21), L21,604, doi:10.1029/2009GL040570.

Lamb, M. F., et al. (2001), Consistency and synthesis of Pacific Ocean $CO_2$ survey data, *Deep Sea Research Part II*, *49*(1-3), 21–58, doi:10.1016/S0967-0645(01)00093-5.

Lavigne, H., and J. P. Gattuso (2011), seacarb: seawater carbonate chemistry with R. R package version 2.4.2, *The Comprehensive R Archive Network (CRAN)*.

Le Quéré, C., T. Takahashi, E. T. Buitenhuis, C. Rödenbeck, and S. C. Sutherland (2010), Impact of climate change and variability on the global oceanic sink of $CO_2$, *Global Biogeochemical Cycles*, *24*(4), GB4007, doi:10.1029/2009GB003599.

Lee, K., T.-W. Kim, R. H. Byrne, F. J. Millero, R. A. Feely, and Y.-M. Liu (2010), The universal ratio of boron to chlorinity for the North Pacific and North Atlantic oceans, *Geochimica et Cosmochimica Acta*, *74*(6), 1801–1811, doi:10.1016/j.gca.2009.12.027.

Lewis, E., and D. Wallace (1998), Program developed for $CO_2$ system calculations, *ORNL/CDIAC-105. Carbon dioxide information analysis center. Oak Ridge National Laboratory, U.S. Department of Energy, Oak Ridge*.

Lewis, G. N., and M. Randall (1921), The Activity of Strong Electrolytes, *Journal of the American Chemical Society*, *43*(5), 1112–1154, doi:10.1021/ja01438a014.

Lindeman, R. L. (1942), The Trophic-Dynamic Aspect of Ecology, *Ecology*, *23*, 399–417, doi:10.2307/1930126.

Liu, X., M. C. Patsavas, and R. H. Byrne (2011), Purification and Characterization of meta-Cresol Purple for Spectrophotometric Seawater pH Measurements, *Environmental Science & Technology*, *45*(11), 4862–4868, doi:10.1021/es200665d.

Liu, X., R. H. Byrne, L. Adornato, K. K. Yates, E. Kaltenbacher, X. Ding, and B. Yang (2013), In Situ Spectrophotometric Measurement of Dissolved Inorganic Carbon in Seawater, *Environmental Science & Technology*, *47*(19), 11,106–11,114, doi:10.1021/es4014807.

MacInnes, D. A. (1919), The Activities of the Ions of Strong Electrolytes, *Journal of the American Chemical Society*, *41*(7), 1086–1092, doi:10.1021/ja02228a006.

Marion, G. M., F. J. Millero, M. F. Camões, P. Spitzer, R. Feistel, and C. T. A. Chen (2011), pH of seawater, *Marine Chemistry*, *126*(1-4), 89–96, doi:10.1016/j.marchem.2011.04.002.

Martz, T., J. Connery, and K. Johnson (2010), Testing the Honeywell Durafet® for seawater pH applications, *Limnology and Oceanography: Methods*, *8*, 172–184, doi:10.4319/lom.2010.8.172.

Martz, T. R., H. W. Jannasch, and K. S. Johnson (2009), Determination of carbonate ion concentration and inner sphere carbonate ion pairs in seawater by ultraviolet spectrophotometric titration, *Marine Chemistry*, *115*(3-4), 145–154, doi:10.1016/j.marchem.2009.07.002.

Mathis, J. T., J. N. Cross, N. R. Bates, S. Bradley Moran, M. W. Lomas, C. W. Mordy, and P. J. Stabeno (2010), Seasonal distribution of dissolved inorganic carbon and net community production on the Bering Sea shelf, *Biogeosciences*, *7*(5), 1769–1787, doi:10.5194/bg-7-1769-2010.

Matrai, P. A., E. Olson, S. Suttles, V. Hill, L. A. Codispoti, B. Light, and M. Steele (2013), Synthesis of primary production in the Arctic Ocean: I. Surface waters, 1954-2007, *Progress in Oceanography*, *110*, 93–106, doi:10.1016/j.pocean.2012.11.004.

McGuire, A. D., et al. (2009), Sensitivity of the carbon cycle in the Arctic to climate change, *Ecological Monographs*, *79*(4), 523–555, doi:10.1890/08-2025.1.

Mehrbach, C., C. H. Culberson, J. E. Hawley, and R. M. Pytkowicz (1973), Measurement of the apparent dissociation constants of carbonic acid in seawater at atmospheric pressure, *Limnology and Oceanography*, *18*(6), 897–907.

Metropolis, N., A. W. Rosenbluth, M. N. Rosenbluth, A. H. Teller, and E. Teller (1953), Equation of State Calculations by Fast Computing Machines, *The Journal of Chemical Physics*, *21*(6), 1087–1092, doi:10.1063/1.1699114.

Millero, F., and D. Pierrot (1998), A chemical equilibrium model for natural waters, *Aquatic Geochemistry*, *4(1)*, 153–199.

Millero, F., and R. N. Roy (1997), A chemical equilibrium model for the carbonate system in natural waters, *Croatica Chemica Acta*, *70*, 1–38.

Millero, F., and D. Schreiber (1982), Use of the ion-pairing model to estimate activity coefficients of the ionic components of natural waters, *American Journal of Science*, *282*, 1508–1540.

Millero, F. J. (1986), The pH of estuarine waters, *Limnology and Oceanography*, *31*(4), 839–847.

Millero, F. J. (2001), *Physical Chemistry of Natural Waters*, John Wiley & Sons, New York, NY, USA.

Millero, F. J. (2007), The Marine Inorganic Carbon Cycle, *Chemical Reviews*, *107*(2), 308–341, doi:10.1021/cr0503557.

Millero, F. J. (2010), Carbonate constants for estuarine waters, *Marine and Freshwater Research*, *61*(2), 139–142, doi:10.1071/MF09254.

Millero, F. J., and D. J. Hawke (1992), Ionic interactions of divalent metals in natural waters, *Marine Chemistry*, *40*(1-2), 19–48, doi:10.1016/0304-4203(92)90046-D.

Millero, F. J., T. B. Graham, F. Huang, H. Bustos-Serrano, and D. Pierrot (2006), Dissociation constants of carbonic acid in seawater as a function of salinity and temperature, *Marine Chemistry*, *100*(1-2), 80–94, doi:10.1016/j.marchem.2005.12.001.

Mintrop, L. (2005), MIDSOMMA manual version 2.0, Marine Analytics and Data (MARIANDA), Kiel, Germany.

Mojica Prieto, F. J., and F. J. Millero (2002), The values of $pK_1$ + $pK_2$ for the dissociation of carbonic acid in seawater, *Geochimica et Cosmochimica Acta*, *66*(14), 2529–2540, doi: 10.1016/S0016-7037(02)00855-4.

Morel, F., and J. Hering (1993), Principles and applications of aquatic principles, *John Wiley & Sons, Inc.*, *New York, NY, USA*, 588.

Mosley, L. M., B. M. Peake, and K. A. Hunter (2010), Modelling of pH and inorganic carbon speciation in estuaries using the composition of the river and seawater end members, *Environmental Modelling and Software*, *25*(12), 1658–1663, doi:10.1016/j.envsoft.2010.06.014.

Ohlson, M. (1991), On the Carbonate System in the Baltic and Weddel Seas: Inventories and Influences by Man, *Doctoral thesis*, *University of Göteborg, Gothenburg, Sweden*.

Omstedt, A., J. Elken, A. Lehmann, and J. Piechura (2004), Knowledge of the Baltic Sea physics gained during the BALTEX and related programmes, *Progress in Oceanography*, *63*(1-2), 1–28, doi:10.1016/j.pocean.2004.09.001.

Orr, J. C., and J. M. Epitalon (2014), Improved routines to model the ocean carbonate system: mocsy 1.0, *Geos. Model Dev. Discuss.*, *submitted*.

Orr, J. C., S. Pantoja, and H.-O. P"ortner (2005), Introduction to special section: The Ocean in a High-$CO_2$ World, *Journal of Geophysical Research: Oceans*, *110*(C9), C09S01, doi:10.1029/2005JC003086.

Orr, J. C., et al. (2009), Research Priorities for Ocean Acidification, report from the Second Symposium on the Ocean in a High-$CO_2$ World, *Monaco*, *October 6-9, 2008, convened by SCOR, UNESCO-IOC, IAEA, and IGBP*, 25 pp.

Orr, J. C., J.-M. Epitalon, and J.-P. Gattuso (2014), Comparison of seven packages that compute ocean carbonate chemistry, *Biogeosciences Discussions*, *11*(4), 5327–5397, doi:10.5194/bgd-11-5327-2014.

O'Sullivan, D. W., and F. J. Millero (1998), Continual measurement of the total inorganic carbon in surface seawater, *Marine Chemistry*, *60*(1-2), 75–83, doi:10.1016/S0304-4203(97)00079-0.

Patsavas, M. C., R. H. Byrne, and X. Liu (2013a), Physical-chemical characterization of purified cresol red for spectrophotometric pH measurements in seawater, *Marine Chemistry*, *155*(0), 158–164, doi:10.1016/j.marchem.2013.06.007.

Patsavas, M. C., R. H. Byrne, and X. Liu (2013b), Purification of meta-cresol purple and cresol red by flash chromatography: Procedures for ensuring accurate spectrophotometric seawater pH measurements, *Marine Chemistry*, *150*(0), 19–24, doi:10.1016/j.marchem.2013.01.004.

Pelletier, G., E. Lewis, and D. W. R. Wallace (2007), CO2SYS.XLS: A calculator for the $CO_2$ system in seawater for Microsoft Excel/VBA, *Washington State Department of Ecology*, *Brookhaven National Laboratory, Olympia, WA/Upton, NY, USA*.

Peng, T.-H., T. Takahashi, W. S. Broecker, and J. O. N. Olafsson (1987), Seasonal variability of carbon dioxide, nutrients and oxygen in the northern North Atlantic surface water: observations and a model*, *Tellus B*, *39B*(5), 439–458, doi:10.1111/j.1600-0889.1987.tb00205.x.

Peng, T.-H., R. Wanninkhof, J. L. Bullister, R. A. Feely, and T. Takahashi (1998), Quantification of decadal anthropogenic $CO_2$ uptake in the ocean based on dissolved inorganic carbon measurements, *Nature*, *396*(6711), 560–563, 10.1038/25103.

Perrette, M., A. Yool, G. D. Quartly, and E. E. Popova (2011), Near-ubiquity of ice-edge blooms in the Arctic, *Biogeosciences*, *8*(2), 515–524, doi:10.5194/bg-8-515-2011.

Pfeil, B., et al. (2013), A uniform, quality controlled Surface Ocean $CO_2$ Atlas (SOCAT), *Earth Syst. Sci. Data*, *5*(1), 125–143, doi:10.5194/essd-5-125-2013.

Pierrot, D. (2002), Thermodynamic Investigations using the Pitzer Formalism: Extension of the Model and its Applications, *Doctoral thesis*, *University of Miami, Miami, USA*.

Pierrot, D., E. Lewis, and D. W. R. Wallace (2006), MS Excel Program Developed for $CO_2$ System Calculations, ORNL/CDIAC-105a, *Carbon Dioxide Information Analysis Center*, *Oak Ridge National Laboratory, U.S. Department of Energy, Oak Ridge, Tennesee, USA*.

Pierrot, D., et al. (2009), Recommendations for autonomous underway $pco_2$ measuring systems and data-reduction routines, *Deep Sea Research Part II*, *56*(8-10), 512–522, doi: 10.1016/j.dsr2.2008.12.005.

Pitzer, K. (1995), *Thermodynamics, Third Edition*, McGraw-Hill Series in Advanced Chemistry, 626 pp., McGraw-Hill, New York, NY, USA.

Pitzer, K. S. (1991), *Activity coefficients in electrolyte solutions*, $2^{nd}$ edition, CRC Press, Boca Raton, FL, USA.

Pitzer, K. S., and G. Mayorga (1974), Thermodynamics of electrolytes. III. Activity and osmotic coefficients for 2-2 electrolytes, *Journal of Solution Chemistry*, *3*(7), 539–546, doi: 10.1007/BF00648138.

Pratt, K. W. (2014), Measurement of $pH_T$ Values of Tris Buffers in Artificial Seawater at Varying Mole Ratios of Tris:Tris - HCl, *Marine Chemistry*, (In press), doi: 10.1016/j.marchem.2014.03.003.

Årthun, M., R. B. Ingvaldsen, L. H. Smedsrud, and C. Schrum (2011), Dense water formation and circulation in the Barents Sea, *Deep Sea Research Part I*, *58*(8), 801–817, doi: 10.1016/j.dsr.2011.06.001.

Redfield, A. C., B. H. Ketchum, and F. A. Richards (1963), The influence of organisms on the composition of sea water., in *The Sea, Vol. 2*, vol. 2, edited by M. Hill, pp. 26–77, Wiley, New York.

Reigstad, M., P. Wassmann, R. C. Wexels, S. ygarden, and F. Rey (2002), Variations in hydrography, nutrients and chlorophyll *a* in the marginal ice-zone and the central Barents Sea, *Journal of Marine Systems*, *38*(1-2), 9–29, doi:10.1016/S0924-7963(02)00167-7.

Reigstad, M., J. Carroll, D. Slagstad, I. Ellingsen, and P. Wassmann (2011), Intra-regional comparison of productivity, carbon flux and ecosystem composition within the northern Barents Sea, *Progress in Oceanography*, *90*(1-4), 33–46, doi:10.1016/j.pocean.2011.02.005.

Rhein, M., et al. (2013), Observations: Ocean, in *Climate Change 2013: The Physical Science Basis. Contribution of Working Group I to the Fifth Assessment Report of the Intergovernmental Panel on Climate Change*, edited by T. Stocker, D. Qin, G.-K. Plattner, M. Tignor,

S. Allen, J. Boschung, A. Nauels, Y. Xia, V. Bex, and P. Midgley, Cambridge University Press, Cambridge, United Kingdom and New York, NY, USA.

Riebesell, U., V. J. Fabry, L. Hansson, and J. P. Gattuso (2010), in *Guide to best practices for ocean acidification research and data reporting*, edited by U. Riebesell, V. J. Fabry, L. Hansson, and J. P. Gattuso, 260 p. Luxembourg: Publications Office of the European Union.

Robbins, L., M. E. Hansen, J. Kleypas, and S. Meylan (2010), CO2calc: a user-friendly carbon calculator for Windows, Mac OS X, and iOS (iPhone), *USGS Open-File Report*, *2010-1280*.

Roy, R. N., L. N. Roy, K. M. Vogel, C. Porter-Moore, T. Pearson, C. E. Good, F. J. Millero, and D. M. Campbell (1993), The dissociation constants of carbonic acid in seawater at salinities 5 to 45 and temperatures 0 to 45 °C, *Marine Chemistry*, *44*(2-4), 249–267, doi:10.1016/0304-4203(93)90207-5.

Rudels, B., E. P. Jones, L. G. Anderson, and G. Kattner (1994), On the Intermediate Depth Waters of the Arctic Ocean, in *The Polar Oceans and Their Role in Shaping the Global Environment*, edited by O. M. Johannessen, R. D. Muench, and J. E. Overland, pp. 33–46, American Geophysical Union.

Rudels, B., L. G. Anderson, and E. P. Jones (1996), Formation and evolution of the surface mixed layer and halocline of the Arctic Ocean, *Journal of Geophysical Research*, *101*(C4), 8807, doi:10.1029/96jc00143.

Rudels, B., et al. (2012), Observations in the Ocean, in *Arctic Climate Change*, vol. 43, edited by P. Lemke and H.-W. Jacobi, chap. 4, pp. 117–198, Atmospheric and Oceanographic Sciences Library, Springer Netherlands, doi:10.1007/978-94-007-2027-5_4.

Sabine, C. L., and T. Tanhua (2010), Estimation of Anthropogenic $CO_2$ Inventories in the Ocean, *Annual Review of Marine Science*, *2*(1), 175–198, doi:10.1146/annurev-marine-120308-080947.

Sabine, C. L., et al. (2004), The Oceanic Sink for Anthropogenic $CO_2$, *Science*, *305*(5682), 367–371, doi:10.1126/science.1097403.

Sabine, C. L., H. Ducklow, and M. Hood (2010), International carbon coordination: Roger Revelle's legacy in the Intergovernmental Oceanographic Commission, *Oceanography*, *23*(3), 48–60, doi:10.5670/oceanog.2010.23.

Sakshaug, E. (2004), Primary and Secondary Production in the Arctic Seas, in *The Organic Carbon Cycle in the Arctic Ocean*, edited by R. Stein and R. MacDonald, chap. 3, pp. 57–81, Springer Berlin Heidelberg.

Sarmiento, J. L., and N. Gruber (2006), Ocean biogeochemical dynamics, *Princeton University Press*, *Princeton, NJ, USA*, 503.

Schauer, U., B. Rudels, E. P. Jones, L. G. Anderson, R. D. Muench, G. Björk, J. H. Swift, V. Ivanov, and A. M. Larsson (1999), Confluence and redistribution of Atlantic water in the Nansen, Amundsen and Makarov basins, *Annals of Geophysics*, *20*(2), 257–273, doi: 10.5194/angeo-20-257-2002.

Schlitzer, R. (2002), Interactive analysis and visualization of geoscience data with Ocean Data View, *Computers & Geosciences*, *28*(10), 1211–1218, doi:10.1016/S0098-3004(02)00040-7.

Schneider, B., G. Nausch, H. Kubsch, and I. Petersohn (2002), Accumulation of total $CO_2$ during stagnation in the Baltic Sea deep water and its relationship to nutrient and oxygen concentrations, *Marine Chemistry*, *77*(4), 277–291, doi:10.1016/S0304-4203(02)00008-7.

Schneider, B., S. Kaitala, M. Raateoja, and B. Sadkowiak (2009), A nitrogen fixation estimate for the Baltic Sea based on continuous $pCO_2$ measurements on a cargo ship and total nitrogen data, *Continental Shelf Research*, *29*(11-12), 1535–1540, doi:10.1016/j.csr.2009.04.001.

Schneider, B., G. Nausch, and C. Pohl (2010), Mineralization of organic matter and nitrogen transformations in the Gotland Sea deep water, *Marine Chemistry*, *119*(1-4), 153–161, doi: 10.1016/j.marchem.2010.02.004.

Schneider, B., E. Gustafsson, and B. Sadkowiak (2014), Control of the mid-summer net community production and nitrogen fixation in the central Baltic Sea: An approach based on $pCO_2$ measurements on a cargo ship, *Journal of Marine Systems*, (accepted article), doi: 10.1016/j.jmarsys.2014.03.007.

Skoog, A., M. Wedborg, and E. Fogelqvist (2011), Decoupling of total organic carbon concentrations and humic substance fluorescence in a an extended temperate estuary, *Marine Chemistry*, *124*(1-4), 68–77, doi:10.1016/j.marchem.2010.12.003.

Steinacher, M., F. Joos, T. L. Frölicher, G. K. Plattner, and S. C. Doney (2009), Imminent ocean acidification in the Arctic projected with the NCAR global coupled carbon cycle-climate model, *Biogeosciences*, *6*(4), 515–533, doi:10.5194/bg-6-515-2009, bG.

Steiner, N. S., W. G. Lee, and J. R. Christian (2013), Enhanced gas fluxes in small sea ice leads and cracks: Effects on $CO_2$ exchange and ocean acidification, *Journal of Geophysical Research: Oceans*, *118*(3), 1195–1205, doi:10.1002/jgrc.20100.

Sterner, R. W., T. Andersen, J. J. Elser, D. O. Hessen, J. M. Hood, E. McCauley, and J. Urabe (2008), Scale-dependent carbon:nitrogen:phosphorus seston stoichiometry in marine and freshwaters, *Limnology and Oceanography*, *53*(3), 1169–1180, doi: 10.4319/lo.2008.53.3.1169.

Stumm, W., and J. Morgan (1996), Aquatic chemistry, third edition, *John Wiley & Sons, Inc.*, *New York, NY, USA*, 1022.

Svensson, B. R., and C. E. Woodward (1988), Widom's method for uniform and non-uniform electrolyte solutions, *Molecular Physics*, *64*(2), 247–259, doi:10.1080/00268978800100203.

Sweeney, C., E. Gloor, A. R. Jacobson, R. M. Key, G. McKinley, J. L. Sarmiento, and R. Wanninkhof (2007), Constraining global air-sea gas exchange for $co_2$ with recent bomb $^{14}c$ measurements, *Global Biogeochemical Cycles*, *21*(2), GB2015, doi:10.1029/2006GB002784.

Takahashi, T., W. S. Broecker, and S. Langer (1985), Redfield ratio based on chemical data from isopycnal surfaces, *Journal of Geophysical Research: Oceans*, *90*(C4), 6907–6924, doi:10.1029/JC090iC04p06907.

Tanhua, T., A. Körtzinger, K. Friis, D. W. Waugh, and D. W. R. Wallace (2007), An estimate of anthropogenic $CO_2$ inventory from decadal changes in oceanic carbon content, *Proceedings of the National Academy of Sciences*, *104*(9), 3037–3042, doi:10.1073/pnas.0606574104.

Tanhua, T., N. R. Bates, and A. Körtzinger (2013), The Marine Carbon Cycle and Ocean Carbon Inventories, in *Ocean Circulation and Climate, International Geophysics Series 103*, edited by G. Siedler, S. Griffies, J. Gould, and J. Church, pp. 787–815, Academic Press, Oxford, United Kingdom and Amsterdam, The Netherlands, doi:10.1016/B978-0-12-391851-2.00030-1.

Thacker, W. C. (2012), Regression-based estimates of the rate of accumulation of anthropogenic $CO_2$ in the ocean: A fresh look, *Marine Chemistry*, *132-133*(0), 44–55, doi:10.1016/j.marchem.2012.02.004.

Thomas, H., and B. Schneider (1999), The seasonal cycle of carbon dioxide in Baltic Sea surface waters, *Journal of Marine Systems*, *22*(1), 53–67, doi:10.1016/S0924-7963(99)00030-5.

Thomas, H., J. Pempkowiak, F. Wulff, and K. Nagel (2003), Autotrophy, nitrogen accumulation and nitrogen limitation in the Baltic Sea: A paradox or a buffer for eutrophication?, *Geophysical Research Letters*, *30*(21), 2130, doi:10.1029/2003GL017937.

Thomas, H., Y. Bozec, H. J. W. de Baar, K. Elkalay, M. Frankignoulle, L. S. Schiettecatte, G. Kattner, and A. V. Borges (2005), The carbon budget of the North Sea, *Biogeosciences*, *2*(1), 87–96, doi:10.5194/bg-2-87-2005, bG.

Touratier, F., and C. Goyet (2004a), Applying the new TrOCA approach to assess the distribution of anthropogenic $CO_2$ in the Atlantic Ocean, *Journal of Marine Systems*, *46*(1-4), 181–197, doi:10.1016/j.jmarsys.2003.11.020.

Touratier, F., and C. Goyet (2004b), Definition, properties, and Atlantic Ocean distribution of the new tracer TrOCA, *Journal of Marine Systems*, *46*(1-4), 169–179, doi:10.1016/j.jmarsys.2003.11.016.

Turner, D. R., M. Whitfield, and A. G. Dickson (1981), The equilibrium speciation of dissolved components in freshwater and seawater at 25 °C and 1 atmosphere pressure, *Geochimica et Cosmochimica Acta*, *45*, 855–881.

Uppström, L. R. (1974), The boron/chlorinity ratio of deep-sea water from the Pacific Ocean, *Deep Sea Research and Oceanographic Abstracts*, *21*(2), 161–162, doi:10.1016/0011-7471(74)90074-6.

van Heuven, S. (2013), Determination of the rate of oceanic storage of anthropogenic $CO_2$ from measurements in the ocean interior: the South Atlantic Ocean, *Doctoral thesis*, *Rijksuniversiteit Groningen, Groningen, The Netherlands*.

Van Heuven, S., D. Pierrot, E. Lewis, and D. W. R. Wallace (2011), MATLAB Program Developed for $CO_2$ System Calculations, ORNL/CDIAC-105b, *Carbon Dioxide Information Analysis Center*, *Oak Ridge National Laboratory, U.S. Department of Energy, Oak Ridge, Tennesee, USA*.

Vázquez-Rodríguez, M., et al. (2009), Anthropogenic carbon distributions in the Atlantic Ocean: data-based estimates from the Arctic to the Antarctic, *Biogeosciences*, *6*(3), 439–451, doi: 10.5194/bg-6-439-2009, bG.

Wallace, D. W. R. (1995), Monitoring global ocean carbon inventories, *OOSDP Background Report*, *No. 5, Texas A&M University, College Stations, TX, USA*.

Walsh, D., I. Polyakov, L. Timokhov, and E. Carmack (2007), Thermohaline structure and variability in the eastern Nansen Basin as seen from historical data, *Journal of Marine Research*, *65*(5), 685–714, doi:10.1357/002224007783649466.

Wang, J., G. F. Cota, and J. C. Comiso (2005), Phytoplankton in the Beaufort and Chukchi Seas: Distribution, dynamics, and environmental forcing, *Deep Sea Research Part II*, *52*(24-26), 3355–3368, doi:10.1016/j.dsr2.2005.10.014.

Wang, Z. A., X. Liu, R. H. Byrne, R. Wanninkhof, R. E. Bernstein, E. A. Kaltenbacher, and J. Patten (2007), Simultaneous spectrophotometric flow-through measurements of pH, carbon dioxide fugacity, and total inorganic carbon in seawater, *Analytica Chimica Acta*, *596*(1), 23–36, doi:10.1016/j.aca.2007.05.048.

Wanninkhof, R., and K. Thoning (1993), Measurement of fugacity of $CO_2$ in surface water using continuous and discrete sampling methods, *Marine Chemistry*, *44*(2-4), 189–204, doi: 10.1016/0304-4203(93)90202-Y.

Wanninkhof, R., W. E. Asher, D. T. Ho, C. Sweeney, and W. R. McGillis (2009), Advances in Quantifying Air-Sea Gas Exchange and Environmental Forcing*, *Annual Review of Marine Science*, *1*(1), 213–244, doi:doi:10.1146/annurev.marine.010908.163742.

Waters, J. F. (2012), Measurement of Seawater pH: A Theoretical and Analytical Investigation, *Open Access Dissertations*, *Paper 908*, University of Miami.

Waters, J. F., and F. J. Millero (2013), The free proton concentration scale for seawater pH, *Marine Chemistry*, *149*(0), 8–22, doi:10.1016/j.marchem.2012.11.003.

Weiss, R. F. (1974), Carbon dioxide in water and seawater: the solubility of a non-ideal gas, *Marine Chemistry*, *2*(3), 203–215, doi:10.1016/0304-4203(74)90015-2.

Weiss, R. F., and B. A. Price (1980), Nitrous oxide solubility in water and seawater, *Marine Chemistry*, *8*(4), 347–359, doi:10.1016/0304-4203(80)90024-9.

Whitfield, M. (1975), An improved specific interaction model for seawater at 25°C and 1 atmosphere total pressure, *Marine Chemistry*, *3*(3), 197–213, doi:10.1016/0304-4203(75)90002-X.

Widom, B. (1963), Some Topics in the Theory of Fluids, *The Journal of Chemical Physics*, *39*(11), 2808–2812, doi:10.1063/1.1734110.

Williams, P. J. l. (1993), Fundamental issues in measurement of primary production, *ICES Marine Sciences Symposium 197*, pp. 3–8.

Wolf-Gladrow, D. A., R. E. Zeebe, C. Klaas, A. Körtzinger, and A. G. Dickson (2007), Total alkalinity: The explicit conservative expression and its application to biogeochemical processes, *Marine Chemistry*, *106*(1-2), 287–300, doi:10.1016/j.marchem.2007.01.006.

Yakushev, E. V., F. Pollehne, G. Jost, I. Kuznetsov, B. Schneider, and L. Umlauf (2007), Analysis of the water column oxic/anoxic interface in the Black and Baltic seas with a numerical model, *Marine Chemistry*, *107*(3), 388–410, doi:10.1016/j.marchem.2007.06.003.

Yang, B., M. C. Patsavas, R. H. Byrne, and J. Ma (2014), Seawater pH measurements in the field: A DIY photometer with 0.01 unit pH accuracy, *Marine Chemistry*, *160*(0), 75–81, doi:10.1016/j.marchem.2014.01.005.

Yao, W., and R. H. Byrne (2001), Spectrophotometric Determination of Freshwater pH Using Bromocresol Purple and Phenol Red, *Environmental Science & Technology*, *35*(6), 1197–1201, doi:10.1021/es001573e.

Zeebe, R. E. (2014), Interactive comment on "Comparison of seven packages that compute ocean carbonate chemistry" by J. C. Orr et al., *Biogeosciences Discuss.*, *11*, C763–C769, doi:http://www.biogeosciences-discuss.net/11/C763/2014/.

Zeebe, R. E., and D. A. Wolf-Gladrow (2001), $CO_2$ in seawater: Equilibrium, kinetics, isotopes, *Elsevier Oceanography Series*, *65*, 1–346, doi:10.1016/S0422-9894(01)80001-5.

Zhang, H., and R. H. Byrne (1996), Spectrophotometric pH measurements of surface seawater at in-situ conditions: absorbance and protonation behavior of thymol blue, *Marine Chemistry*, *52*(1), 17–25, doi:10.1016/0304-4203(95)00076-3.